Graduate Theses and Dissertations

Iowa State University Capstones, Theses and Dissertations

2012

Integrating plug-in electric vehicles into the electric power system

Di Wu
Iowa State University

Follow this and additional works at: https://lib.dr.iastate.edu/etd

Part of the Electrical and Electronics Commons

Recommended Citation

www.manaraa.com

Integrating plug-in electric vehicles into the electric power system

by

Di Wu

A dissertation submitted to the graduate faculty

in partial fulfillment of the requirements for the degree of

DOCTOR OF PHILOSOPHY

Major: Electrical Engineering

Program of Study Committee:

Dionysios C. Aliprantis, Major Professor

Konstantina Gkritza

James D. McCalley

Ron M. Nelson

Lizhi Wang

Lei Ying

Iowa State University

Ames, Iowa

2012

TABLE OF CONTENTS

LIST OF TABLES

LIST OF FIGURES

ACKNOWLEDGMENTS

I express my sincere gratitude to Dr. Dionysios C. Aliprantis, the major advisor of my Ph.D. studies, for his guidance, patience, and support throughout my research work and the writing of this dissertation. His insights and words of encouragement have often inspired me and renewed my hopes for completing my Ph.D. studies at Iowa State University.

Of the many people who have been enormously helpful in the preparation of this dissertation, I am especially thankful to my committee members, Dr. Konstantina Gkritza, Dr. James D. McCalley, Dr. Ron M. Nelson, Dr. Lizhi Wang, and Dr. Lei Ying, for their efforts and contributions to this work. I also recognize the contribution from the faculty members and students in the NETSCORE-21 research project. Further, I acknowledge the financial support from the Department of Electrical and Computer Engineering at Iowa State University and the National Science Foundation[1].

I dedicate this dissertation to my parents, Jinming Wu and Huanhong Li, and my wife Yimo for their unconditional love and support in every way possible throughout the process of this dissertation and beyond.

ABSTRACT

This dissertation contributes to our understanding of how plug-in hybrid electric vehicles (PHEVs) and plug-in battery-only electric vehicles (EVs)—collectively termed plug-in electric vehicles (PEVs)—could be successfully integrated with the electric power system. The research addresses issues at a diverse range of levels pertaining to light-duty vehicles, which account for the majority of highway vehicle miles traveled, energy consumed by highway travel modes, and carbon dioxide emissions from on-road sources. Specifically, the following topics are investigated: (i) On-board power electronics topologies for bidirectional vehicle-to-grid and grid-to-vehicle power transfer; (ii) The estimation of the electric energy and power consumption by fleets of light-duty PEVs; (iii) An operating framework for the scheduling and dispatch of electric power by PEV aggregators; (iv) The pricing of electricity by PHEV aggregators and how it affects the decision-making process of a cost-conscious PHEV owner; (v) The impacts on distribution systems from PEVs under aggregator control; (vi) The modeling of light-duty PEVs for long-term energy and transportation planning at a national scale.

1. GENERAL INTRODUCTION

The electrification of transportation has become a cornerstone of our efforts to conserve energy, protect the environment, and reduce our nation's dependence on fossil fuels, which are a geopolitically insecure and dwindling energy source. This dissertation studies light-duty plug-in electric vehicles, because they represent a very significant and timely electric transportation technology. Plug-in electric vehicles (PEVs)—either plug-in hybrid electric vehicles (PHEVs) or pure electric vehicles—adopt similar drivetrains as hybrid electric vehicles (HEVs), but are equipped with higher-capacity batteries, allowing electricity from the power system to displace a significant portion of petroleum consumed in the transportation sector. Accelerating the development of PEV technology is recognized as an essential part of the solution to the energy and environmental problems around the world [1].

The contributions of this dissertation can be classified into three levels, namely:

1. the vehicle level, where a novel power electronics topology was proposed to enable the bidirectional exchange of energy with the power system;

2. the power system level, where the focus is on load estimation from fleets of PEVs, charging control algorithms, and potential impacts on the power system.

3. the national level, where appropriate PEV models are proposed for long-term energy and transportation planning studies.

1.1 Dissertation Organization

The dissertation's chapters correspond to journal and conference papers that I have authored or co-authored.

In Chapter 2, a novel power electronics topology is proposed, which enables bidirectional

power transfer between HEVs and the grid for a variety of drivetrain configurations. The topology utilizes only the pre-existing vehicles' internal power converters and electric machines, which are normally used to provide traction, and thus eliminates the requirement for an additional (on-board or off-board) battery charger. The proposed method can help to reduce costs and vehicle weight. In addition, with the capability for bidirectional power transfer, that is, charging the battery from the grid or discharging the stored electrochemical energy to the grid, these vehicles could be used to assist power system operation by providing ancillary services (e.g., voltage and frequency regulation, capacity reserve, or peak load shaving), thus increasing the security and reliability of the power system [2, 3].

The emerging fleet of PEVs will introduce a considerable amount of additional load on the power system, which needs to be forecast. To this end, Chapter 3 proposes methodologies to estimate the electric energy and power consumption by light-duty PEVs. This study is based on a probabilistic formulation, where various aspects have been taken into consideration. For example, we are using a realistic light-duty vehicle travel pattern obtained from the National Household Travel Survey (NHTS). In addition, PEV operation is reasonably modeled considering all possible drivetrain configurations, such as series and parallel topologies. We also consider whether a public charging infrastructure is available or not, which would allow drivers to charge their vehicles away from home. Finally, different voltage and current levels are considered for the charging circuits. Using the proposed method, the PEVs' daily energy and power consumption are estimated for two uncontrolled charging scenarios. The results of this work indicate that under uncontrolled charging, a significant amount of charging will take place during peak hours when the wholesale electricity is expensive, resulting in higher charging cost. The coincidence between peaks of PEV and other load also requires additional capacity in generation, transmission, and distribution in order to maintain the adequacy of the nation's power system.

PEVs constitute a type of "energy load" that is in fact more flexible than traditional load. For example, the majority of PEV owners return home early in the evening, and may not have a preference about when their vehicles are being charged as long as the batteries are fully charged by the next morning. To utilize this flexibility, appropriate algorithms for charging control and

management must be designed. This control will be performed by PEV aggregators, either existing load serving entities with new financial contracts specific for PEV loads, or new for-profit entities that will participate in the wholesale electricity market. Chapter 4 proposes an operating framework and sets forth algorithms for the scheduling and dispatch of electric power for PEV aggregators, whose main objective is the maximization of energy trading profits. The aggregators are assumed to operate in the current wholesale electric energy market framework. First, a minimum-cost load scheduling algorithm is designed, which determines the purchase of energy in the day-ahead market based on the forecast electricity price and PEV power demands. Second, a dynamic dispatch algorithm is developed, used for distributing the purchased energy to PEVs on the operating day. The algorithms were developed by taking into account realistic vehicle travel patterns from the NHTS database. Simulation results are used to evaluate the proposed algorithms, and to demonstrate the potential impact of an aggregated PEV fleet on the power system.

By participating in an aggregator-controlled off-peak charging program, a PHEV owner relinquishes control of the battery's state of charge, in exchange for a reduced electricity rate. In this case, some charging that normally would have occurred during on-peak hours may not be allowed by the aggregator, and so a fraction of the PHEVs' daily miles traveled may shift from the charge-depleting to the charge-sustaining mode. Hence, a greater portion of the tractive energy would be derived from gasoline, increasing PHEV owners' fuel expenses. In Chapter 5, the decision-making process of a cost-conscious PHEV owner who is trying to minimize his/her transportation energy costs is studied. The analysis leads to a set of outcomes determined by the prices of electricity and gasoline, and yields certain interesting insights pertaining to the pricing of electricity by PHEV aggregators.

On the bulk power transmission level, the PEV additional load is manageable, and may not cause serious supply adequacy problems at least in the short term. However, the emerging fleet of PEVs could overload local distribution systems, especially in feeders with high concentration of PEVs. The problem might be more urgent for cities in coastal regions in the U.S., since it is expected that PEVs will initially penetrate the market in these locations [4]. Chapter 6 proposes a method to evaluate potential impacts on distribution systems from light-duty PEVs.

As an example, we study the potential impacts from PEVs under the control of aggregators who maximize their energy trading-related profits using the method of Chapter 4.

Finally, the emerging PEV fleet will increase the interdependency between the electricity and transportation sectors. Since electricity can be generated from various resources such as hydro, wind, solar, nuclear, coal, and natural gas, PEV technology provides an opportunity to diversify the primary energy sources for transportation, and reduce our dependence on petroleum. New investments in the energy infrastructure will be required to satisfy the additional PEV energy demand. Emissions from vehicle tailpipes will be shifted to power plants (or will disappear altogether if renewable energy sources are used), so the net emissions from the integrated system will change. Therefore, PEV modeling is important for studying the design of the national energy and transportation infrastructures. Realizing this need, Chapter 7 proposes models for light-duty PEVs, appropriate for identifying the impacts of vehicle technologies on the national energy and transportation infrastructures. The models are parameterized using an array of publicly available data, and are implemented within an advanced national energy and transportation planning tool called NETPLAN that has been recently developed at Iowa State University.

Chapter 8 summarizes our research findings, and proposes areas for extending this work in the future.

2. BIDIRECTIONAL POWER TRANSFER BETWEEN HEVS AND GRID WITHOUT EXTERNAL POWER CONVERTERS

A paper published in the *Proceedings of the IEEE Energy 2030 Conference*, Atlanta, GA, Nov. 17–18, 2008.

Di Wu, Hao Chen, Trishna Das, and Dionysios C. Aliprantis

Abstract

This paper proposes methodologies to realize bidirectional power transfer between hybrid electric vehicles (HEVs) and the power grid for the most common HEV configurations. Only the internal power electronics and electric machines of the vehicle's propulsion system are being used, thus avoiding additional external power converters. Theoretical analysis and simulation results verify the effectiveness of the proposed methodologies.

2.1 Introduction

With the growing emphasis on energy conservation and environmental protection, hybrid electric vehicles (HEVs) are becoming increasingly popular because of their high fuel economy and reduced emissions compared with conventional petroleum fueled vehicles [5–7]. From the viewpoint of energy, HEVs can be considered as a special multi-energy reservoir. The electric and chemical energy stored in the battery and fuel tank can be transformed to mechanical energy for propulsion by the power electronics and drive system [8]. On the other hand, a large fleet of HEVs represents an enormous distributed energy storage potential, which can be exploited to support the power grid.

Conventional HEV batteries are charged through the use of the on-board internal combustion engine (ICE) and electric generator, or by the electric generator only during the "regenerative braking" process [9]. There is no provision to charge the batteries externally, let alone discharging stored energy to the grid. With an additional bidirectional power transfer capability, that is, charging the battery from the grid or discharging the stored electric/chemical energy to the grid, plug-in HEVs become ideal candidates to assist power system operation providing, for instance, voltage and frequency regulation, power quality improvement, peak load shaving and grid ancillary services, thus increasing the security and reliability of the power system [2]. This capability is also referred to as grid-to-vehicle (G2V) and vehicle-to-grid (V2G) [3].

A method is introduced in [10] to utilize a series-parallel HEV (Toyota Prius) as an emergency power source in the event of power outage for a local isolated load without additional power electronics devices. This paper proposes methodologies to realize bidirectional power transfer between HEVs and the grid for different types of HEVs by utilizing only the vehicles' internal power converters and electric machines, which are normally used to provide traction. In this study, the electric motor is assumed to be a permanent magnet synchronous machine (PMSM), which is widely used in HEV applications [8,11]. Matlab/Simulink is used for modeling, simulation and analysis of the proposed strategies.

2.2   Bidirectional Power Transfer Strategy

Bidirectional power transfer implies that power can flow from the grid to the HEV and vice versa. During G2V operation, the batteries are being charged. During V2G operation, it is advantageous to enable the discharge of energy not only from the batteries but also from the fuel tank. Since the capacity of battery is limited, the energy stored in the fuel tank can further enhance HEVs' V2G capability.

As is well known, the ICE efficiency is a function of torque and speed, and varies significantly with operation point. It is beneficial to operate the ICE in the high-efficiency region to increase fuel economy [6]. Thus, when discharging the energy stored in the fuel tank, the torque and speed of the generator that is loading the ICE should be controllable. It should be noted that when the engine is operated to provide power for V2G application, the vehicle could be

located outdoors or indoors if sufficient ventilation for exhaust and cooling requirements is provided [12].

2.3   Proposed Methodologies

Three common existing HEV configurations [6, 8] are shown in Figure 2.1. Note that the series and series-parallel configurations make use of two electric machines, each with its own converter. In the parallel configuration, there is only one motor and one inverter.

(a) Series HEVs

(b) Parallel HEVs

(c) Series-Parallel HEVs
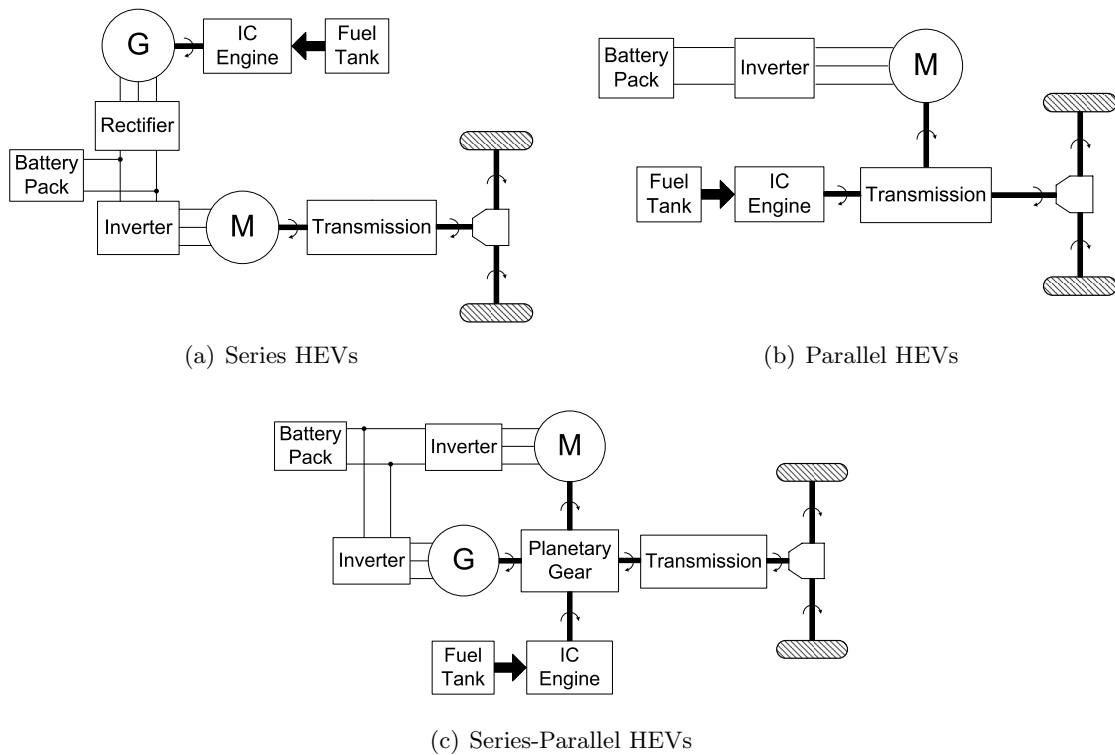
Figure 2.1   HEV Configurations.

2.3.1   Series and Series-Parallel HEVs

The proposed topology for series and series-parallel HEVs is shown in Figure 2.2, where the c-phase is disconnected from the inverter and the grid is connected with the a-phase in series after opening switches K_1, K_3 and closing switch K_2–K_2' [12]. This constitutes a simple single-phase H-bridge inverter [13]. When the battery is being charged/discharged from/to the grid,

the generator and its corresponding rectifier/inverter are not in operation. When the energy stored in the fuel tank is discharged (through the engine and the generator), the generator is loading the ICE and controlled to operate ICE at a given torque and speed point (e.g., the one that corresponds to maximum efficiency). Since the vehicle is stationary, no propulsion torque is needed from the motor. Thus, the motor-side inverter is available and can be changed to an H-bridge inverter.
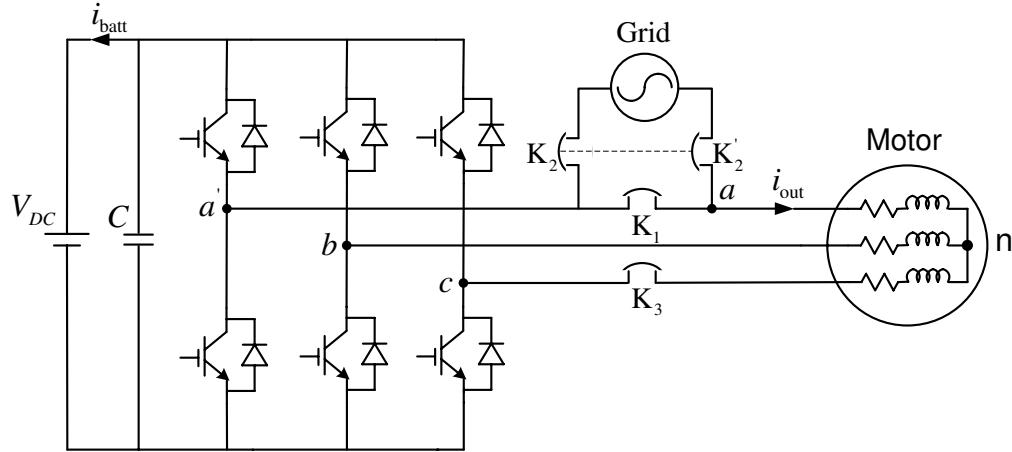
Figure 2.2 Topology for bidirectional power transfer in series and series-parallel HEVs.

Because the voltage of the power grid is essentially constant, the output current can be controlled to achieve the desired active and reactive power. To this end, hysteresis modulation can be used. It is interesting to note that the stator windings of the motor are employed in Figure 2.2. With this configuration, no additional filter is required to filter out the high-frequency harmonic components in the output current. In the ensuing analysis, the equivalent inductance value for this configuration will be derived.

The stator voltage equation in the rotor reference frame is [14, 15]

$$\mathbf{v}_{qd0s}^r = (\mathbf{r}_s + \mathbf{L}_{qd0s}p)\mathbf{i}_{qd0s}^r + \omega_r \boldsymbol{\lambda}_{dqs}^r \,, \tag{2.1}$$

where

$$\mathbf{v}_{qd0s}^r = \begin{bmatrix} v_{qs}^r & v_{ds}^r & v_{0s}^r \end{bmatrix}^T \,,$$

$$\mathbf{i}_{qd0s}^r = \begin{bmatrix} i_{qs}^r & i_{ds}^r & i_{0s}^r \end{bmatrix}^T \,,$$

$$\boldsymbol{\lambda}_{dqs}^r = \begin{bmatrix} \lambda_{ds}^r & -\lambda_{qs}^r & 0 \end{bmatrix}^T ,$$

$$\mathbf{r}_s = \begin{bmatrix} r_s & 0 & 0 \\ 0 & r_s & 0 \\ 0 & 0 & r_s \end{bmatrix} ,$$

$$\mathbf{L}_{qd0s} = \begin{bmatrix} L_q & 0 & 0 \\ 0 & L_d & 0 \\ 0 & 0 & L_{ls} \end{bmatrix} ,$$

r_s is the stator's resistance, L_{ls} is the leakage inductance, L_q and L_d are the qd-axes self-inductances, ω_r is the speed of the rotor reference frame, and p denotes differentiation with respect to time.

Since the motor will be locked, ω_r is equal to zero. Therefore, the second term in (2.1) is eliminated. Hence, the voltages and currents in abc variables can be obtained using the reference frame transformation

$$\begin{aligned} \mathbf{v}_{abcs} &= (\mathbf{K}_s^r)^{-1}\mathbf{v}_{qd0s}^r \\ &= (\mathbf{K}_s^r)^{-1}(\mathbf{r}_s + \mathbf{L}_{qd0s}p)\mathbf{i}_{qd0s}^r \\ &= (\mathbf{K}_s^r)^{-1}(\mathbf{r}_s + \mathbf{L}_{qd0s}p)(\mathbf{K}_s^r)\mathbf{i}_{abcs} \\ &= (\mathbf{r}_s + \mathbf{L}_s p)\mathbf{i}_{abcs} , \end{aligned} \qquad (2.2)$$

where

$$\mathbf{v}_{abcs} = \begin{bmatrix} v_{as} & v_{bs} & v_{cs} \end{bmatrix}^T ,$$

$$\mathbf{i}_{abcs} = \begin{bmatrix} i_{as} & i_{bs} & i_{cs} \end{bmatrix}^T ,$$

$$\mathbf{L}_s = (\mathbf{K}_s^r)^{-1}\mathbf{L}_{qd0s}\mathbf{K}_s^r ,$$

$$\mathbf{K}_s^r = \frac{2}{3} \begin{bmatrix} \cos\theta_r & \cos(\theta_r - 120^\circ) & \cos(\theta_r + 120^\circ) \\ \sin\theta_r & \sin(\theta_r - 120^\circ) & \sin(\theta_r + 120^\circ) \\ 1/2 & 1/2 & 1/2 \end{bmatrix}$$

is the abc-$qd0$ rotor reference frame transformation matrix, $(\mathbf{K}_s^r)^{-1}$ is the inverse transformation matrix, and θ_r is the angle between a-phase axis and rotor axis.

The abc-phase currents are

$$\mathbf{i}_{abcs} = \begin{bmatrix} i_{as} & i_{bs} & i_{cs} \end{bmatrix}^T = \begin{bmatrix} i_{\text{out}} & -i_{\text{out}} & 0 \end{bmatrix}^T . \qquad (2.3)$$

Substituting $\mathbf{i}_{abcs}$ in (2.2) by (2.3) yields

$$v_{as} = [r_s + (\mathbf{L}_s(1,1) - \mathbf{L}_s(1,2))p]i_{\text{out}}$$

$$v_{bs} = [-r_s + (\mathbf{L}_s(2,1) - \mathbf{L}_s(2,2))p]i_{\text{out}} . \tag{2.4}$$

The machine's inductance matrix is symmetric, so $\mathbf{L}_s(1,2) = \mathbf{L}_s(2,1)$, and hence

$$v_{ab} = v_{as} - v_{bs}$$

$$= \{2r_s + [\mathbf{L}_s(1,1) + \mathbf{L}_s(2,2) - 2\mathbf{L}_s(1,2)]p\}i_{\text{out}}$$

$$= (2r_s + L_{eq}p)i_{\text{out}} , \tag{2.5}$$

where

$$L_{eq} = (L_q + L_d) + (L_q - L_d)\cos(2\theta_r + 60°) . \tag{2.6}$$

The torque of a PMSM can be expressed as [15]

$$T_e = \frac{3}{2}\frac{P}{2}\left[(L_{md} - L_{mq})i_{ds}^r i_{qs}^r + L_{md}I_m i_{qs}^r\right] , \tag{2.7}$$

where P denotes the number of poles, L_{mq} and L_{md} are the qd-axes magnetizing inductances, and I_m represents the magnetizing current of the permanent magnets. The currents i_{qs}^r and i_{ds}^r in (2.7) can be calculated by

$$\mathbf{i}_{qd0s}^r = \mathbf{K}_s^r\mathbf{i}_{abcs} . \tag{2.8}$$

Hence, (2.7) becomes after trigonometric manipulations

$$T_e = -\frac{\sqrt{3}}{2}P\left[(L_{md} - L_{mq})\frac{2}{\sqrt{3}}\cos(\theta_r - 60°)i_{\text{out}} + L_{md}I_m\right]\sin(\theta_r - 60°)\,i_{\text{out}} . \tag{2.9}$$

As the desired output current i_{out} is normally a sinusoidal function of time with constant frequency (e.g., 60 Hz), randomly choosing θ_r can cause a pulsating torque whose magnitude may be comparable to the motor's rated torque. This can be avoided by controlling θ_r equal to 60° or 240° in the proposed topology. At this position, $L_{eq} = 2L_d$, which is large enough to filter the high-frequency harmonic components of the output current, thus avoid the need for an additional filter. When K_1 is closed and K_2–K_2' is open, the rotor is controlled to rotate to the desired position (60° or 240°) and is then locked.

It should be noted that at this position the permanent magnets are aligned with the armature field, and could be demagnetized if the output current amplitude exceeds a certain value. This upper bound of the output current will depend on the permanent-magnet materials used.

2.3.2 Parallel HEVs

Charging/discharging the battery from/to the grid in parallel HEVs is similar to the series and series-parallel HEVs. However, when discharging the stored energy in fuel tank, the traction motor must be operated as a generator. The motor's torque (which is loading the ICE) needs to be controlled to operate the ICE at the desired (e.g., the most efficient) point. No additional power electronics devices within the HEV exist to construct the H-bridge inverter. Therefore, the method discussed in the previous section is not feasible in this case. A new topology to realize bidirectional power transfer for parallel HEVs is shown in Figure 2.3. The midpoint of the DC link (**g**) and the neutral point of the motor (**n**) are connected to the grid through a filter that improves the quality of the output current. The main idea is to realize both torque and output current control through the same converter by an appropriate control strategy.
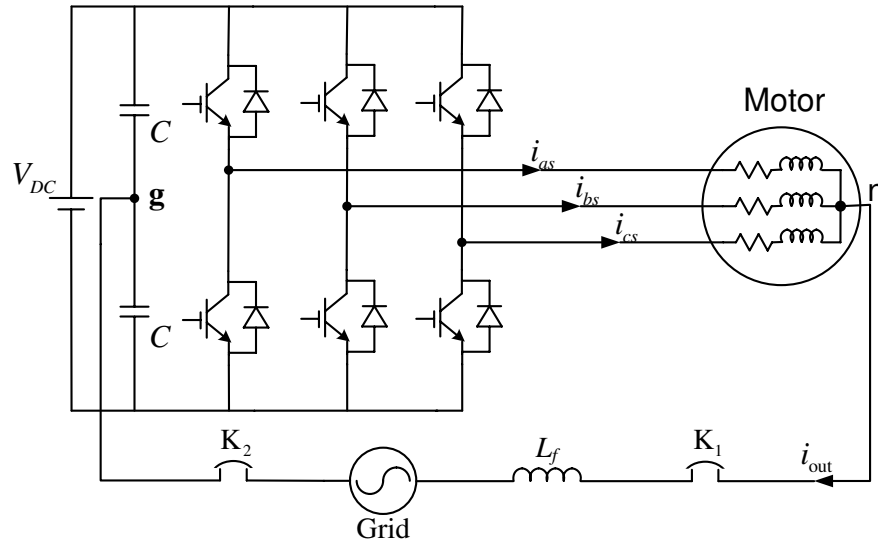
Figure 2.3   Topology for bidirectional power transfer in parallel HEVs.

The output current is given by

$$i_{\text{out}} = i_{as} + i_{bs} + i_{cs} \,, \tag{2.10}$$

and

$$\mathbf{i}_{abcs} = (\mathbf{K}_s^r)^{-1}\mathbf{i}_{qd0s}^r. \tag{2.11}$$

Based on (2.10) and (2.11), the output current is

$$i_{\text{out}} = 3i_{0s}^r, \tag{2.12}$$

which implies that the output current can be controlled via the 0-axis current. Typically, a motor is only intended to provide a desired amount of torque. Since i_{0s}^r does not contribute to electromagnetic torque, balanced three-phase currents are always used resulting in zero 0-axis current. In the proposed topology, however, i_{0s}^r is simultaneously controlled to follow the desired value that is dictated by the power output to the grid.

Torque control is realized by controlling the qd-axes currents. For a simplified controller, it is not uncommon to set the d-axis current command to zero and vary the q-axis current command linearly with the torque command. However, this setting is not optimal, and sometimes infeasible when discharging the energy stored in the fuel tank, as will be discussed later in subsection 2.4.2.

The abc-phase currents can be calculated by (2.11), for example,

$$i_{as} = i_{qs}^r \cos\theta_r + i_{ds}^r \sin\theta_r + i_{0s}^r. \tag{2.13}$$

In "steady state[1]," and ignoring the harmonic terms, (2.13) becomes

$$\begin{aligned} i_{as} &= I_{qs}^r \cos\theta_r + I_{ds}^r \sin\theta_r + \sqrt{2}I_{0s}\sin\theta \\ &= I_{qs}^r \cos(\omega_r t + \theta_{r0}) + I_{ds}^r \sin(\omega_r t + \theta_{r0}) + \sqrt{2}I_{0s}^r \sin(\omega t + \phi), \end{aligned} \tag{2.14}$$

where I_{qs}^r, I_{ds}^r are the qd-axes currents (constants), I_{0s}^r is the rms value of the 0-axis current, θ_{r0} is the rotor position at $t = 0$, ω is the radial frequency of the grid voltage and ϕ is the output current phase angle.

In general, ω_r can be different from ω. Therefore, assuming that the phase current limit for the motor windings is I_s (rms), the $qd0$-axes currents must satisfy

$$\frac{(I_{qs}^r)^2 + (I_{ds}^r)^2}{2} + (I_{0s}^r)^2 \le I_s^2. \tag{2.15}$$

---

[1] "Steady state" implies the case wherein PI controller outputs have become constant and are equal on average with the actual controlled quantities, e.g., currents and electromagnetic torque.

The stator phase voltage can be derived in a similar fashion, for example,

$$v_{as} = v_{qs}^r \cos\theta_r + v_{ds}^r \sin\theta_r + v_{0s}^r. \tag{2.16}$$

In the "steady state," and ignoring the harmonic terms, (2.1) can be reduced to

$$V_{qs}^r = r_s I_{qs}^r + \omega_r(L_d I_{ds}^r + L_{md}I_m)$$

$$V_{ds}^r = r_s I_{ds}^r - \omega_r L_q I_{qs}^r$$

$$v_{0s}^r = r_s i_{0s}^r + L_{ls}pi_{0s}^r, \tag{2.17}$$

where in the 0-axis voltage equation, lowercase variables are used to signify that these voltages and currents are not constants (they have a frequency of 60 Hz). Hence, (2.16) becomes

$$v_{as} = V_{qs}^r \cos\theta_r + V_{ds}^r \sin\theta_r + v_{0s}^r$$

$$= V_{qs}\cos(\omega_r t + \theta_{r0}) + V_{ds}\sin(\omega_r t + \theta_{r0}) + v_{0s}^r. \tag{2.18}$$

From Figure 2.3, taking **g** as the potential's reference point, we obtain

$$v_{ag} = v_{as} + v_{ng}$$

$$= v_{as} + v_{\text{grid}} + v_f, \tag{2.19}$$

where v_{grid} is the grid voltage, and v_f is the voltage across the inductive filter. Assuming that the DC link voltage is V_{DC}, the following inequality must hold for correct operation of the inverter,

$$|v_{ag}(t)| \leq \frac{V_{DC}}{2}. \tag{2.20}$$

Replacing v_{as} in (2.19) by (2.18) and ignoring the resistive voltage drops and v_{0s} (which is relatively small) yields the following sufficient condition for (2.20):

$$(L_q I_{qs}^r)^2 + (L_d I_{ds}^r + L_{md}I_m)^2 \leq \left(\frac{\frac{V_{DC}}{2} - |v_{\text{grid}} + v_f|}{\omega_r}\right)^2. \tag{2.21}$$

The motor's power is equal to $T_e \cdot \omega_{rm}$, where ω_{rm} is the mechanical rotor speed ($\omega_{rm} = 2\omega_r/P$). Thus, power can be increased by either T_e or ω_r under the condition that (2.15) and (2.21) are satisfied. In order to maximize the efficiency of the power conversion, the maximum-torque-per-stator-ampere (MTPA) control strategy is used herein [16, 17]. For a given torque

and output current command, the *qd*-axes current commands are determined by (2.7), while the 0-axis current is determined by (2.12). The *abc* current commands are computed by (2.11). Hysteresis modulation is used to control the *abc*-phase currents.

2.4   Simulation Results

Simulation results of bidirectional power transfer application for series, parallel and series-parallel HEVs were obtained using Matlab/Simulink. The parameters of the PMSM in this study are given in Table 2.1. The DC link voltage is assumed to be 400 V and the stator current limit is assumed to be 40 A. Considering a typical US household electrical installation, the power transfer limit is assumed to be 1.65 kW (110 V/15 A).

Table 2.1   Electrical parameters of a 20kVA PMSM

param.	value	param.	value
r_s	0.0437 Ω	L_{ls}	0.8865 mH
L_{mq}	6.95 mH	L_{md}	3.25 mH
P	8	I_m	100 A

2.4.1   Series and Series-Parallel HEVs

In the topology for series and series-parallel HEVs, the output current and its command (15 A rms in this study) are shown separately in Figure 2.4 and together in detail in Figure 2.5. Clearly, i_{out} closely followed the command i_{out}^*. Arbitrary active and reactive power output can be achieved by adjusting the 0-axis current command's magnitude and phase with respect to grid voltage.

The electromagnetic torque of the motor under 15 A output current for various rotor angles is shown in Figure 2.6. Randomly choosing θ_r may result in large torque pulsations; e.g., $\theta_r = 0°$, which results in a pulsating torque with a magnitude of 100 N·m. To avoid this, one can choose $\theta_r = 60°$ or $\theta_r = 240°$ as discussed in subsection 2.3.1. Equation (2.9) predicts the existence of three components (namely, dc, 60 Hz, and 120 Hz) in the pulsating torque, whereas

it seems that only the 60 Hz component is created. In this specific case, this is due to the fact that $(L_{md} - L_{mq})i_{\text{out}} \ll L_{md}I_m$.
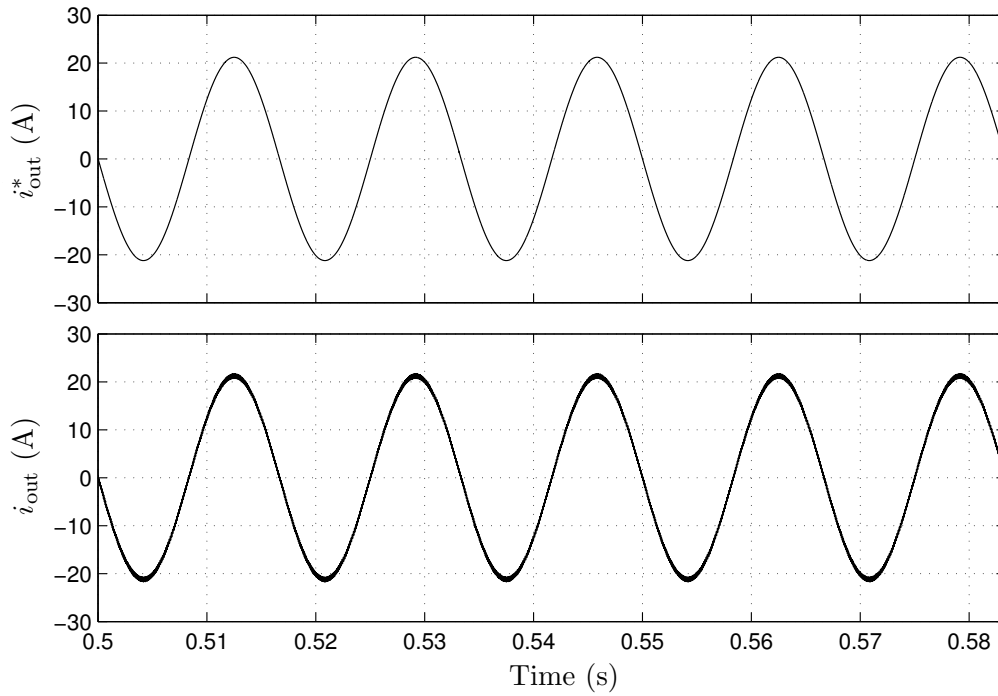
Figure 2.4   Output current for series and series-parallel HEVs.
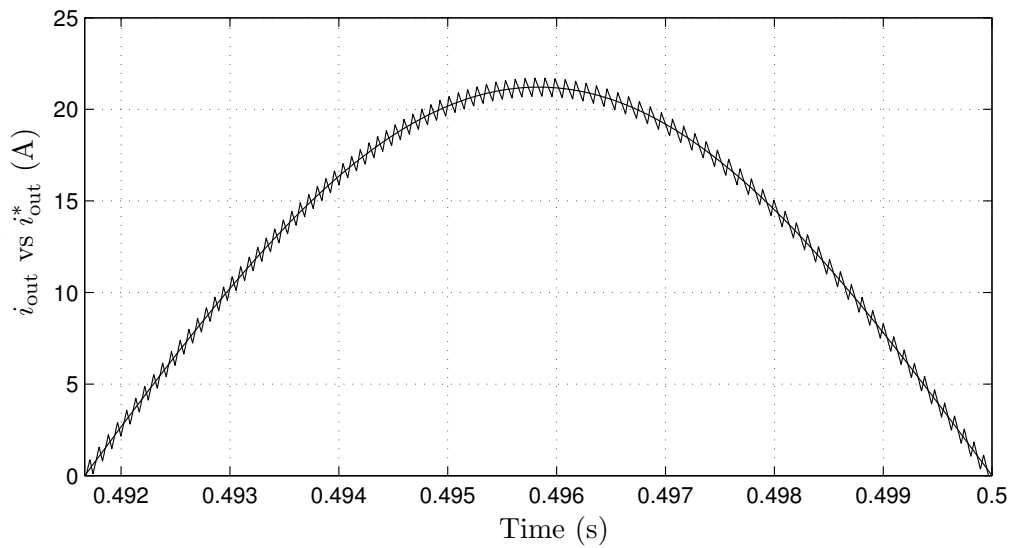
Figure 2.5   Output current in detail for series and series-parallel HEVs.
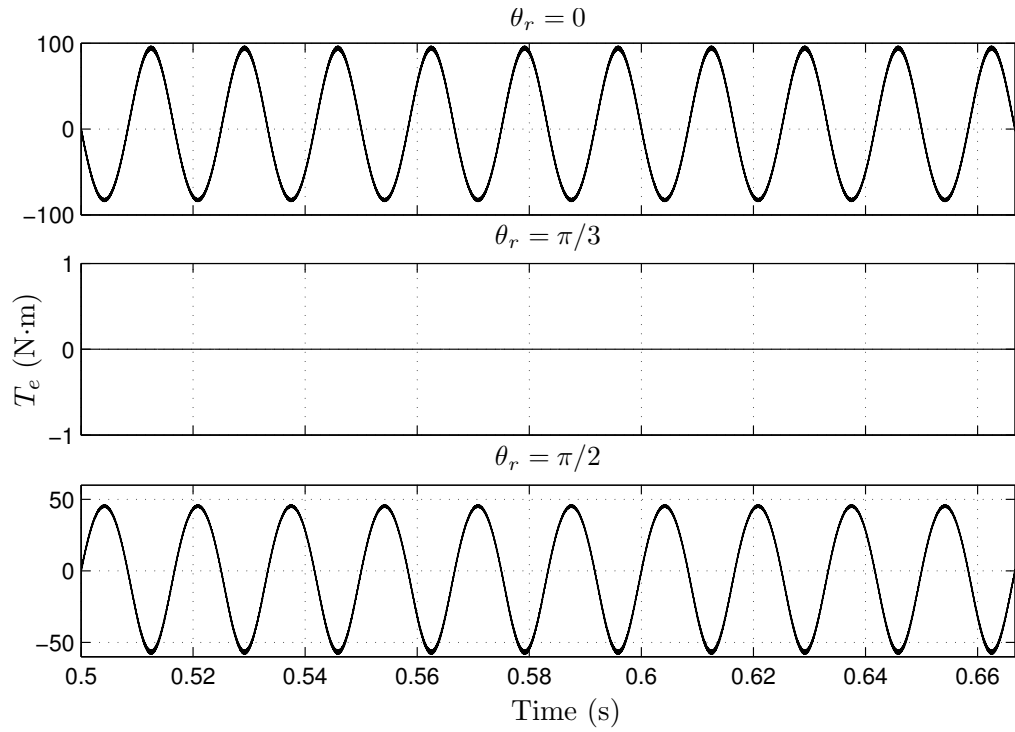
Figure 2.6   Pulsating torque at different θ_r for series and series-parallel HEVs.
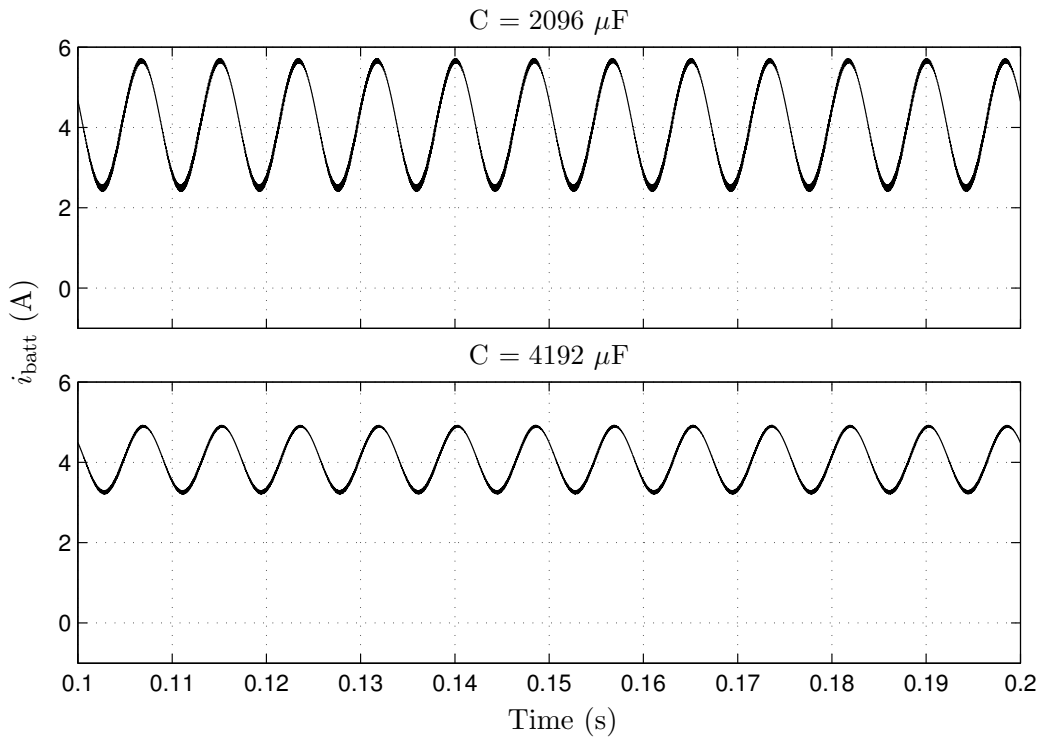
Figure 2.7   Battery charging current for series and series-parallel HEVs.

An example of the battery's charging current in G2V operation is shown in Figure 2.7, where it is assumed that the battery's internal resistance is 2 Ω and the dc-link capacitance is 2096 and 4192 μF. As can be seen, the ripple of the charging current waveform is reduced with more capacitance.

2.4.2 Parallel HEVs

In the topology for parallel HEVs, the output current waveform is similar to the previous case and is not repeated. The stator currents of the motor are shown in Figure 2.8. These currents have two components—the qd-axes currents for torque control and the 0-axis current. The frequencies and magnitudes of these two components can be different. The frequency of the qd-axes currents is determined by the rotor speed and the frequency of the 0-axis current is the grid frequency. In this study, these two components are (33 Hz, 34.4 A) and (60 Hz, 5 A), respectively.
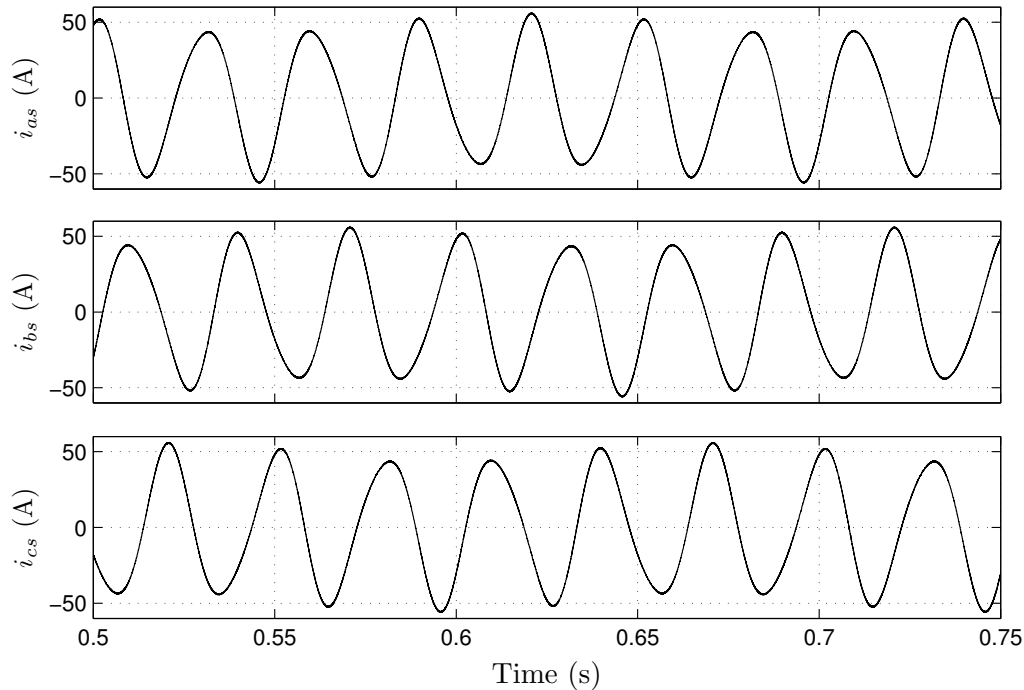
Figure 2.8   Stator phase currents for parallel HEVs.

Herein, the MTPA control strategy is used to obtain the qd-axes current commands. The

following example is a case where the MTPA control outperforms the control where torque is generated from the q-axis current only (i.e., $i_{ds}^r = 0$). When the motor is commanded to generate 1.65 kW at $\omega_r = 2\pi(33)$ rad/s, $T_e = 31.8$ N·m, keeping $i_{ds}^r = 0$, the voltage limit (2.21) is violated[2], resulting in output current distortion, as shown in Figure 2.9. The motor's electromagnetic torque is also distorted, compared with the torque under MTPA control strategy in Figure 2.10.
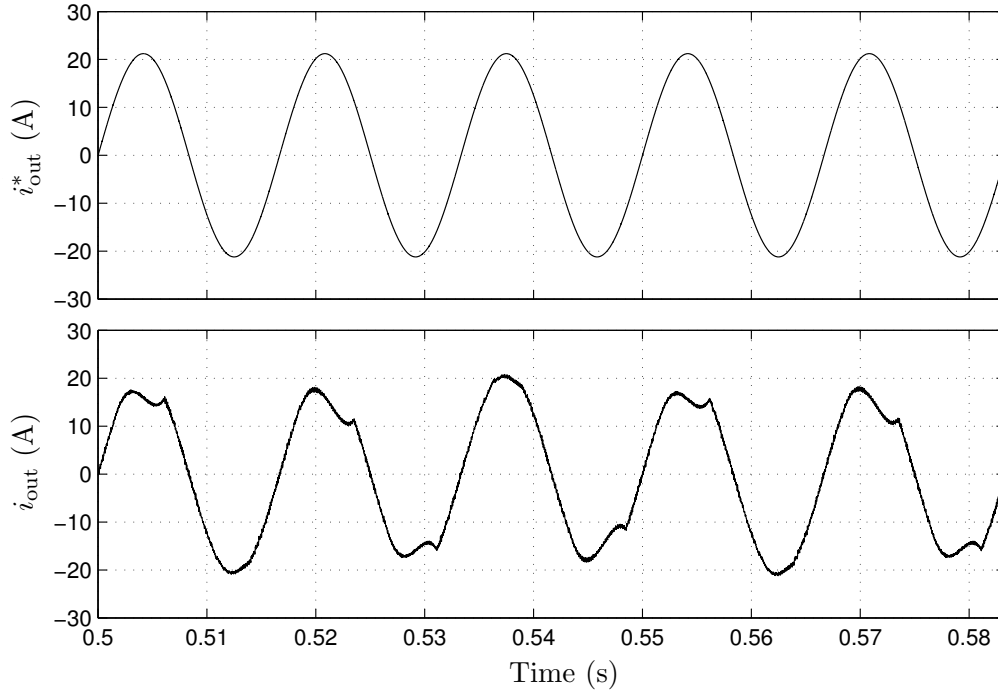
Figure 2.9   Distortion of output current due to voltage limit violation when torque is generated by q-axis current component only ($i_{ds}^r = 0$) for parallel HEVs.

The maximum theoretical power that the motor can provide and the corresponding torque as a function of ω_r are shown in Figure 2.11. This result was obtained by using (2.21). As can be seen, under the MTPA control strategy the motor can be operated within a much wider range. It is interesting to note that the motor can generate up to 3.5 kW, which could be used to provide 1.65 kW to grid and simultaneously charge the battery.

---

[2]Under this case, the DC link voltage at least needs to be 478 V to satisfy the voltage limit. V_{DC} is only 400 V in this example.
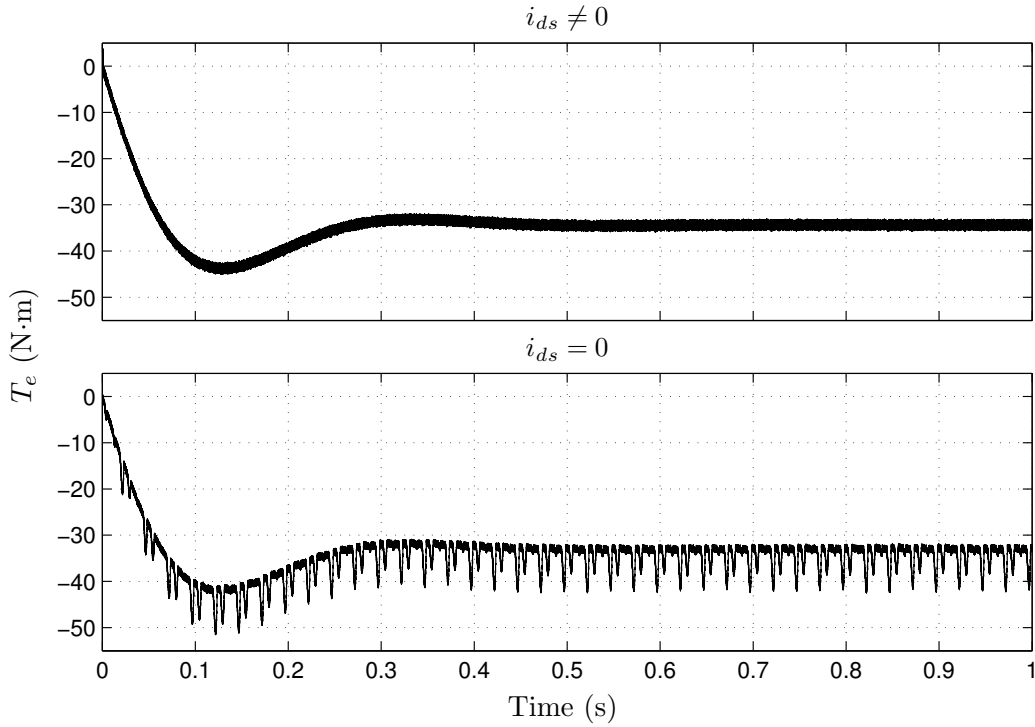
Figure 2.10   Electromagnetic torque for MTPA and $i_{ds}^r = 0$ control strategies for Parallel HEVs.
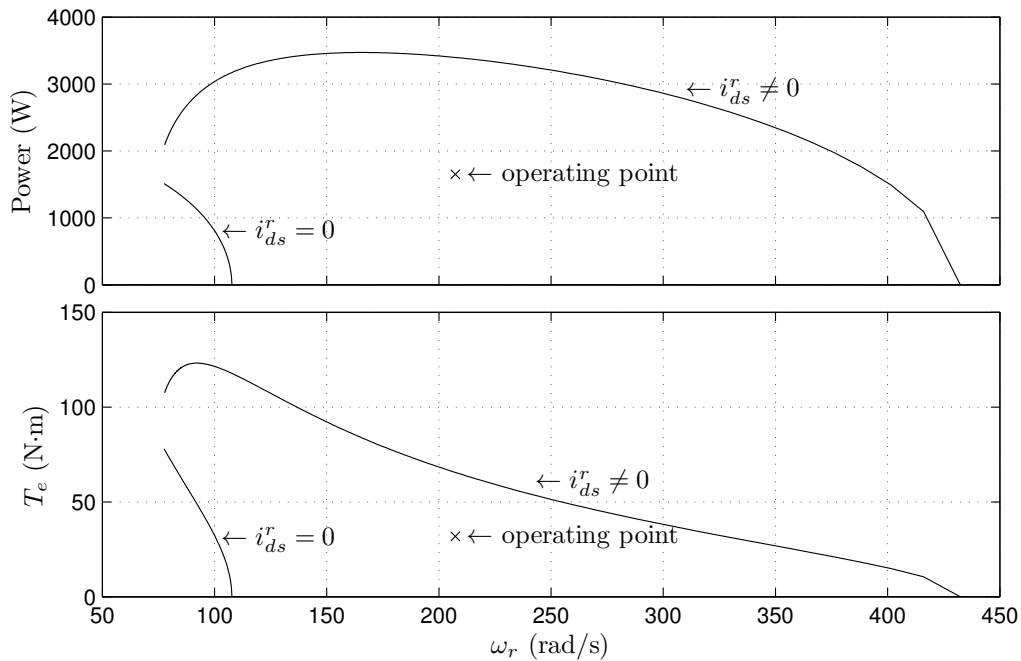
Figure 2.11   Maximum power transfer under different control strategies for parallel HEVs.

2.5   Conclusion

With a suitable control strategy, bidirectional power transfer for HEVs can be achieved by utilizing the vehicle's drivetrain, without additional external hardware (other than an inductive choke, if required). Theoretical analysis and simulation results demonstrate the feasibility of the proposed strategies for series, parallel and series-parallel HEVs.

3. ELECTRIC ENERGY AND POWER CONSUMPTION BY LIGHT-DUTY PLUG-IN ELECTRIC VEHICLES

Di Wu, Dionysios C. Aliprantis, and Konstantina Gkritza

Abstract

This paper proposes methodologies to estimate the electric energy and power consumption by light-duty plug-in electric vehicles (PEVs). Using the travel patterns of light-duty vehicles in the U.S. obtained from the 2009 National Household Travel Survey, the PEVs' energy and power consumption are estimated for two uncontrolled charging scenarios.

Index Terms

Land vehicles, load forecasting, probability, road vehicle electric propulsion, stochastic approximation.

Nomenclature

a	all-electric range
c_{fr}	fraction of daily vehicle miles traveled (VMT) in all-electric mode
d	charge-depleting range
$E(\mathbf{x})$	expected value of random variable (RV) $\mathbf{x}$
f_x	probability density function of RV $\mathbf{x}$

F_x cumulative distribution function of RV $\mathbf{x}$

h_{e} portion of h_{tr} from the electrical traction subsystem

h_{tr} tractive energy per mile at the wheels

m daily VMT

m_{a} daily VMT in all-electric mode

m_{cd} daily VMT in charge-depleting mode

$M_N(t)$ sample mean of power consumption at time t over a sample size N

W_n daily energy consumption of a fleet of n PEVs

$\mathbf{x}$ random variable

$\mathbf{x}(t)$ stochastic process

$\hat{x}$ estimate of a random variable's expected value

$Y_n(t)$ power consumption at time t of a fleet of n PEVs

$\delta(x)$ Dirac delta function

ϵ daily electric energy consumption of a PEV

η wall-to-wheels efficiency

ξ fraction of tractive energy derived from electricity

$\sigma(\mathbf{x})$ standard deviation of RV $\mathbf{x}$

3.1   Introduction

Plug-in electric vehicles (PEVs) have been identified as a vital technology to reduce carbon emissions and dependence on petroleum [1]. An expectation has been set for one million PEVs on U.S. roads alone by 2015. PEVs—either plug-in hybrid electric vehicles (PHEVs) or pure electric vehicles (EVs)—adopt similar drivetrain configurations as hybrid electric vehicles (HEVs) [18], but are characterized by larger battery capacity and the capability of being recharged from the electric grid. Therefore, a portion of the energy obtained from gasoline can be replaced by electricity from the power system.

The emerging fleet of PEVs will introduce a considerable amount of additional load on the power system. Several studies have been devoted to this topic during the last few years, at both national and regional scales [19–26]. In most of these, all PEVs in a fleet are assigned

the same all-electric range (AER)[1] and the corresponding amount of usable energy in their batteries. The daily electric energy consumption is then estimated assuming that the charging frequency is once per day. Power consumption is typically estimated based on the results of the energy calculations.

Previous work has adopted assumptions that lead to inaccurate results. First, some PEVs will be incapable of being always driven in all-electric mode, but rather they will be operated in blended mode, requiring occasional support from their internal combustion engine [28]. Second, the electric energy consumption is often estimated without considering vehicle travel patterns. For example, in [21–23] and [26], all vehicles leave home with fully charged batteries and return home with the entire usable energy exhausted. However, some PEVs may not travel at all on a day, or will travel less than their electric range, thus consuming only a fraction of their battery energy. Therefore, this leads to an overestimation of electric energy consumption. Third, when estimating power consumption, some studies use models that represent situations unlikely to occur. In [19], off-peak electricity is consumed by the entire PEV fleet, whereas in reality some vehicles may be traveling, and some will be unable to receive any more energy from the grid because their batteries will be fully charged. In [22], all PEVs begin charging simultaneously at 5 p.m. or 10 p.m. In the uncontrolled charging scenarios of [23], all PEVs leave home evenly between 8 a.m. and 9 a.m., and return home between 6 p.m. and 9 p.m. Obviously, these simplifying assumptions do not account for real-world travel patterns, so the validity of the results obtained is questionable.

Herein, a more accurate methodology to estimate the electric energy and power consumption of light-duty PEVs is set forth. The analysis is based on the actual U.S. travel patterns, as captured by the 2009 National Household Travel Survey (NHTS). The formulation is probabilistic and makes use of the NHTS statistical data to represent the travel patterns of the U.S. light-duty vehicle (LDV) fleet.[2] LDV travel accounts for 92% of the highway vehicle miles traveled (VMT) [30], 76% of the energy consumed by highway travel modes [31], and 74% of

---

[1]AER is defined as the distance from the beginning of a driving cycle with initially fully charged battery to the exact point at which the internal combustion engine turns on [27].

[2]The U.S. fleet of light-duty vehicles consists of cars and light trucks, including minivans, sport utility vehicles (SUVs) and trucks with gross vehicle weight less than 8,500 pounds [29].

the carbon dioxide emissions from on-road sources [32].

The remainder of this paper is structured as follows: Section 3.2 discusses travel patterns and the NHTS database. Section 3.3 describes the basics of PEV operation. In Section 3.4, an analytical methodology to estimate PEV electric energy consumption is presented. Section 3.5 illustrates a simulation-based methodology for calculating PEV power and energy consumption. In Section 3.6, some concluding remarks are offered.

3.2   Travel Patterns

A fundamental underlying assumption of this analysis is that the driving behavior of PEV owners will be similar to the behavior of drivers of conventional nonelectric vehicles. In other words, it is assumed that PEVs will not affect daily travel patterns and lifestyles in any significant fashion: people will have the same travel demands as before, and will use their vehicles (either PEVs or not) to run the same everyday errands. It could be argued that this assumption is not entirely correct, because PEV owners may drive differently than the average driver. This change could be attributed to either a PEV (being a different type of vehicle) impacting the travel patterns, or to specific attributes of PEV owners, such as increased environmental awareness or income level [33]. At least initially, when PEVs enter the market, this argument could be valid. However, as the penetration of PEVs increases, then the PEV driver will "converge" to the average driver.

The 2009 NHTS collects information on the travel behavior of a national representative sample of U.S. households, such as mode of transportation, trip origin and purpose, and trip distance. The database files can be found online at [34]. For this analysis, information contained in the "travel day trip" database file (DAYPUBLL) and the "vehicle" database file (VEHPUBLL) is needed. The survey consists of 150,147 households and 294,408 LDVs. Table 3.1 shows the distribution of the LDV fleet by vehicle class, in urban or rural areas in the U.S.

It was observed that vehicle travel patterns vary by household area (urban or rural) and day of the week (weekday or weekend). Therefore, the vehicle travel pattern is examined separately for the following four cases: (i) trip in an urban area on a weekday ('urban weekday'), (ii) trip

Table 3.1   Distribution of LDV Fleet by Vehicle Class and Area Type

	Car	Van	SUV	Pickup truck
Urban	56.9%	9.2%	19.6%	14.3%
Rural	42.9%	8.0%	19.1%	30.0%
All	53.0%	8.9%	19.4%	18.7%

in an urban area during the weekend ('urban weekend'), (iii) trip in a rural area on a weekday ('rural weekday'), and (iv) trip in a rural area during the weekend ('rural weekend'). These four area/day cases are represented by 141,011; 56,677; 68,979; and 27,741 LDVs, respectively. Because the NHTS data set contains trips spread throughout a year, and because herein these trips are not further distinguished with respect to the date they occurred on, the results obtained should be interpreted as statistics of energy and power consumption for an arbitrary urban/rural weekday/weekend of the year.

It should be noted that not all LDVs travel on a given day. The probability that a random LDV (in an urban or a rural area) travels (on a random weekday or weekend) can be estimated by using the information included in the DAYPUBLL and VEHPUBLL files. The derived vehicle travel probabilities are in the range 45–65%. Previous reports have not taken this fact explicitly into account, and have assumed that all PEVs travel every day, resulting in an overestimation of the energy and power consumption [20].

The parking start/end times and location (e.g., home, work, shopping mall, etc.) for every vehicle throughout the day can be extracted from the vehicle database. This kind of information is required for the determination of the charging profile. The probability of a vehicle to be parked anywhere (including at home) or be parked at home is shown in Figure 3.1. These plots provide valuable insights to comprehend the outcome of the power consumption estimation, which will be carried out in Section 3.5.

3.3   Basics of PEV Operation

There is still uncertainty regarding the size and configuration of future PEVs. The market will contain an array of models with different drivetrain topologies and electric ranges. Some
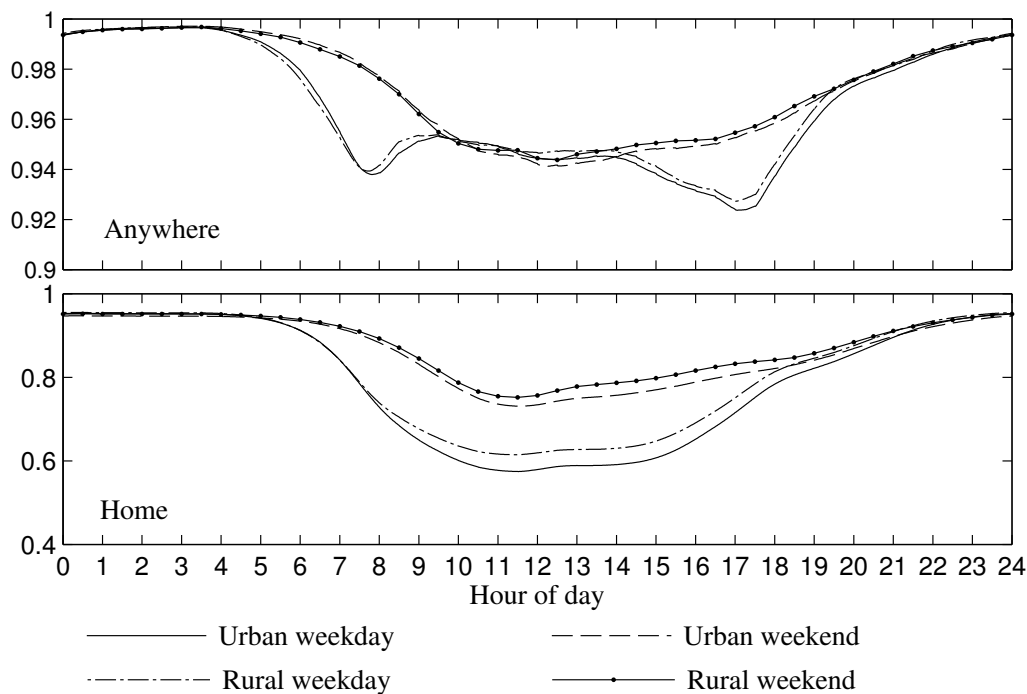
Figure 3.1   Probability of a random LDV to be parked. [Top: parked anywhere (including at home). Bottom: parked at home.]

PEVs may be pure EVs, without an internal combustion engine. Others may be designed to operate initially in EV mode, and then switch to a charge-sustaining mode (e.g., series PHEVs). However, a clearly defined switch from one mode of operation to the other is not the only possible operation strategy. PEVs can be also operated in blended mode, where the internal combustion engine occasionally assists the electric motor in supplying the tractive energy (e.g., a parallel PHEV with a relatively weak electric traction motor).

Therefore, the operation of PEVs can be classified into the charge-depleting (CD) mode and the charge-sustaining (CS) mode [27]. In CD mode, the vehicle is gradually depleting the energy stored in the batteries, with either a fraction of or the entire tractive energy coming from the battery pack. The total distance that a PEV can travel in CD mode with its batteries initially fully charged is defined as its "charge-depleting range" (CDR). After all the usable battery energy is exhausted, the operation of the PEV enters CS mode, where it is operated similarly to a conventional HEV, with all tractive energy derived from the fuel. Several of the previous studies treat CD operation the same as all-electric (i.e., EV) operation. In those, the

designation "PHEV-x" simply represents a PHEV that, starting with a fully charged battery, can travel x miles in EV mode without consuming any fuel in the tank. In order to encompass all possible operating strategies, this analysis is performed based on the more comprehensive concepts of CD operation and CDR.

To represent the uncertainty regarding future PEVs, a probabilistic formulation is provided, with all parameters expressed as random variables (RVs). Herein, RVs are denoted by boldface symbols; for instance, the daily VMT ($\mathbf{m}$) or the tractive energy per mile at the wheels ($\mathbf{h}_{tr}$) of a random PEV.

The tractive energy per mile that is provided by the battery in CD mode (h_e) is a fraction (ξ) of the total tractive energy per mile (h_{tr}) required to overcome aerodynamic drag, rolling resistance, and vehicle inertia [25, 27]: $h_e = \xi h_{tr}$. The tractive energy depends on several parameters, such as vehicle weight, aerodynamic drag coefficient, personal driving habits, geographic location, driving cycle, weather conditions, road conditions, and others. In this study, $\mathbf{h}_{tr}$ is assumed to have a normal distribution with mean value determined by the vehicle class—0.21 kWh/mile for cars, 0.33 kWh/mile for vans, 0.37 kWh/mile for SUVs, and 0.40 kWh/mile for pickup trucks[3]—and standard deviation equal to 10% of the mean.

In order to capture the entire spectrum of possible PEV operation—from "light" parallel to pure EV, it is assumed that $\boldsymbol{\xi}$ is an RV with the following PDF:

$$f_\xi(x) = \begin{cases} 1 & \text{for } 0.2 \leq x < 1 \,, \\ 0.2\delta(x - 1) & \text{for } x = 1 \,. \end{cases} \tag{3.1}$$

In other words, it is assumed that 20% of PEVs will be operated as pure EVs in CD mode. Furthermore, it is assumed that $\boldsymbol{\xi}$ is independent of $\mathbf{h}_{tr}$, leading to

$$E(\mathbf{h}_e) = E(\boldsymbol{\xi})E(\mathbf{h}_{tr}) \,. \tag{3.2}$$

This is a safe assumption to make as long as future PEV drivetrain topologies will be independent of vehicle class. However, if, for instance, smaller vehicles will tend to be correlated with higher ξ, while larger vehicles with smaller ξ, this assumption will have to be revisited. Nevertheless, the above assumptions are warranted by lack of better information presently.

---

[3]These numerical values were derived using information found in [25, 35, 36].

3.4   Electric Energy Consumption

This section presents an analytical methodology to estimate the energy consumption of PEVs, under the assumption that charging occurs once per day (after all trips are completed). A methodology to estimate the energy when multiple daily charges in-between trips are possible is presented in Section 3.5.

For a random PEV in an urban (or rural) area, on a random weekday (or weekend), the daily electric energy consumption (ϵ) depends on the product of two RVs, namely $\mathbf{h}_e$ and $\mathbf{m}_{cd}$ (daily VMT in CD mode):

$$\epsilon = \frac{1}{\eta}\mathbf{h}_e\mathbf{m}_{cd}\,, \tag{3.3}$$

where $\eta = 67.2\%$ accounts for the overall wall-to-wheels efficiency, and is assumed to be constant.[4] The VMT in CD mode depend on both the travel patterns and the CDR. When assuming that the charging frequency is once per day and that the PEV starts with a fully charged battery, m_{cd} can be expressed as a function of VMT (m) and CDR (d):

$$m_{cd} = \begin{cases} m & \text{for } m \le d\,, \\ d & \text{for } m > d\,. \end{cases} \tag{3.4}$$

If $\mathbf{h}_e$ is assumed to be independent of $\mathbf{m}$ and $\mathbf{d}$, then $\mathbf{h}_e$ is independent of $\mathbf{m}_{cd}$. Again, this simplifying assumption—namely, that drivetrain topology, vehicle class, VMT, and CDR are all mutually independent—is required to proceed with the analysis due to insufficient data (but it is recognized that it might not portray reality accurately). Under these assumptions, the expected value of ϵ is

$$E(\epsilon) = \frac{1}{\eta}E(\mathbf{h}_e)E(\mathbf{m}_{cd})\,. \tag{3.5}$$

---

[4]It is assumed that the efficiencies of charger, battery (roundtrip), on-board power electronics, traction motor, and mechanical transmission plus accessory loads (e.g., air-conditioning, on-board electronics) are: 95% [25], 92% [37], 95% [25, 38], 92% [38], and 88% [39], respectively; this results in an overall efficiency from the wall outlet to the wheels of 67.2%. In particular, the selected value for efficiency of mechanical transmission and accessory loads (88%) represents the overall efficiency of a fleet of PEVs that consists of: hybrid electric vehicles with gearbox and mechanical driveline, and pure EVs or series PEVs that drive the wheels and power the accessory loads directly.

3.4.1 Previous work

In previous studies, it is often assumed that PEVs are operated as pure EVs within their CD range ($\xi = 1$). As a result, the CDR (d) obtains the meaning of an AER (a), and $\mathbf{h}_\text{e}$ becomes synonymous to $\mathbf{h}_\text{tr}$. In this case, (3.5) becomes

$$E(\boldsymbol{\epsilon}) = \frac{1}{\eta} E(\mathbf{h}_\text{tr}) \, E(\mathbf{m}_\text{a}) \,, \tag{3.6}$$

where $\mathbf{m}_\text{a}$ is the daily VMT in all-electric mode, as expressed in (3.4) with d replaced by a. In [21–23] and [26], it is assumed further that $m_\text{a} = a$. In other words, it is assumed that all PEVs are operated as pure EVs until they completely deplete their batteries by being driven at least as far as their all-electric range on a daily basis. Hence, (3.6) becomes

$$E(\boldsymbol{\epsilon}) = \frac{1}{\eta} E(\mathbf{h}_\text{tr}) \, a \,. \tag{3.7}$$

This estimation is simple and facilitates calculations, but it is inaccurate because the effect of travel patterns on the energy consumption is ignored. The estimated energy consumption becomes equal to the entire usable energy, irrespective of how a PEV travels.

In fact, the expected value of daily VMT powered from electricity is only a fraction of the expected daily VMT. In order to include effects of travel patterns on the electric energy consumption, [35] defined a 'battery usage factor' as a function of AER based on the 1995 Nationwide Personal Travel Survey data.[5] This can be expressed as

$$c_\text{fr}(a) = \frac{E(\mathbf{m}_\text{a})}{E(\mathbf{m})} = \frac{\int_0^a x f_m(x) \, dx + a \int_a^\infty f_m(x) \, dx}{\int_0^\infty x f_m(x) \, dx} \,. \tag{3.8}$$

Replacing $E(\mathbf{m}_\text{a})$ by $c_\text{fr}(a)E(\mathbf{m})$ in (3.6) yields

$$E(\boldsymbol{\epsilon}) = \frac{1}{\eta} E(\mathbf{h}_\text{tr}) \, c_\text{fr}(a) E(\mathbf{m}) \,. \tag{3.9}$$

Such an estimation was performed in [19, 20].

Although (3.9) is more accurate than (3.6) and (3.7), blended mode operation ($\xi < 1$) is still not considered. Moreover, rather than being assigned a unique value a, the CDR (instead of the AER) should be represented by a random variable. In order to take these facts into account, an improved estimation method is proposed in the next subsection.

---

[5]In [40], a 'utility factor' is similarly defined, except that the concept of CDR is used rather than AER. This factor represents the fraction of daily VMT in CD mode.

3.4.2 Proposed method

Substituting (3.2) into (3.5) yields the more general formula:

$$E(\boldsymbol{\epsilon}) = \frac{1}{\eta} E(\boldsymbol{\xi}) E(\mathbf{h}_{\mathrm{tr}}) E(\mathbf{m}_{\mathrm{cd}}) . \tag{3.10}$$

One can proceed with calculations of the three expected values in the right-hand side of (3.10) as follows:

1. The first term, $E(\boldsymbol{\xi})$, is the mean value of the distribution of the PEV drivetrain electrification parameter (see Section 3.3), which is equal to 0.68 for the proposed PDF (3.1).

2. The second term is $E(\mathbf{h}_{\mathrm{tr}}) = \sum_{k=1}^{4} r_k E(\mathbf{h}_{\mathrm{tr},k})$, where r_k are the ratios of different vehicle classes (Table 3.1), and $E(\mathbf{h}_{\mathrm{tr},k})$ are given in Section 3.3. The results are provided in Table 3.2.

3. The calculation of the third term, $E(\mathbf{m}_{\mathrm{cd}})$, requires knowledge of the PDF of $\mathbf{m}_{\mathrm{cd}}$ ($f_{m_{\mathrm{cd}}}$). Given that $\mathbf{m}$ and $\mathbf{d}$ are assumed independent, the corresponding CDF can be expressed in terms of probabilities as

$$\begin{aligned} F_{m_{\mathrm{cd}}}(x) &= P[\mathbf{m}_{\mathrm{cd}} \leq x] \\ &= P[\mathbf{d} \leq x] + P[\mathbf{m} \leq x, \mathbf{d} > x] \\ &= P[\mathbf{d} \leq x] + (P[\mathbf{m} \leq x] - P[\mathbf{m} \leq x, \mathbf{d} \leq x]) . \end{aligned} \tag{3.11}$$

Differentiating (3.11) yields, after manipulations,

$$f_{m_{\mathrm{cd}}}(x) = f_m(x) \int_x^\infty f_d(v)\, dv + f_d(x) \int_x^\infty f_m(u)\, du . \tag{3.12}$$

The above equation highlights the interplay between travel patterns and technological advances when determining $E(\mathbf{m}_{\mathrm{cd}})$. The PDF f_m can be readily extracted from the 2009 NHTS data. For f_d, two distinct cases are considered, namely two log-normal distributed RVs, $f_{d,1}$ and $f_{d,2}$, with $(E(\mathbf{d}),\ \sigma(\mathbf{d}))$ equal to $(40, 10)$ and $(70, 20)$, respectively.[6] These two hypothetical cases are devised to highlight the effect on energy consumption of possible future technological improvements (which could enable longer CDRs).

---

[6]The log-normal PDF has the convenient property of $(0, +\infty)$ support. The parameters (40,10) and (70,20) represent the expected value and standard deviation of the lognormal distribution (i.e., they do not represent the parameters of the RV's natural logarithm).

The electric energy consumption estimation results are provided in Table 3.2. The following observations confirm a priori expectations: (i) vehicles in rural areas consume more energy than vehicles in urban areas; (ii) during the weekends, the energy consumption is smaller.

Table 3.2   Daily Energy Consumption Estimation Results (per PEV)

	$E(\mathbf{h}_{\mathrm{tr}})$	$E(\mathbf{m}_{\mathrm{cd}})$ miles		$E(\boldsymbol{\epsilon})$ kWh		$\sigma(\boldsymbol{\epsilon})$ kWh	
	kWh/mile	$f_{d,1}$	$f_{d,2}$	$f_{d,1}$	$f_{d,2}$	$f_{d,1}$	$f_{d,2}$
Urban weekday	0.28	14.70	17.89	4.16	5.06	5.36	7.31
Urban weekend	0.28	11.41	14.10	3.23	3.99	4.98	6.92
Rural weekday	0.31	15.70	20.24	4.88	6.29	6.43	9.10
Rural weekend	0.31	11.92	15.29	3.70	4.75	5.87	8.28

The formulation using RVs also allows calculation of the standard deviation of the daily energy consumption. This is found by

$$
\begin{aligned}
\sigma(\boldsymbol{\epsilon}) &= \sqrt{E(\boldsymbol{\epsilon}^2) - E^2(\boldsymbol{\epsilon})} \\
&= \sqrt{E(\boldsymbol{\xi}^2)E(\mathbf{h}_{\mathrm{tr}}^2)E(\mathbf{m}_{\mathrm{cd}}^2)/\eta^2 - E^2(\boldsymbol{\epsilon})}\,,
\end{aligned}
\tag{3.13}
$$

where RV independence has been assumed. Moreover, $E(\boldsymbol{\xi}^2) = \int_0^1 x^2 f_\xi(x)\,dx$, $E(\mathbf{m}_{\mathrm{cd}}^2) = \int_0^\infty x^2 f_{m_{\mathrm{cd}}}(x)\,dx$, and $E(\mathbf{h}_{\mathrm{tr}}^2) = \sum_{k=1}^4 r_k E(\mathbf{h}_{\mathrm{tr},k}^2) = \sum_{k=1}^4 r_k[E^2(\mathbf{h}_{\mathrm{tr},k}) + \sigma^2(\mathbf{h}_{\mathrm{tr},k})]$. These calculations are straightforward to perform once the PDFs have been defined.

The results are provided in Table 3.2. The standard deviations are large compared to the expected values. Hence, the daily electric energy consumption of an individual PEV cannot be precisely predicted. However, the results can be utilized to estimate the overall energy consumption of a PEV fleet. Assuming there are n PEVs, the total daily energy consumption, $\mathbf{W}_n = \sum_{i=1}^n \boldsymbol{\epsilon}_i$, is also a random variable. If the $\boldsymbol{\epsilon}_i$'s are assumed independent, then the covariance of any two $\boldsymbol{\epsilon}_i$ and $\boldsymbol{\epsilon}_j$ is zero.[7] Hence, for identically independently distributed $\boldsymbol{\epsilon}_i$'s, $E(\mathbf{W}_n) = nE(\boldsymbol{\epsilon})$, $\sigma(\mathbf{W}_n) = \sqrt{n}\,\sigma(\boldsymbol{\epsilon})$, and the coefficient of variation $\sigma(\mathbf{W}_n)/E(\mathbf{W}_n)$ is proportional to $1/\sqrt{n}$. For a fleet size of one million "urban-weekday" PEVs with $E(\mathbf{d}) = 40$ miles, the energy consumption has $E(\mathbf{W}_n) = 4{,}160$ MWh and $\sigma(\mathbf{W}_n) = 5.36$ MWh. In addition,

---

[7]In reality, the covariance will not be zero because of external factors, such as the weather or gasoline prices, which can affect travel demand. However, this is not taken into account in this study.

according to the central limit theorem, $\mathbf{W}_n$ will have an approximately normal distribution with the above parameters. Note that the estimated electric energy consumption is at the outlet, excluding transmission and distribution losses.

3.4.3 Sensitivity analysis

Equation (3.10) can be used to gauge the estimation error due to uncertainty in knowing the true values of the parameters' expected values; namely, the drivetrain electrification coefficient, the tractive energy, and—indirectly via the VMT in CD mode—the charge-depleting range. As a matter of fact, any RV distribution that can be devised about PEVs at this point in time represents only a "best guess." (Similarly, the assumed value of η might be incorrect.) Hence, the true mean values can be related to their estimates as $E(\mathbf{x}) = \hat{x} + \Delta x$. (Also, formally, $\eta = \hat{\eta} + \Delta\eta$.) Using a Taylor series expansion of (3.10), the following first-order approximation of the relationship between relative estimation errors can be obtained:

$$\frac{\Delta\epsilon}{\hat{\epsilon}} \approx \frac{\Delta\xi}{\hat{\xi}} + \frac{\Delta h_{\mathrm{tr}}}{\hat{h}_{\mathrm{tr}}} + \frac{\Delta m_{\mathrm{cd}}}{\hat{m}_{\mathrm{cd}}} - \frac{\Delta\eta}{\hat{\eta}}\,, \tag{3.14}$$

where $\hat{\epsilon} = \hat{\xi}\hat{h}_{\mathrm{tr}}\hat{m}_{\mathrm{cd}}/\hat{\eta}$.

Also, instead of considering only two distinct cases for f_d, namely, $f_{d,1}$ and $f_{d,2}$, it is possible to compute the variation of $E(\mathbf{m}_{\mathrm{cd}})$ as a function of $E(\mathbf{d})$ and $\sigma(\mathbf{d})$. This is depicted in Figure 3.2. It can be observed that the miles driven in CD mode (hence, the absorbed electrical energy) will generally increase with $E(\mathbf{d})$, whereas $\sigma(\mathbf{d})$ has a secondary effect on the result.[8] It is also interesting to note that the energy consumption will increase only incrementally after approximately $E(\mathbf{d}) = 80$ miles. Increasing the CDR even further might be beneficial to the marketability of PEVs, but it will not provide significant benefits to the average driver [41]. The intersection of this surface with the $\sigma(\mathbf{d}) = 0$ plane is identical to $c_{\mathrm{fr}}(d)E(\mathbf{m})$ (using (3.8) with $d = a$). This plot reveals that the estimation of the miles driven in CD mode using the unique value $d = E(\mathbf{d})$ (rather than modeling the CDR as a distributed RV) does indeed introduce some error; it leads to an overestimation by 5–15%.

---

[8]In fact, it can be shown that the gradient vector of this function always points towards increasing $E(\mathbf{d})$ and decreasing $\sigma(\mathbf{d})$.

Finally, one might question the choice of the log-normal distribution for f_d, lacking a clear physical justification. However, it has been found that other probabilistic models, such as the gamma, the Weibull, and even the uniform distribution, provide remarkably similar results to the ones shown in Table 3.2 and Figure 3.2.
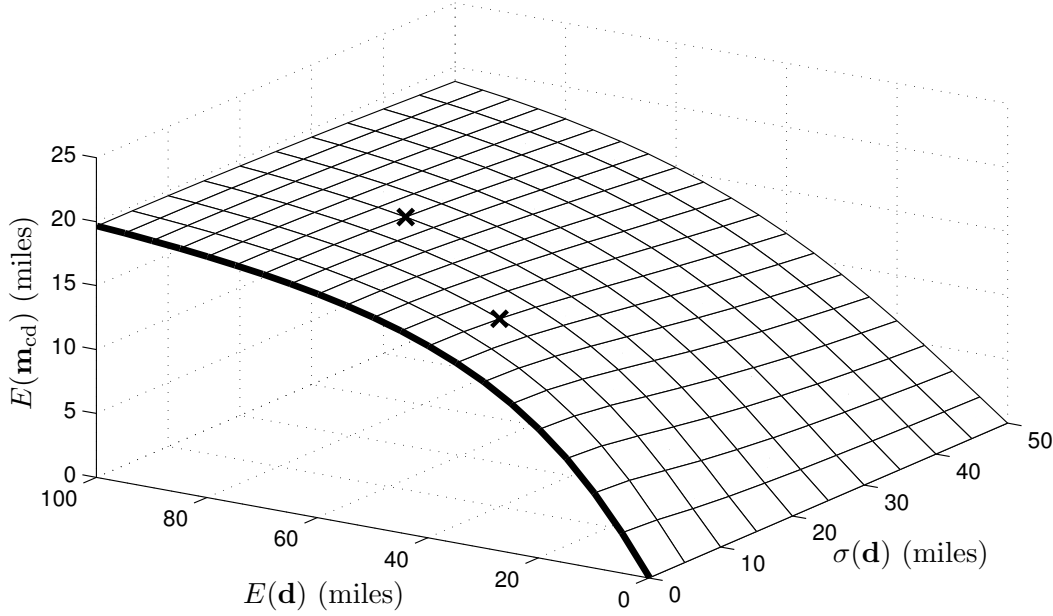
Figure 3.2 $E(\mathbf{m}_{cd})$ vs. $E(\mathbf{d})$ and $\sigma(\mathbf{d})$ for an urban weekday. [Note: The two '$\times$' symbols correspond to $f_{d,1}$ and $f_{d,2}$.]

3.5   Electric Power Consumption

3.5.1   Previous work

The estimation of electric power consumption by PEVs is more complicated than computing the total energy consumption, because of the inherent difficulty in predicting when a PEV will be plugged in, and the duration of its connection to the grid. Previous studies have thus estimated power consumption based on estimates of electric energy consumption, obtained first using either (3.6) or (3.9), by simply assuming a constant power draw during a predefined time period [22,23]. To account for all PEVs on the road, the total power is increased proportionally.

Alternative charging scenarios that include some sort of time-of-day dependence have been devised, such as uncontrolled charging, delayed charging, and off-peak charging [19, 22, 23].

These can be further classified in accordance with the location of charging into: charging only at home, delayed charging only at home, charging only at home and work, charging at any place, etc. In previous work, these scenarios have been analyzed using similar simplifications.

Clearly, this type of methodology leads to unrealistic results. First, it is unreasonable to expect that all PEVs begin charging simultaneously. Some may be parked with their batteries fully charged already, and some may be traveling. Second, charging may occur in-between trips, that is, the charging frequency does not need to be limited to once per day. In general, this method overestimates the peak value of power consumption [22, 23].

3.5.2 Proposed methodology

For an estimation of power consumption, the travel patterns should be taken into account. The proposed methodology consists of simulating daily trips using the 2009 NHTS data. The following two scenarios are simulated:

(A)   uncontrolled charging any time the vehicle is parked at home, and

(B)   uncontrolled "opportunistic" charging at any location (home, shopping mall, work, etc.).

These scenarios might not be completely representative of the actual behavior of PEV drivers; for instance, it might be unrealistic to expect that drivers would decide to charge their car every single time they return home. Nevertheless, they represent two possible futures characterized by extreme cases of public charging infrastructure investment (from minimum to maximum). In particular, scenario (B) provides an upper bound for PEV energy consumption. Other scenarios, such as controlled charging (where time of charging is influenced by an electricity price or other signal) or exchanging batteries at battery stations, are not considered; these can be addressed in future work.

The charging circuit significantly affects the power consumption curve. Two ac charging levels have been recently standardized, with a third dc level currently under development [42]. For a normal household circuit breaker and wiring installation, typical options for charging circuits [35] are shown in Table 3.3, where 'charger size' denotes the nominal power consumption at the wall outlet. It is assumed that a PEV is always charged with a constant power draw—equal to the charger size. Even though this does not correspond to an actual battery charging

profile [43], it has been found that this simplification does not affect the results significantly. The results provided herein will account for the cases where (i) all PEVs utilize a single charger type, and (ii) PEVs are randomly assigned a home charger type based on an (arbitrarily) pre-determined ratio, also shown in Table 3.3. For scenario (B), it is assumed that the public charging infrastructure involves only 6-kW chargers (i.e., the most expensive option).

Table 3.3   Charging Circuits

Charging circuit	Charger size (kW)	Ratio
120 V, 15 A (Level 1)	1.4	1/3
120 V, 20 A (Level 1)	2	1/3
240 V, 30 A (Level 2)	6	1/3

The proposed methodology proceeds as follows. For each of the four area/day cases considered, a random vehicle (along with its travel pattern) is selected from the corresponding set of vehicles in the NHTS. These sets contain all vehicles, even those that do not travel on a given day. The selected vehicle is probabilistically assigned a tractive energy based on its type as per Section 3.3. Thus the interdependency between vehicle type and its travel pattern is now captured. (These two RVs were assumed independent in the analysis of Section 3.4.) In addition, the vehicle is virtually converted into a PEV by being assigned values of ξ and d based on the distributions given in previous sections. Then its power consumption throughout the day is observed using a computer simulation. To initialize the simulations, it is assumed that all vehicles start their first trip of the day with fully charged batteries, where 'first trip' is defined as the first trip that takes place after 4 am. Each simulation starts at the instant where the vehicle first departs, and ends after 24 hours, even if its battery is not fully charged at this point in time. In essence, this method generates instances of the stochastic process $\mathbf{x}(t)$ that describes the daily power consumption of a random PEV.

For a fleet of n PEVs charging independently of each other, the overall power consumption is $\mathbf{Y}_n(t) = \sum_{i=1}^{n} \mathbf{x}_i(t)$, with $E(\mathbf{Y}_n(t)) = nE(\mathbf{x}(t))$[9] and $\sigma(\mathbf{Y}_n(t)) = \sqrt{n}\,\sigma(\mathbf{x}(t))$. The coefficient of variation $\sigma(\mathbf{Y}_n(t))/E(\mathbf{Y}_n(t))$ is equal to $\sigma(\mathbf{x}(t))/\sqrt{n}E(\mathbf{x}(t))$. For large n, the central limit

---

[9]The reader is cautioned that this notation does not imply an averaging process over time, but rather an averaging of all possible outcomes of an experiment conducted at a specific point in time.

theorem suggests that the distribution of $\mathbf{Y}_n(t)$ will be approximately Gaussian.

According to the law of large numbers, the expected power draw per PEV, $E(\mathbf{x}(t))$ can be approximated by finding the sample mean of the power consumed by a large number N of PEVs, $\mathbf{M}_N(\mathbf{x}(t)) = \frac{1}{N} \sum_{i=1}^{N} \mathbf{x}_i(t)$. This is essentially the procedure followed herein. It is illustrated using a hypothetical vehicle with parameters $\xi = 0.8$, $h_{\mathrm{tr}} = 0.25$ kWh/mile, and $d = 40$ miles. The usable energy initially contained in the fully charged battery is $E_0 = (0.8)(0.25)(40)/\eta_1 = 8/\eta_1$ kWh, where η_1 is the battery-to-wheels efficiency. At $t_0 = 09{:}57$, the vehicle departs from home with E_0 stored in the battery. After traveling a total of $m_1 = 24.7$ miles, the vehicle returns home at $t_1 = 11{:}49$, and begins charging at once. The usable energy that remains in the battery at t_1 can be calculated by

$$E_1 = \begin{cases} E_0 - (\xi\, h_{\mathrm{tr}}\, m_1)/\eta_1 & \text{for } E_0 - (\xi\, h_{\mathrm{tr}}\, m_1)/\eta_1 > 0\,, \\ 0 & \text{for } E_0 - (\xi\, h_{\mathrm{tr}}\, m_1)/\eta_1 \leq 0\,. \end{cases} \tag{3.15}$$

In this case, $E_1 = 3.06/\eta_1$ kWh, and an amount of energy $(E_0 - E_1)/\eta_2 = \xi\, h_{\mathrm{tr}}\, m_1/\eta = 7.35$ kWh is required from the outlet to fully recharge the battery, where η_2 is the wall-to-battery efficiency. If a 2-kW charger is used, a complete recharge takes 3 hours and 40 minutes, so it concludes at $t_2 = 15{:}29$. Of course, the simulations permit vehicles to begin their next trip before their batteries become fully charged. These subsequent trips (if any) are simulated in the same manner. By repeating a simulation for every PEV included in the survey, the sample mean $\mathbf{M}_N(\mathbf{x}(t)) \approx E(\mathbf{x}(t))$ is found.

Furthermore, the simulations can be used to find $\sigma(\mathbf{x}(t))$, and thus to calculate a confidence interval for the power consumption estimation. For the simple case where all PEVs have a single charger type, rated at c kW, a random PEV's charging at time t is a Bernoulli trial: $\mathbf{x}(t) \in \{0, c\}$. So, if $p(t)$ is the probability of it being charged, $E(\mathbf{x}(t)) = cp(t)$, and $\sigma^2(\mathbf{x}(t)) = c^2 p(t)(1 - p(t))$. If there exists a mix of K distinct charger ratings c_k, with $k = 1, \ldots, K$, and if $p_k(t)$ is the probability of a random PEV being charged at a rate c_k, then $E(\mathbf{x}(t)) = \sum_{k=1}^{K} c_k p_k(t)$ and $\sigma^2(\mathbf{x}(t)) = \sum_{k=1}^{K} c_k^2 p_k(t) - (\sum_{k=1}^{K} c_k p_k(t))^2$. The probability $p_k(t)$ that appears in the above expressions can be obtained from the simulations.

It should be noted that the distribution of vehicles by class in the survey is slightly different from the actual nationwide distribution. Therefore, to improve the accuracy of the estimate, the power consumption is adjusted by appropriate weight factors (included in the NHTS), which are calculated for each of the four cases considered.

Simulation results for the two scenarios are shown in Figure 3.3. These curves depict the expected daily power consumption per PEV on U.S. roads, measured at the "outlet." (The curves account for all registered household light-duty PEVs, even those that are not driven on a given day.) The following observations can be made:

- The load profiles are somewhat different from the ones that have been presented in previous studies [22,23], which tend to overestimate the peak of the power consumption. The two main reasons for this are: (i) ignoring the travel probability (see Section 3.2), and (ii) assuming that PEVs can only charge after ca. 18:00, whereas some PEVs might be plugged-in during the morning and early afternoon hours.

- During the workweek in scenario (A), the power peaks around 18:00, while people are returning home from work (cf. Figure 3.1). At that time, the number of PEVs being charged reaches a maximum. In contrast, in scenario (B), three peaks are apparent—around 8:00, noon, and 18:00—coincident with people arriving at work, driving to and from lunch, and returning home from work. Interestingly, even though charging can occur anywhere vehicles can park, the 18:00 peak value is similar.

- During weekends, the load profiles are smoother and have lower peak values than on weekdays.

- The variation with respect to charger size is quite significant. Smaller charger sizes tend to reduce the peak value of power consumption, but spread the load to longer time periods. It should be noted that the peaks of the power curves are not proportional to charger size (e.g., the 6-kW peak is not equal to three times the 2-kW peak). It is interesting to observe that the expected peak of power consumption per PEV is always less than 1 kW (even with the 6-kW chargers).

- The difference between the power curves with $f_{d,1}$ and $f_{d,2}$ (not shown due to space limitations) is not significant. This occurs because apparently a 40-mile average CDR can satisfy

most daily travel requirements (cf. Figure 3.2). On the other hand, if the average CDR is reduced below 40 miles, simulations predict a significant decrease in power consumption.
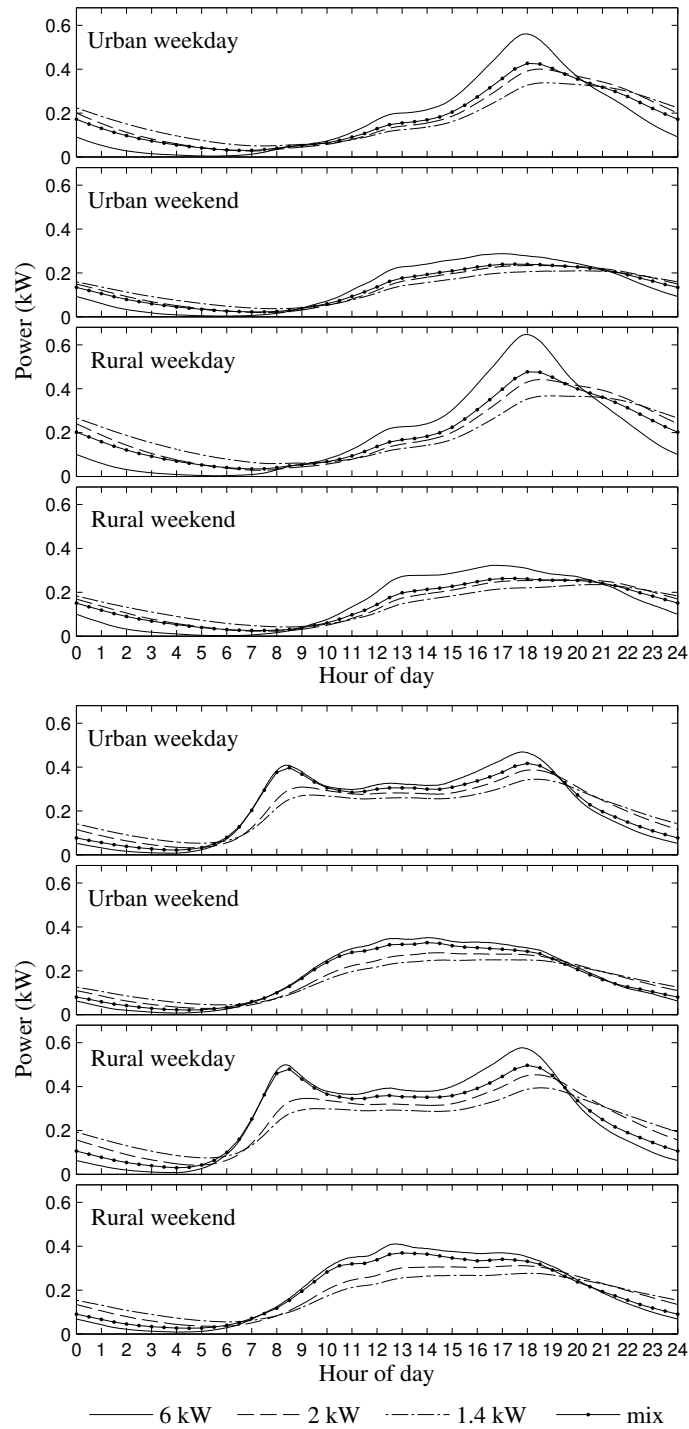
Figure 3.3   Average power consumption per PEV with $f_{d,1}$. [Top: scenario (A). Bottom: scenario (B).]

To assess the impact of a large PEV fleet on a power system, the computed PEV load is added to the Midwest ISO (MISO) load profile, as shown in Figure 3.4. The $f_{d,1}$ CDR PDF is used and a mix of chargers is assumed, as previously described. The PEVs' power consumption is converted from the outlet to the substation level, assuming that distribution losses are 5%. The solid load curves represent the average weekday and weekend load as reported by MISO [44] in 2009. The number of LDVs in the MISO footprint today is approximately 28 million [45], with ca. 75% of these in urban areas [34]. About 17% are in the eastern time zone, and the remaining are in the central time zone. Notably, the impact on power consumption of one million PEVs on MISO's system would be relatively small. Further increases will require additional peaking capacity to be installed, because the peak PEV load will be more or less synchronous with the peak of the MISO load curve. Therefore, some form of time-dependent pricing scheme would be greatly beneficial in shifting the PEV load to off-peak periods.
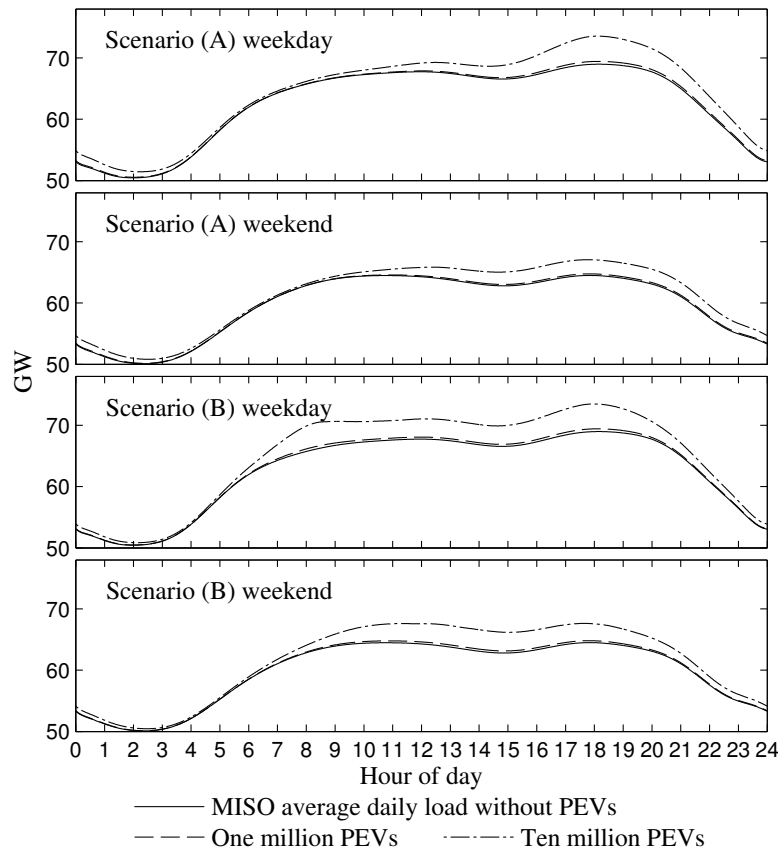
Figure 3.4 PEV fleet power load superimposed on MISO load curve. [The horizontal axis shows the hour of day in the central time zone.]

Lastly, the daily electric energy consumption can be obtained by numerically integrating the power consumption curve. These results are provided in Table 3.4, which also contains the results of the analytical computation of subsection 3.4.2 (column labeled 'Table 3.2') for convenience. The following can be observed:

- Energy consumption increases with charger size. This could signify a potentially undesirable situation where chargers are inadequately powerful to completely recharge some PEVs overnight.

- Investments in public charging infrastructure will lead to an increase in electric energy consumption.

- The results of the analytical calculation method of subsection 3.4.2 are consistent with the simulation results. However, the latter can reveal interesting interactions between charger size, travel patterns, and CDR.

Table 3.4   Energy Estimation by Integrating Power (in kWh/PEV)

		Table 3.2	Scenario (A)				Scenario (B)			
			6 kW	2 kW	1.4 kW	mix	6 kW	2 kW	1.4 kW	mix
$f_{d,1}$	U. w/day	4.16	4.24	4.13	4.09	4.15	5.39	5.12	4.94	5.30
	U. w/end	3.23	3.22	3.14	3.10	3.16	4.23	3.92	3.80	4.13
	R. w/day	4.88	4.82	4.66	4.59	4.69	6.53	6.07	5.84	6.42
	R. w/end	3.70	3.57	3.43	3.41	3.47	4.86	4.46	4.27	4.72
$f_{d,2}$	U. w/day	5.06	4.93	4.80	4.72	4.82	5.72	5.46	5.25	5.64
	U. w/end	3.99	3.77	3.67	3.59	3.68	4.57	4.35	4.18	4.46
	R. w/day	6.29	5.87	5.75	5.60	5.74	7.06	6.65	6.37	6.92
	R. w/end	4.75	4.32	4.15	4.10	4.19	5.36	4.99	4.79	5.17

3.6   Conclusions

In this paper, a theoretical framework for assessing light-duty PEVs as a power system load has been set forth. The most authoritative source of national travel patterns (i.e., the 2009 NHTS database) was utilized to obtain a PEV load forecast. Uncontrolled PEV charging will almost certainly increase the power system's peak load in the U.S.

This work can become the starting point for incorporating vehicle travel patterns in studies such as: quantifying the effect that time-dependent pricing of electricity can have on PEV load leveling; analyzing the impact of the additional PEV load on locational marginal prices; estimating PEV impacts on greenhouse gas emissions; studying localized effects on power grids by introducing the spatial distribution of vehicles; and examining the potential of PEVs to act as distributed generation sources using vehicle-to-grid technologies.

Acknowledgment

4. LOAD SCHEDULING AND DISPATCH FOR AGGREGATORS OF PLUG-IN ELECTRIC VEHICLES

Di Wu, Dionysios C. Aliprantis, and Lei Ying

Abstract

This paper proposes an operating framework for aggregators of plug-in electric vehicles (PEVs). First, a minimum-cost load scheduling algorithm is designed, which determines the purchase of energy in the day-ahead market based on the forecast electricity price and PEV power demands. The same algorithm is applicable for negotiating bilateral contracts. Second, a dynamic dispatch algorithm is developed, used for distributing the purchased energy to PEVs on the operating day. Simulation results are used to evaluate the proposed algorithms, and to demonstrate the potential impact of an aggregated PEV fleet on the power system.

Index Terms

Electric vehicles, power demand, power system economics, smart grids.

Nomenclature

c_j	Rated power of charger type j
e_i	Departure time (slot) for the first trip in the morning for PEV i
$\mathcal{E}$	Overall energy required to charge all PEVs

$\mathcal{E}_i$	Energy required to charge PEV i
$\mathcal{H}_i$	Set of time slots where PEV i will be charged
K	Number of slots within the charging period
l_i	Charging time (number of slots) of PEV i
$n(l,j,s,e)$	Number of PEVs with charging duration l, charger type j, arrival slot s, and departure slot e
N	Number of PEVs under the aggregator's control
N_1	Number of PEVs charged with energy purchased through long-term bilateral contracts
N_2	Number of PEVs charged with energy purchased in the day-ahead market
p_i	Charger power rating of PEV i
$p_{i,k}$	Scheduled power for PEV i at time slot k
$\mathcal{P}_k$	Total scheduled charging power at time slot k
$R_{s+1,e}(\tau_k)$	Rank of τ_k for time slots between $s+1$ and e
s_i	Arrival time (slot) for the last trip at night for PEV i
ΔT	Duration of time slot
τ_k	Wholesale electrical energy price in time slot k

4.1   Introduction

The transportation sector accounts today for a significant portion of all nations' petroleum consumption and carbon emissions. For instance, in the U.S. in 2009, 94% of the transportation energy was obtained from petroleum, while 63% of the crude oil was imported [46]. This dependency on dwindling oil resources represents an ever-increasing risk to national security and poses grave environmental concerns. The electrification of transportation and, in particular, the development of plug-in electric vehicle (PEV) technology has been recognized as a key part of the solution to energy and environmental problems worldwide [1,47]. PEVs—either plug-in hybrid electric vehicles or pure electric vehicles—are equipped with adequate battery energy storage to travel for several miles using (mostly) electricity, and are recharged from the electric grid, thus allowing electricity to displace a portion of petroleum.

The emerging fleet of PEVs will introduce a considerable amount of additional load on the power system. In the simplest case, this can be treated as a traditional (i.e., uncontrollable) load, being served whenever a PEV is plugged in, and billed at a normal retail rate. In [48], the power consumption from a fleet of uncontrolled light-duty PEVs has been estimated based on the travel pattern obtained from the 2009 National Household Travel Survey (NHTS) [34]. The analysis of [48] and other reports [19–26, 49–51] have predicted that a significant amount of PEV charging will take place during peak hours when the wholesale electricity price is high. Moreover, the coincidence between peaks of PEV and non-PEV load will require investments in generation, transmission, and distribution, in order to maintain the reliability of the power system. Fortunately, PEVs are more flexible than traditional load, because the majority of PEV owners return home early in the evening, and may not have a preference about the exact time that their vehicles will be charged, as long as the batteries are full by the next morning. To utilize this flexibility, appropriate algorithms for charging control and management must be designed.

This control will be performed by PEV aggregators, which will be either existing utilities that will offer new financial contracts specific for PEV loads, or new for-profit entities that will participate in the wholesale electricity market. A broad array of aggregators is described in [4], and a conceptual framework to integrate the aggregated PEVs with vehicle-to-grid (V2G) capability into the grid is proposed in [52]. The PEV aggregator considered herein has a significantly large customer base so that it can purchase energy at wholesale. The aggregator could also provide ancillary services to the power system. This has been the focus of previous work, wherein the possible ancillary services that could be offered by aggregated PEVs have been reported [4]. For example, controlling PEVs with or without V2G capability to maximize the revenue from frequency regulation is discussed in [53] and [54], respectively.

In contrast to these previous approaches, where the objective is profit maximization from ancillary services, this paper focuses on the actions of an aggregator who wishes to maximize its energy trading-related profits. In this analysis, the contracts with the PEV owners stipulate that charging will only occur during off-peak hours, e.g., from 10 p.m. to 7 a.m., because most vehicles are not in use and the wholesale electricity price is generally low during this

period. Aggregators coordinate and control PEV charging. PEV owners relinquish control of their batteries' state of charge, in exchange for a fixed reduced electricity rate. We are considering a risk-averse aggregator, who would purchase the bulk of its electricity through long-term bilateral contracts and/or by participating in the day-ahead markets (there are 24 hourly markets); the real-time market would be used for balancing purposes only. Specifically, it is assumed that this aggregator controls a fleet of $N = N_1 + N_2$ PEVs; N_1 PEVs are charged with energy purchased through bilateral contracts, while the remaining N_2 PEVs are charged with energy purchased in the day-ahead market. This split is arbitrary, and in the extreme case, either N_1 or N_2 could be zero. Setting $N_1 = 0$ would increase the aggregator's financial risk, so it might not be a prudent choice. Also, because the number of PEVs that subscribe to this aggregator can change on a daily basis, N_2 realistically cannot be zero, unless the aggregator updates its bilateral contracts daily, which is highly unlikely. In any case, it should be noted that this paper does not delve on the determination of the optimal split between N_1 and N_2, but rather on what happens once this split is given. Due to the assumption of a fixed retail rate, profit maximization is equivalent to minimization of the purchased energy cost. Therefore, this aggregator would take advantage of the flexibility of the PEV load, and would charge PEVs with the cheapest possible electricity, which typically occurs during off-peak hours at night. Also, in the presence of several competing aggregating entities, the reduction of energy cost would be necessary to gain market share.

This paper has two main objectives:

1. To set forth algorithms that aggregators can use to schedule and dispatch the PEV load so that their energy cost is reduced (and ideally minimized), using information about the forecasted charging demand for the coming day. The proposed scheduling algorithm can be applied for negotiating long-term bilateral contracts, based on the offered electricity price (especially if this price is time-varying); or for participating in the day-ahead market, based on the forecasted electricity price. The proposed dispatch algorithm is used to distribute the purchased energy to the individual PEVs during the operating day. "Scheduling" and "dispatch" are familiar terms in power system analysis, applicable to generators in the context of unit commitment and economic dispatch, respectively. Herein, these terms are applied

to the charging of PEV batteries. In particular, "dispatch" refers to the determination of the charging time for each PEV (dynamically, in real time) so that the actual aggregated power consumption follows the "scheduled" load curve purchased by the aggregator.

2. To identify how an aggregated PEV load would impact the power system, assuming that the aggregator would operate under the current electric energy market structure. The analysis shows that the PEV load can have an unusual stepped pattern, which could be detrimental to the proper operation of the power system. It also suggests that new market mechanisms might be necessary to provide load-leveling and load-smoothing incentives to aggregators.

The rest of this paper is organized as follows: Section 4.2 outlines assumptions made in this analysis. In Section 4.3, potential issues with simple uncontrolled off-peak charging are presented. In Section 4.4, a scheduling algorithm is proposed for minimizing the expected electric energy cost according to the price variation and the charging demand. In addition, a dynamical dispatch algorithm is set forth. In Section 4.5, simulation results are discussed. Finally, Section 4.6 concludes the paper.

4.2   Analysis Assumptions

The proposed algorithms are developed and validated using the actual U.S. travel patterns as captured by the 2009 NHTS, and the simulation method of [48]. The NHTS statistical data represent the travel patterns of the U.S. light-duty vehicle (LDV) fleet[1], and contain information on the travel behavior of a national representative sample of U.S. households, such as mode of transportation, trip origin and purpose, and trip distance. LDV travel accounts for 92% of the highway vehicle miles traveled [30], 76% of the energy consumed by highway travel modes [31], and 74% of the carbon dioxide emissions from on-road sources [32]. For the purposes of this analysis, the NHTS database is used to extract statistics of electric energy consumption, charging duration, and arrival and departure times, under reasonable assumptions of PEV drivetrain configurations and charger sizes. In the future, an aggregator will have access to more accurate statistics by monitoring the actual composition, travel pattern, and energy

---

[1]The U.S. fleet of light-duty vehicles consists of cars and light trucks, including minivans, sport utility vehicles (SUVs), and trucks with gross vehicle weight less than 8,500 pounds [29].

consumption of its own fleet.

The PEV charging infrastructure will be available at the garages or driveways of PEV owners' residences[2] and at some public locations, such as parking lots of commercial buildings and shopping malls. However, it is conceivable that, when charging at public locations, a PEV driver might be hesitant to permit controlled charging, especially if the driver needs to ensure that the battery will be charged as much as possible, uninterrupted throughout the duration of the stop. (A notable exception is the charging that would occur during normal business hours, when employees' vehicles would remain plugged in at the parking lot of their workplace.) Therefore, for simplicity, in this analysis it is assumed that the proposed controlled charging program is associated only with home charging. Nevertheless, in case it becomes necessary to account for the charging at public locations as well, the proposed scheduling and dispatch methods would still apply.

The proposed methods require that the aggregator utilizes techniques for forecasting the day-ahead electricity price, such as the ones presented in [57–60]. Herein, it is assumed that day-ahead locational marginal price (LMP) can be forecasted with reasonable accuracy, and the error associated with the forecast is ignored. It is important to note that the LMP forecast's absolute value is not critical. Rather, for minimizing cost, it is the *ranking* of the hourly LMPs that is critical, and should be predicted as accurately as possible. In addition, it is assumed that aggregators' actions do not affect the relative ranking of hourly LMPs.

Finally, any charging constraints that would arise at the distribution level (e.g., from transformer overloading) or distribution system optimization [61] are ignored. This analysis is performed at the bulk power level, and it is further assumed that the aggregator can schedule arbitrarily large amounts of power. Extending this work to systems with detailed distribution feeder models is worthwhile, but is left for future study.

---

[2]Most probably, people will not consider purchasing a PEV if they cannot charge their vehicle at home. Chargers are currently available for 120-V or 240-V circuits, both typically available at U.S. residences [55]. Often, PEV manufacturers and the U.S. federal government offer assistance and financial incentives for the installation of the required equipment [56].

4.3 Uncontrolled Off-peak Charging

Figure 4.1 depicts the average percentage of vehicles parked at home through a day, calculated using the NHTS data. As can be seen, more than 90% of vehicles are parked at home between 9 p.m. and 6 a.m. Recognizing this opportunity, several charging strategies have been previously proposed for shifting the PEV load to off-peak hours, in order to utilize less expensive electricity and reduce the peak of the overall load. For example, all the vehicles begin charging at 10 p.m. in the "delayed charging" scenario of [20]; half of the vehicles are charged at 10 p.m. and half at 11 p.m. in the "night charge" scenario in [22]; vehicles are only charged between 12 a.m. and 6 a.m. in the "delayed night charging" scenario in [23]. These studies, however, do not take into account realistic travel patterns. So, herein, a similar scenario is considered using the travel pattern obtained from the 2009 NHTS, with charging only allowed between 10 p.m. and 7 a.m. During this period, PEVs will be charged whenever they are parked at home until their batteries reach full capacity. Computer simulations are performed using the method and parameters presented in [48].
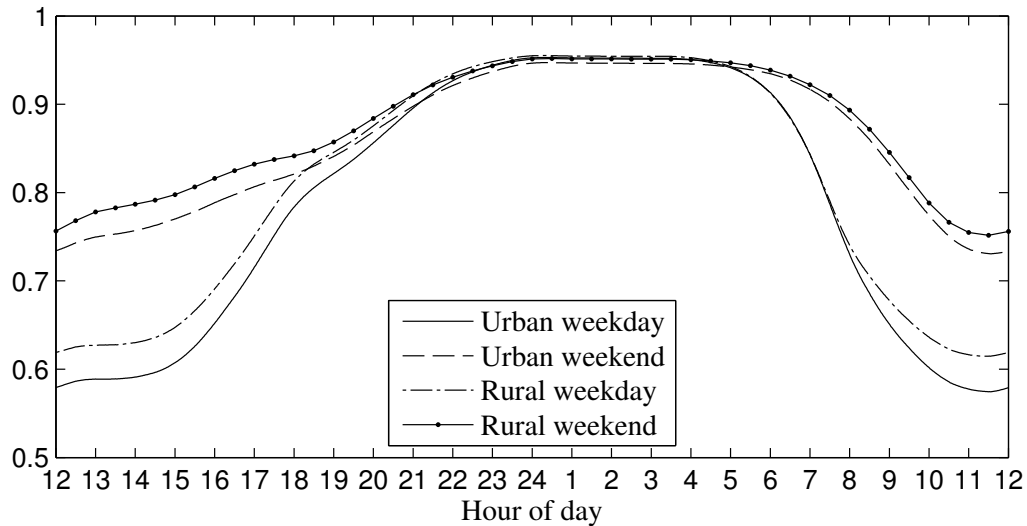
Figure 4.1   Average percentage of vehicles parked at home in 2009.

The simulation results provide the average power consumption that is shown in Figure 4.2 (b). It can be observed that the resulting peak load per PEV is much higher than the uncontrolled charging scenario shown in Figure 4.2 (a). This happens because charging tends to concentrate

at the beginning of the charging-allowed period, whereas it would be naturally distributed with time if left uncontrolled. This PEV load is also superimposed on MISO's load curve in Figure 4.3, for 1 million and 10 million PEVs (which amounts to about one third of the current LDV fleet size in the MISO area).

These findings contradict the conclusions of previous studies (which are obtained with simplified travel patterns) that suggest simple-delayed charging strategies are better than uncontrolled charging in terms of reducing the peak load. In addition, even though the cost of electric energy in this charging scenario would be probably reduced compared to uncontrolled charging, this is not necessarily the most economic way to charge the PEV fleet. The electricity cost could be further reduced by optimally shifting PEV charging to periods with the lowest LMP.
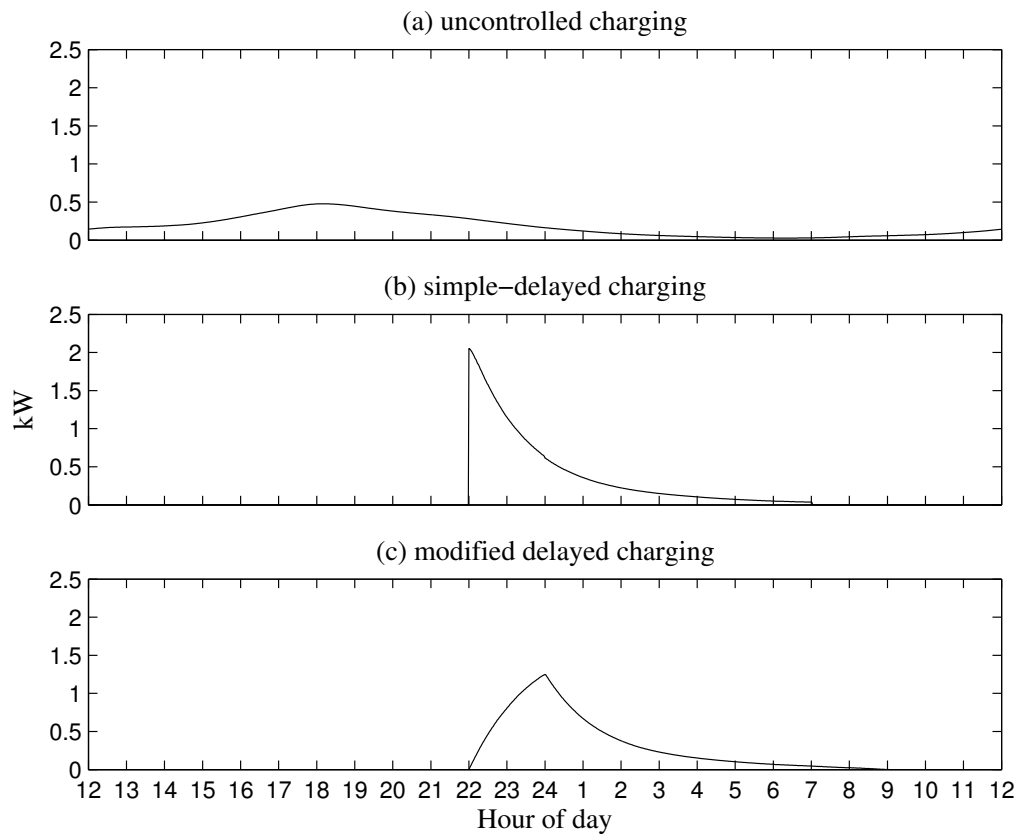
Figure 4.2   Average power consumption per PEV (in an urban area on a weekday).

The adverse sharp peak can be avoided with a simple modification, namely, by uniformly

distributing the charging start time over a predefined period (e.g., from 10 p.m. to 12 a.m.). This leads to lower peaks, as shown in Figure 4.2 (c) and Figure 4.3 (c). In fact, it might even be possible to solve the inverse problem of finding the distribution of charging start times that would generate some desirable load pattern. The aggregator would in turn reflect this distribution to the financial contracts with PEV owners. Although this method would be rather simple to implement, it would be static and inflexible, and it would not allow dynamic coordination among PEVs. Also, the peak of the aggregated load would not be synchronized with the lowest LMP, because this varies on a daily basis.

Other more advanced charging control algorithms have been proposed to fill the overnight valley, such as the decentralized control strategy described in [62]. However, flattening the overall load may increase the aggregators' energy cost in the wholesale electricity market. A different strategy is required to maximize the aggregators' profits from energy trading. This is described in the next section.

4.4   Proposed Algorithms

In the proposed framework, aggregators control PEV charging during the off-peak period from 10 p.m. to 7 a.m. It is also assumed that they are contractually bound to maximize the state of charge of the batteries by the departure time declared by each PEV owner[3] (unless a battery cannot be fully charged overnight given its state of charge on arrival and the charger rating). The charging period is discretized into a finite number of slots. The proposed scheduling algorithm determines the amount of energy to purchase in each time slot, according to the price (either the bilateral contract price or the forecasted day-ahead LMP) and the PEV charging demands. On the operating day, aggregators need to dispatch the PEV load according to the committed load. The dispatch algorithm determines the time slots where each PEV will be charged.

---

[3]It is conceivable that some PEV owners would try to ensure that their vehicle gets charged by reporting false (i.e., earlier than the actual) departure time. Hence, they must be incentivized to report their true departure time, or penalized when they consistently report false departure times. The design of such mechanisms would fall within the aggregator's responsibility, but is outside the scope of this paper.
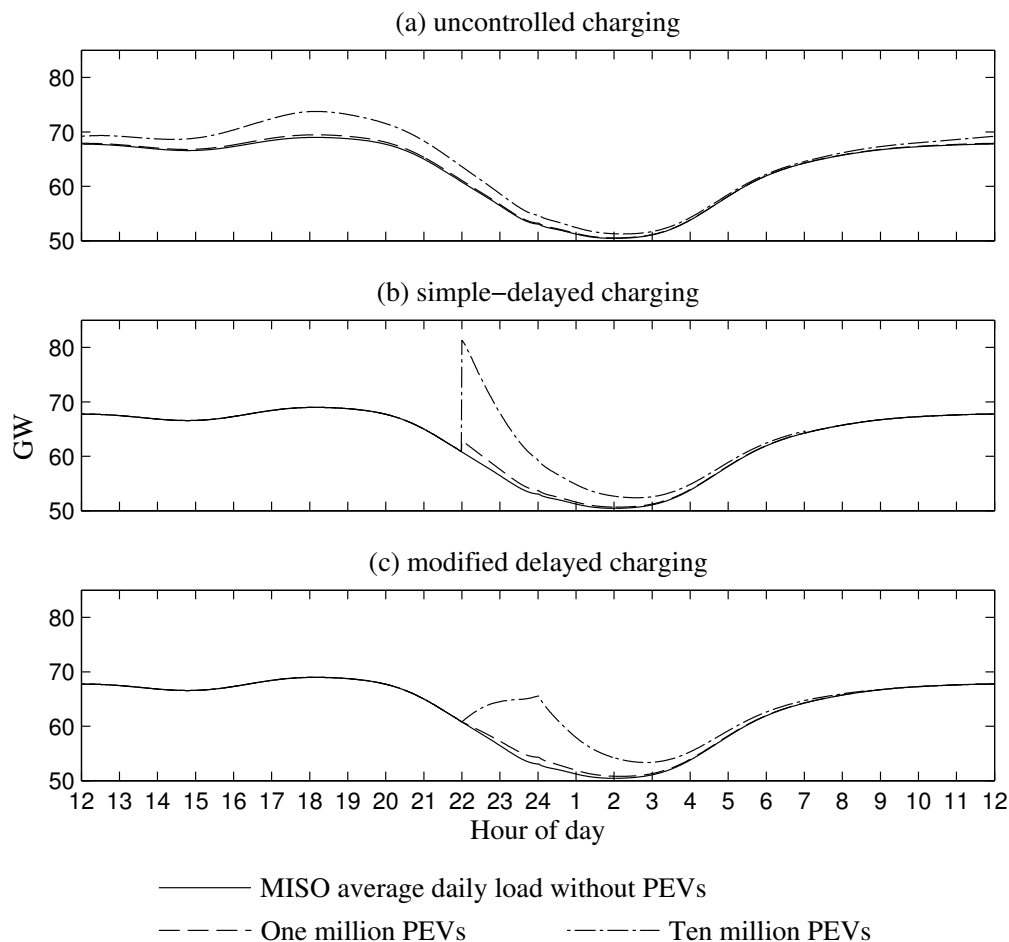
Figure 4.3   PEV fleet power load superimposed on MISO load curve.

4.4.1   Scheduling

Consider an aggregator that is controlling a fleet of N_x PEVs, $x \in \{1, 2\}$, which are indexed by i. Let p_i denote the charger rating of vehicle i, which belongs to a set $\{c_1, \cdots, c_j, \cdots, c_J\}$, where c_j is the rating of charger type j among a number of charger types J. For a normal residential wiring installation, typical options for charging circuits [35] are shown in Table 4.1, where "charger rating" denotes the nominal power consumption (continuous rated power) at the wall outlet. The "ratio" column shows that these are equally distributed within the hypothetical fleet of PEVs herein for simulation purposes. It is conceivable that there might exist commercial charger models with the capability to modulate the charging power from zero to a rated value based on an external control signal. Nevertheless, in the proposed minimum-cost scheduling

and dispatch scheme, all PEVs are charged with either zero or maximum rate. In fact, optimal battery charging follows a varying power profile [43]. However, it has been found that modeling this profile in detail does not affect the simulation results significantly.

Table 4.1   Charging Circuits

Charging circuit	Charger rating (kW)	Ratio
120 V, 15 A (Level 1)	1.4	1/3
240 V, 30 A (Level 2)	3.3 (limited by on-board charger)	1/3
	6	1/3

The charging period is discretized into K time slots, indexed by k, with the duration of each time slot equal to ΔT. The parameter ΔT is independent of the rate that market operations take place (e.g., on an hourly basis for the day-ahead market), and will be on the order of one minute. Such a fine resolution might be necessary to ensure proper charging of the PEVs, i.e., to better accommodate vehicles that arrive or leave at arbitrary times, or whose charging time is not an integer number of hours. The charging time of PEV i, denoted by l_i, is defined as the number of time slots during which charging would take place with full rate p_i, under a simple-delayed charging scenario; in this scenario, vehicles are plugged in as soon as they arrive home, the only restriction on the charging is that it must take place within a prescribed time period, and there is no other advanced control whatsoever. Clearly, $0 \le l_i \le K$. The total energy required to charge all vehicles is $\mathcal{E} = \Delta T \sum_{i=1}^{N_x} p_i l_i$. Furthermore, let τ_k denote the price (either from the bilateral contract or the forecasted day-ahead LMP) during time slot k, and $n(l, j, s, e)$ denote the number of vehicles with charging time l and charger type j, which arrive home at time slot s and leave home at time slot e. (If a vehicle leaves home later than K, then set $e = K$.) Because a vehicle associated with the parameter set $\{l, j, s, e\}$ can be charged for at most $e - s$ time slots (the earliest that charging can start is the $s + 1$ slot), it follows that $l \le e - s$.

It is assumed that reliable estimates of $n(l, j, s, e)$ can be obtained from statistics, based on data that the aggregator can collect on a daily basis from its fleet of PEVs. Herein, such statistics are generated using the 2009 NHTS data set. For illustration purposes, we consider the trips of all urban vehicles that traveled on weekdays, and it is assumed that the driving

patterns of PEVs are similar to those of regular automobiles. Elimination of the vehicles that did not travel on the survey date (ca. 35% of the total number of vehicles), as well as of those that for any reason did not return home at the end of the day (ca. 5.8% of the vehicles that traveled), yields a total of approximately 86,000 vehicles, whose trips are used to generate the statistics. First, each vehicle is categorized according to its arrival and departure time, using 20 minute-long time slots. This results in the two-dimensional probability distribution shown in Figure 4.4. As can be observed, the majority of vehicles (ca. 82%) arrive at home before 10:20 p.m., and leave home after 6:40 a.m., but several other bins contain substantial vehicle numbers as well. It is important to note that the travel patterns differ between these groups of vehicles. For example, further examination of the NHTS data reveals that vehicles that arrive home later at night and leave earlier in the morning usually travel longer distances than the rest (as is intuitively expected); this is depicted by the cumulative distribution functions (CDFs) of vehicle-miles traveled (VMT) shown in Figure 4.5. Finally, the electrical energy required to charge the PEVs is computed using the above VMT information and the method described in [48]; some representative results from these statistics are illustrated in Figure 4.6. The end result of these calculations is $n(l, j, s, e)$.
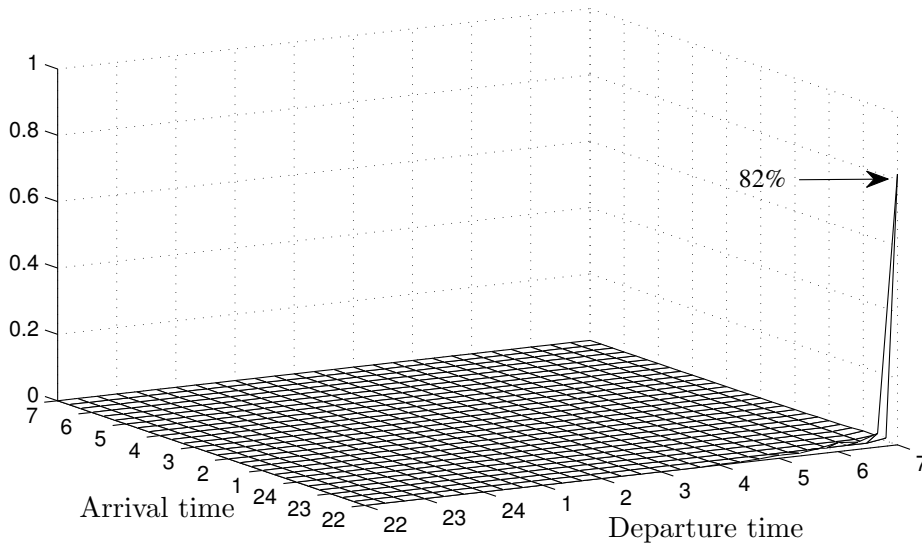
Figure 4.4 Probability of vehicle arrival and departure time. Note: The vehicles in the 10:00-10:20 p.m. arrival time or 6:40-7:00 a.m. departure time category arrived home before 10:20 p.m. or left home after 6:40 a.m., respectively.
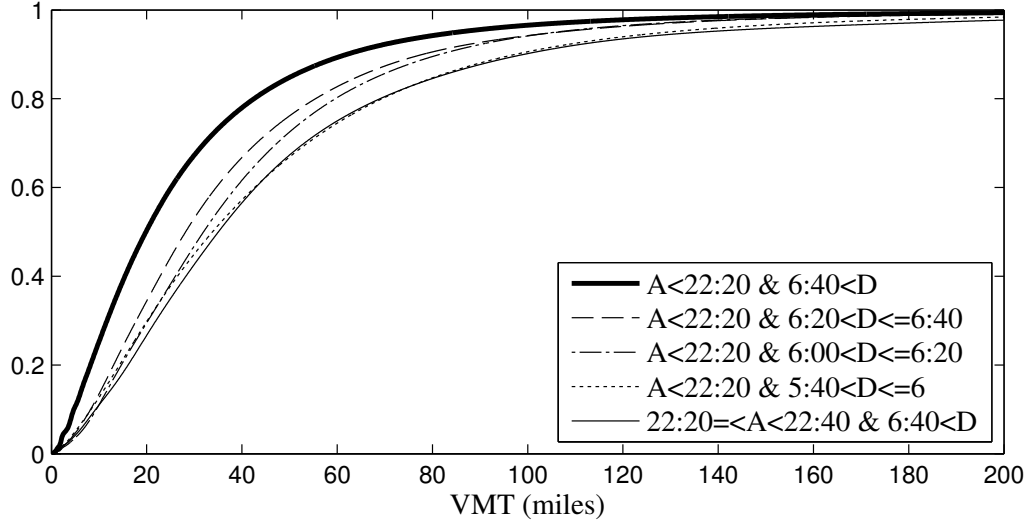
Figure 4.5   CDF of daily VMT for several combinations of arrival and departure times.

Given τ_k and $n(l, j, s, e)$, a load scheduling that minimizes the wholesale energy cost is outlined below as Algorithm 1. (If τ_k represents the forecasted day-ahead price, then it is the expected energy cost that is minimized.) The basic idea is to charge each vehicle in the time slots where the lowest electricity price occurs. PEVs can only be charged when they are parked (at home), so for each vehicle i only the time slots between s_i and e_i need to be considered. The time slots are ranked by electricity price from low to high, and the l_i time slots associated with the least expensive electricity are selected for charging.

Algorithm 1 solves the following linear program:

$$\min_{p_{i,k}} \Delta T \sum_{i=1}^{N_x} \sum_{k=1}^{K} \tau_k p_{i,k} \tag{4.1}$$

$$\text{subject to } \sum_{k=1}^{K} p_{i,k} = p_i l_i, \text{ for all } i$$

$$0 \le p_{i,k} \le p_i, \text{ for all } i, k$$

$$p_{i,k} = 0 \text{ for } k \le s_i \text{ and } k > e_i, \text{ for all } i$$

The solution that is produced is (for all i)

$$p_{i,k} = p_i, \text{ for } k \text{ such that } R_{s_i+1,e_i}(\tau_k) \le l_i, \text{ and} \tag{4.2}$$

$$p_{i,k} = 0, \text{ otherwise.} \tag{4.3}$$
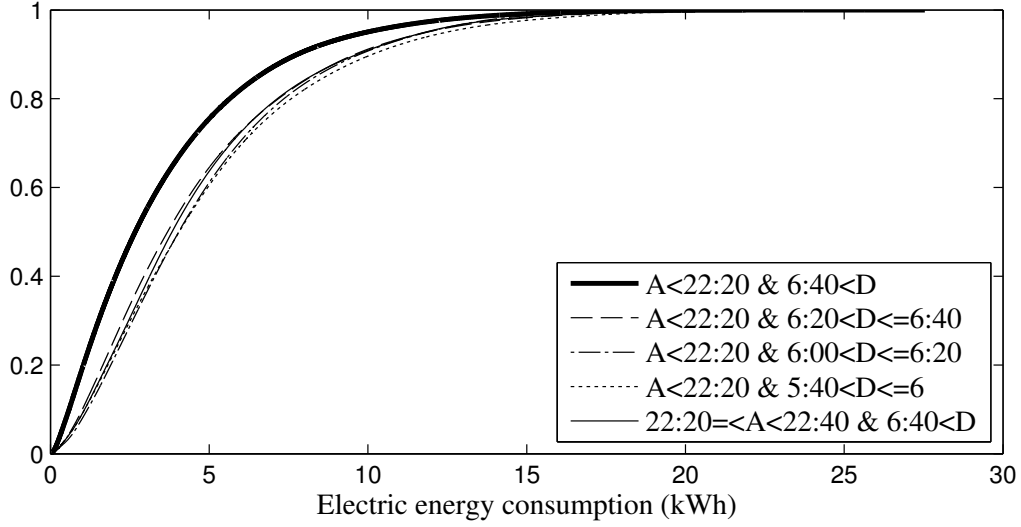
Figure 4.6   CDF of daily PEV electric energy requirement for several combinations of arrival
and departure times.

This solution corresponds to one of the extreme points on the boundary of the feasible region, and is optimal by construction. The algorithm outputs a schedule for the minimum-cost power purchase, $\mathcal{P}_k$. It is possible to use a commercial solver to obtain a numerical solution to this problem. However, this solution will not have a clear physical significance. On the other hand, the proposed algorithm, via the use of the ranking function R, provides a way to affect the shape of the PEV load, as will be demonstrated later.

It is interesting to observe that there might be other equally optimal solutions to this problem, yielding the same energy cost. For instance, consider a PEV i that has been parked at home since early in the evening, and that needs to charge for 90 minutes, so $l_i = 90$ if $\Delta T = 1$ min. Also, assume that the price remains constant for hour-long intervals (as usual for the LMP of the day-ahead market). Obviously, this PEV's charging will be spread over two hourly intervals (which could be non-adjacent), corresponding to the two lowest LMPs occurring between s_i and e_i, say, between 1–2 a.m. (the lowest), and 4–5 a.m (the second lowest). Therefore, this PEV will get charged for all 60 slots between 1–2 a.m., but the remaining 30 slots can be selected arbitrarily from the 60 slots of the 4–5 a.m. period (there are $\binom{60}{30}$ combinations if the slots are not contiguous, or 30 different combinations of contiguous time slots). Alternatively, the PEV could be charged during the entire 4–5 a.m. period, but at

---

Algorithm 1   Min-Cost Load Scheduling

1: Input: τ_k for $1 \leq k \leq K$, and $n(l, j, s, e)$ for $1 \leq s < e \leq K$, $0 \leq l \leq e - s \leq K$ and $1 \leq j \leq J$.

2: **for** $k = 1$ **to** K **do**

3:      $\mathcal{P}_k \leftarrow 0$

4: **end for**

5: **for** $s = 1$ **to** K **do**

6:      **for** $e = s + 1$ **to** K **do**

7:          Rank the price τ_k for $s < k \leq e$ from lowest to highest. The ranking function is denoted by $R_{s+1,e}(\tau_k)$, and takes the values $\{1, \ldots, e - s\}$. If different time slots have equal τ_k, they are ranked according to the index k from low to high.

8:          **for** $m = 1$ **to** $e - s$ **do**

9:              Compute the power which should be purchased for the time slot with the mth cheapest price among time slots $s + 1$ to e, which is

$$\chi_m \leftarrow \sum_{j=1}^{J} c_j \sum_{l=m}^{e-s} n(l, j, s, e).$$

10:          **end for**

11:          **for** $k = s + 1$ **to** e **do**

12:              Update the charging power $\mathcal{P}_k$ for time slot k:

$$\mathcal{P}_k \leftarrow \mathcal{P}_k + \chi_{R_{s+1,e}(\tau_k)}.$$

13:          **end for**

14:      **end for**

15: **end for**

16: **return** $\mathcal{P}_k$

---

reduced (half) power if this capability is provided by the charger, or for some other combination of time slots/power level if the battery charging tail end profile is considered. The proposed Algorithm 1 would use the first 30 slots of the 4–5 a.m. interval, because of its definition of the ranking function $\mathcal{R}$ (see step 7). Various other minimum-cost algorithms, each using a different slot selection algorithm, can be conceived. This flexibility could be used to provide regulation services to the power system [54].

The relative ranking of hourly day-ahead LMPs will probably not be affected under a mild PEV penetration level, say, within the next five to ten years. However, this could occur under higher PEV penetration levels. In this case, the aggregator would use a modified min-cost

scheduling algorithm, whose basic idea is as follows: First, PEV load will be scheduled during the cheapest hour of day, until the price becomes equal to the second cheapest price. After this point, additional PEV load will be distributed between these two hours of the day. If the PEV load makes the price reach the level of the third cheapest price, then any additional PEV load will be distributed over these three hours, and so forth. The use of advanced day-ahead LMP forecasting algorithms, such as the ones in [57–60], will be again necessary.

4.4.2 Dispatch

The purpose of the proposed dispatch algorithm (Algorithm 2) is to distribute the purchased energy to the PEVs, with as little deviation from the schedule ($\mathcal{P}_k$) as possible. It is assumed that the aggregator does not engage in arbitrage. The charger ratings (p_i) of all PEVs controlled by the aggregator are known beforehand. The algorithm keeps running throughout the nightly charging period, and dynamically updates the list of PEVs and their charging time slots. The plug-in time (s_i) and required energy ($\mathcal{E}_i$) are communicated by PEV i to the aggregator as soon as it is plugged in. Simultaneously, the PEV owners report their expected departure time (e_i). For the vehicles that are expected to depart after the end of the charging period, the departure time is set to K. The charging duration (l_i) is calculated based on the above information, from $\mathcal{E}_i = \Delta T l_i p_i$. Decisions are made dynamically in real time for each arriving PEV, which is assigned the next l_i least expensive time slots, as long as these slots still have available power. At time slot k, if $k \in \mathcal{H}_i$, the aggregator charges PEV i with rate p_i. It should be noted that Algorithm 2 is not an optimization algorithm. However, its design is related to Algorithm 1, because it also uses the same ranking function R.

4.5   Simulation Results

Figure 4.7 depicts the average load per PEV (i.e., all PEVs under contract, including those do not travel or return home) that would be obtained from Algorithm 1 with a hypothetical day-ahead LMP variation. The Algorithm is run using 1 minute-long time slots, while the price changes on an hourly basis. As can be observed, at the beginning of each hour, the PEV load has a relatively large spike that decreases with time, due to those PEVs that finish charging

---

Algorithm 2 Dispatch

1: Input: $\mathcal{P}_k$ for $k = 1, \ldots, K$, and p_i for $i = 1, \ldots, N_x$.
2: **loop**
3:     **if** PEV i arrives at home and gets plugged in **then**
4:         Receive $\{\mathcal{E}_i, s_i, e_i\}$. Calculate l_i.
5:         Rank the time slots $\{k : s_i + 1 \leq k \leq e_i$ and $\mathcal{P}_k > 0\}$ according to τ_k, from lowest to highest. The rank of slot k is denoted by $R_{s_i+1,e_i}(\tau_k)$.
        $\{\mathcal{P}_k \leq 0$ corresponds to the case where the purchased power at time slot k has been exhausted.$\}$
6:         $\mathcal{H}_i \leftarrow \{k : R_{s_i+1,e_i}(\tau_k) \leq l_i\}$.
7:         $\mathcal{P}_k \leftarrow \mathcal{P}_k - p_i$, for all $k \in \mathcal{H}_i$.
8:     **end if**
9: **end loop**

---

before the hour is over. This load shape is quite different from a traditional load variation. If the penetration of PEVs becomes significant, these abrupt step changes (both upwards but also downwards at the start of each hour) could be problematic for frequency regulation and transient system stability. Perhaps a better solution for the power system would be to average the PEV load throughout the hour. To achieve this, for example, the ranking function $\mathcal{R}$ could be modified so that there is no preference for earlier time slots. This yields the load profile shown in Figure 4.8.

Algorithm 2 (dispatch) is applied to a set of trips randomly generated based on the NHTS data, different than the one used for the scheduling algorithm. In particular, the departure of PEVs at times different from the reported ones is modeled as a Gaussian error term: $e_i^{\text{true}} = e_i + \mathcal{N}(0, \sigma)$. A 10-minute standard deviation is chosen. Since most of the vehicles leave after 7 a.m., such errors are quite insignificant. Even for those PEVs that depart before 7 a.m., an earlier departure may not cause a problem, because their charging might be complete before their actual departure time. The dispatch obtained by Algorithm 2 is shown in Figure 4.7 together with the scheduled load that was previously determined from Algorithm 1. The two curves are almost identical.

Aggregators would have to purchase the estimated average hourly power consumption as hourly energy blocks in the day-ahead market (or by a long-term bilateral contract). Hence,
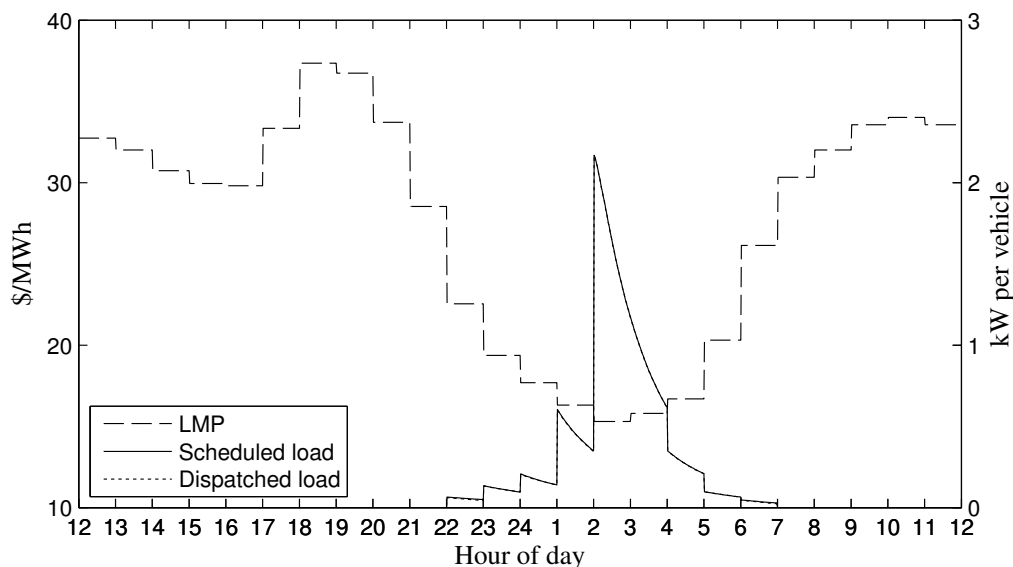
Figure 4.7   LMP and PEV scheduled load obtained by Algorithm 1. Also shown is the PEV load dispatch obtained by Algorithm 2, which is almost identical to the scheduled load curve.

it could be argued that any aggregator would level its hourly load in order to match its actual consumed power with the amount purchased. This would minimize the deviation of its real-time load from the purchased power, reducing (and ideally eliminating) potential penalties or losses incurred from being forced to participate in the real-time markets.

Nevertheless, even this "flatter" load variation is atypical. Even without the pronounced spikes at the beginning of the hour, the step changes—if large enough—could cause problems to system frequency regulation. As mentioned in the Introduction, PEV fleets can be used to provide regulation services to the system to alleviate generation-load unbalance [4, 52–54], whereas the PEV load shape obtained by the min-cost scheduling algorithm will require additional regulation at the beginning of each hour from other sources. (This becomes apparent once the maximization of energy trading-related profits becomes an objective. Previous work on PEV-related frequency regulation has not identified this issue.) Power systems routinely handle MW-level step changes in load, for example, from large industrial customers. The potential problem described here stems from the sheer impact of a large aggregate PEV load (such as several million PEVs in the MISO system that would cause hourly steps on the order of hundreds of MW) coupled with its controllability. This will tend to synchronize the step
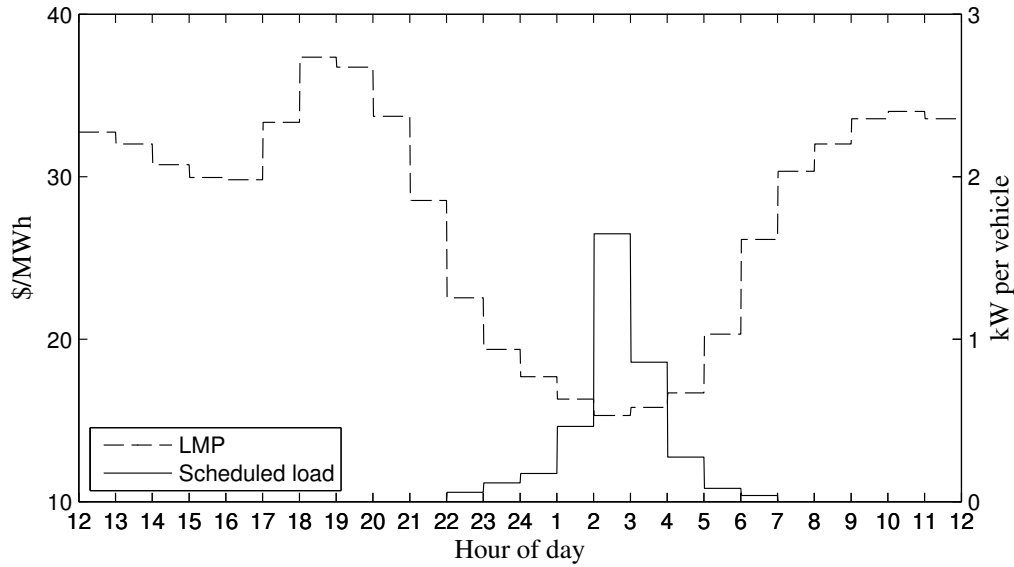
Figure 4.8   LMP and hourly PEV load obtained by a modified Algorithm 1 that uses an alternate ranking function, which has no preference for the earlier time slots.

changes at the beginning of the hour among all aggregators in the system, especially if the prices are calculated on a zonal rather than a nodal basis, or for metropolitan areas with a single LMP where large concentrations of PEVs would exist. This phenomenon could be made less pronounced by purchasing the bulk of the energy via long-term bilateral contracts.[4] Also, the difference of LMP prices at different nodes throughout the power system could be beneficial, unless the correlation of LMP time variation is significant throughout the system. A more accurate analysis that will use LMP calculations obtained from an optimal power flow formulation is left for future study, which should take into account the impact of the additional PEV load on the LMP levels, whose relative ranking is assumed to be predefined in this analysis. But regardless of the calculated LMP levels, the resulting waveform of aggregated PEV power load will probably still have a similar staircase shape, with the bulk of the energy consumed during the hour of lowest LMP.

Aggregators also have the option to bid a price-sensitive load curve in the day-ahead market, but this complicates the scheduling process considerably. To see why this is so, consider the

---

[4]Applying Algorithm 1 to a bilateral long-term contract with a single off-peak price yields an average power consumption that is identical to the curve of Figure 4.2 (b). A large step change in load would still occur, but only once.

case where the contract between the aggregator and the PEV owners stipulates that PEVs must be maximally charged overnight. Assume that during hour h, high prices lead to some PEV load not being served. This lost energy must be acquired during hour $h + 1$ or later. However, the price-sensitive bids are submitted one day in advance, and cannot be modified. This will force an aggregator to acquire the energy deficit in the real-time market, and will increase its financial risk. (Even so, it is not clear at which hour it would be advantageous to purchase the deficit.) So, bidding price-sensitive loads might be a problematic strategy.

The currently implemented two-settlement market structure has been devised with the traditional slowly varying bulk power system load in mind, which has relatively minor real-time deviations. But an emerging controllable PEV fleet represents an important new constant-energy load paradigm, which requires a certain amount of electric energy over a specific period of time, and for which the exact time and rate of power consumption are not critical to the end-user. Our results seem to suggest that perhaps the existing market mechanisms should be modified, in order to provide the appropriate incentives to the PEV aggregators, so that the power system operation is not compromised. For example, it might be beneficial to smoothen the PEV load variation; however, a hypothetical aggregator today would have no incentive to do so, and in fact it might be penalized for deviating significantly from the purchased load level. Perhaps new regulations that impose maximum ramp up/down rates to aggregated PEV loads are necessary, in addition to the ones already in place for generating units. Alternatively, it might be beneficial to use the PEV load to fill the overnight valleys of the overall system load; this has been previously suggested to be one of the major benefits of PEV integration with the power system. Apparently, this will not be the case if aggregators participate in the wholesale energy markets, because the obtained load will not have the required pattern that will exactly level the load curve. The design of appropriate market-based mechanisms remains an open research question.

4.6   Conclusion

This paper set forth algorithms for the scheduling and dispatch of electric power by aggregators of PEV fleets, whose main objective is the maximization of energy trading profits. The

aggregators are assumed to operate in the current wholesale electric energy market framework. The algorithms were developed by taking into account realistic vehicle travel patterns from the NHTS database. The impacts of such fleets on the bulk power system were estimated with computer simulations. A major implication of our findings is that current market regulations and policies associated with PEV load have to be revised, to avoid causing problems to the power system, and to incentivize its utilization in a synergistic manner in order to improve the overall system operation, especially for aggregators without interest in ensuring power system reliability.

5. ON THE CHOICE BETWEEN UNCONTROLLED AND CONTROLLED CHARGING BY OWNERS OF PHEVS

Di Wu, Dionysios C. Aliprantis, and Lei Ying

Abstract

This letter analyzes the decision-making process of owners of plug-in hybrid electric vehicles (PHEVs), when choosing between uncontrolled and controlled charging programs. The minimization of energy cost leads to a set of outcomes determined by electricity and gasoline prices, and impacts the electricity rates of PHEV aggregators.

Index Terms

Aggregators, plug-in hybrid electric vehicles.

5.1 Introduction

Owner of plug-in hybrid electric vehicles (PHEVs) will have the option to choose between two different charging programs: (i) uncontrolled charging (i.e., completely unrestricted, similar to any other appliance) with a regular retail electricity price, and (ii) controlled off-peak charging with a reduced price, offered by PHEV aggregators [4, 52]. Aggregators will coordinate PHEV charging so that it does not occur during peak power system load hours, or so that it does not overload distribution transformers, and will provide ancillary services to the

power system, and thus are expected to play a central role in tomorrow's smart grid. Arguably the most significant factor affecting this decision will be the total energy cost, consisting of expenses for electricity and gasoline.

In this letter, the decision-making process of a cost-conscious PHEV owner who is trying to minimize his/her transportation energy costs is studied. The analysis leads to a set of outcomes determined by the prices of electricity and gasoline, and yields certain interesting insights pertaining to the pricing of electricity by PHEV aggregators. It is shown that under certain conditions, some PHEV owners might prefer uncontrolled charging, thus reducing the market share of aggregators and the benefits of coordinated PHEV charging to the electric power system. It should be emphasized that this letter does *not* delve into the factors that affect the decision of whether to purchase a PHEV or not; rather it is assumed that this decision has been already made.

5.2 Decision-Making Process of PHEV Owners

The operation of PHEVs can be classified into the charge-depleting (CD) and the charge-sustaining (CS) modes [28, 63]. Therefore, the daily vehicle-miles-traveled (VMT), m, can be split into miles in CD and CS modes, $m = m_{\mathrm{cd}} + m_{\mathrm{cs}}$. In the CD mode, the vehicle gradually consumes the energy stored in the batteries, with either a fraction of or the entire tractive energy coming from the battery pack. When a minimum state of charge is reached, the CS mode is activated, and PHEVs operate similarly to conventional hybrid electric vehicles, with all tractive energy coming from the gasoline in the tank.

Therefore, the daily electric energy consumption at the wall outlet can be estimated by

$$\epsilon_e = \frac{\xi h_{\mathrm{tr}} m_{\mathrm{cd}}}{\eta_e} \,, \tag{5.1}$$

where $\xi \leq 1$ is the fraction of tractive energy from electricity in the CD mode, h_{tr} is the required tractive energy per mile at the wheels, and η_e is the wall-to-wheels efficiency. A method to estimate ϵ_e has been presented in [48].

On the other hand, gasoline can be consumed during both the CD mode (under blended operation) and the CS mode. If the tank-to-wheels efficiency (η_g) is assumed the same for both

modes[1], the daily gasoline energy consumption is

$$\epsilon_g = \frac{(1-\xi)h_{\text{tr}}m_{\text{cd}} + h_{\text{tr}}m_{\text{cs}}}{\eta_g} = \frac{h_{\text{tr}}(m - \xi m_{\text{cd}})}{\eta_g}. \tag{5.2}$$

Denoting by r_e the residential retail electricity price for uncontrolled charging (\$/kWh), by e_g the energy content of gasoline (36.6 kWh/gallon higher heating value), and by r_g the retail price of regular gasoline (\$/gallon), a PHEV's daily energy cost in the uncontrolled charging program is expressed

$$C = \frac{r_g h_{\text{tr}} m}{e_g \eta_g} + \xi h_{\text{tr}} \left(\frac{r_e}{\eta_e} - \frac{r_g}{e_g \eta_g} \right) m_{\text{cd}}. \tag{5.3}$$

Here, r_e/η_e and $r_g/(e_g\eta_g)$ have the physical significance of *price of tractive energy* (at the wheels) for electricity and gasoline, respectively. A cost-conscious PHEV owner will try to minimize C, and it is obvious from (5.3) that—all other things being held constant—this decision will be based on the relation between electricity and gasoline prices.

When $r_e/\eta_e > r_g/(e_g\eta_g)$, it is cheaper to drive PHEVs with gasoline instead of electricity. The PHEV owner would decide to make $m_{\text{cd}} = 0$ by never charging the vehicle, thus avoiding consuming any electricity from the grid, and would just keep driving in the CS mode. Conversely, when $r_e/\eta_e < r_g/(e_g\eta_g)$, the PHEV owner would take advantage of all opportunities to charge the vehicle (wherever a charging infrastructure is in place: at home, at work, at the shopping mall, etc.), in order to maximize electricity usage and m_{cd}.

In the U.S., the average residential retail electricity price in 2010 was ca. 0.12 \$/kWh, and is expected to remain at similar levels over the next 25 years [64]. The annual average retail gasoline price in the U.S. has been higher than 2 \$/gallon since 2005, and is expected to increase to 4–6 \$/gallon in the next 25 years (in today's dollars) [65]. Given that $\eta_e \approx 0.65$–0.70 [48] and $\eta_g \approx 0.25$–0.3, it can be readily verified that using electricity rather than gasoline to power PHEVs makes financial sense in most of the U.S. today. For example, in Iowa during 2009, the average $r_e \approx 0.10$ \$/kWh, while the average $r_g \approx 2.3$ \$/gallon, making the tractive energy price of electricity about 60% that of gasoline. Nevertheless, there are some states where retail electricity price is quite high. Such an example is Hawaii where, in 2009, the two rates were

---

[1]PHEVs may have different tank-to-wheels efficiencies in CD vs. CS mode [63], but this (small) difference is ignored herein.

$r_e \approx 0.24$ \$/kWh and $r_g \approx 3.0$ \$/gallon, so the cost of moving PHEVs with electricity would have been about 9% higher.

In the controlled off-peak charging scenario, a PHEV owner relinquishes control of the battery's state of charge, in exchange for a reduced electricity rate ($r_e' < r_e$). In this case, some charging that normally would have occurred during on-peak hours may not be allowed by the aggregator, and so a fraction α of the daily VMT may shift from the CD to the CS mode, hence a greater portion of the tractive energy would be derived from gasoline. Using the simulation method and parameters of [48], based on the 2009 National Household Travel Survey, a statistical analysis on α has been performed, revealing that $\alpha = 0$ for a significant portion of PHEVs, but reaching values as high as $\alpha = 0.5$ (or more) for the remaining PHEVs. The energy cost for controlled charging is (cf. (5.3))

$$C' = \frac{r_g h_{\text{tr}} m}{e_g \eta_g} + \xi h_{\text{tr}} \left(\frac{r_e'}{\eta_e} - \frac{r_g}{e_g \eta_g} \right) (1 - \alpha) m_{\text{cd}} \,. \tag{5.4}$$

The choice of charging program depends on the cost difference

$$C' - C = \xi h_{\text{tr}} m_{\text{cd}} \left[\frac{(1 - \alpha) r_e' - r_e}{\eta_e} + \frac{\alpha r_g}{e_g \eta_g} \right] \,. \tag{5.5}$$

The owner will benefit from joining the controlled charging program only if $C' < C$, which requires

$$r_e' < r_e + \frac{\alpha \eta_e}{1 - \alpha} \left(\frac{r_e}{\eta_e} - \frac{r_g}{e_g \eta_g} \right) = r_e + R \,. \tag{5.6}$$

It is interesting to note that the condition above is independent of (i) ξ, or drivetrain design; (ii) the tractive energy, related to PHEV weight/type; and (iii) m_{cd}, related to battery size.

In summary, the following four cases are identified:

1. If

$$\frac{r_e}{\eta_e} > \frac{r_e'}{\eta_e} > \frac{r_g}{e_g \eta_g} \,, \tag{5.7}$$

then the PHEV owner will prefer driving solely on gasoline, and will never charge the vehicle's battery. All the miles traveled will be driven in the CS mode.

2. If

$$\frac{r_e}{\eta_e} > \frac{r_g}{e_g \eta_g} > \frac{r_e'}{\eta_e} \,, \tag{5.8}$$

then the inequality (5.6) is satisfied. Therefore, the PHEV owner will prefer the controlled charging program.

3. If

$$\frac{r_g}{e_g \eta_g} > \frac{r_e}{\eta_e} > \frac{r'_e}{\eta_e} \tag{5.9}$$

and (5.6) is satisfied, then the PHEV owner will subscribe to the controlled charging program.

4. If

$$\frac{r_g}{e_g \eta_g} > \frac{r_e}{\eta_e} > \frac{r'_e}{\eta_e} \tag{5.10}$$

and (5.6) is not satisfied, then the PHEV owner will join the uncontrolled charging program.

5.3   Concluding Remarks

Based on today's and forecast energy prices, the most probable situation will be either case 3 or 4 (otherwise, with gasoline price lower than electricity, it is unlikely that PHEVs will become popular), where the owner's decision depends on (5.6). A key observation is that setting r'_e slightly below r_e will not suffice to attract every owner; the two rates must differ by at least $|R|$ (an owner-specific parameter), which could be substantial. For example, assuming typical values, $\eta_e = 0.7$, $\eta_g = 0.25$, and $\alpha = 0.2$ for a certain driver, and prices $r_e = 0.12$ \$/kWh and $r_g = 3.5$ \$/gallon, then an aggregator should set its rate $r'_e < 0.083$ \$/kWh to attract this owner. If r_e represents a discounted overnight rate of a time-of-use program, then the aggregator would have to reduce its rates further (e.g., $r_e = 0.08$ \$/kWh leads to $r'_e < 0.033$ \$/kWh). On the other hand, aggregators would be able to increase rates when the price differential between electricity and gasoline is smaller. Alternatively, (5.6) implies that the aggregator should carefully design its control algorithms in order to minimize the "leakage" factor α, while avoiding expensive on-peak charging or overloading distribution circuits.

The average excise tax on gasoline today in the U.S. is 0.48 \$/gallon, of which 0.184 \$/gallon is a federal tax that feeds the Highway Trust Fund (HTF), which has not been adjusted for inflation since 1993. These monies are used to maintain the Interstate Highway System and state/local roads. Due to the higher fuel efficiency of modern automobiles, the HTF has been

recently plagued by a severe capital shortage, which will certainly become worse with the advent of PHEVs, unless this tax is extended to the PHEV owners (as users of the same transportation infrastructure). If such a tax (on the order of few cents per kWh) were to be imposed equally on uncontrollable and controllable PHEV load, it would not affect the difference between r_e and r'_e, but it would affect R (a convergence of electrical and gasoline tractive energy costs would occur). This would have a positive impact on aggregators' market share and revenue, but a negative impact on the transportation costs of individual PHEV owners.

6.   POTENTIAL IMPACTS OF AGGREGATOR-CONTROLLED PLUG-IN ELECTRIC VEHICLES ON DISTRIBUTION SYSTEMS

A paper published in the *Proceedings of the 4th IEEE International Workshop on Computational Advances in Multi-Sensor Adaptive Processing*, San Juan, Puerto Rico, Dec. 13–16, 2011, pp. 105–108.

Di Wu, Chengrui Cai, and Dionysios C. Aliprantis

Abstract

This paper presents potential impacts on distribution systems from light-duty plug-in electric vehicles (PEVs), when these are under the control of aggregators who desire to maximize their energy trading-related profits. The electric load characteristics of light-duty PEVs are developed using the travel pattern from the 2009 National Household Travel Survey. This PEV load is added to the existing non-PEV load within one of the prototypical feeders developed by the Pacific Northwest National Laboratory.

Index Terms

Aggregator, plug-in electric vehicles, power distribution, travel pattern.

6.1   Introduction

Plug-in electric vehicles (PEVs) can help reduce worldwide dependence on petroleum and carbon emissions [1, 47]. Some reports predict one million PEVs on U.S. roads within 5–10 years. The emerging PEV fleet will represent an additional load on the power system. In the

simplest case, this load can be treated the same as a traditional (i.e., uncontrollable) load, being served whenever a PEV is plugged in, and billed at a normal retail rate. In this case, a substantial amount of PEV charging will take place during peak hours [20, 23, 26, 48, 49, 51], increasing the generation cost, and requiring additional investment in generation capacity to maintain the reliability level. On the other hand, PEVs are more flexible than traditional load, because the majority of drivers return home early in the evening, and may not have a preference about the exact time when their vehicles will be charged, as long as the vehicles are ready for use by the next morning. To utilize this flexibility, appropriate charging control and management are required. Such a role could be played by PEV aggregators—either existing utilities that will offer new financial contracts specific for PEV loads, or new for-profit entities that will participate in the wholesale electricity market [4]. Understanding the potential impacts on distribution systems from aggregator-controlled PEVs is important for adapting planning and operation procedures, thereby accelerating the adoption of PEVs. In particular, this paper studies potential distribution system impacts from light-duty PEVs under the control of aggregators whose objective is the maximization of energy trading-related profits.

The rest of this paper is organized as follows: In Section 6.2, key assumptions and assessment tools are presented. Section 6.3 proposes the evaluation method, where the uncertainty in the connecting network location and individual PEV daily power consumption are taken into account. In Section 6.4, simulation results are discussed. Section 6.5 concludes the paper.

6.2 Key Assumptions and Assessment Tools

Aggregated PEVs can be used to provide ancillary services to the power system [4]. Revenue maximization from frequency regulation (one of the possible ancillary services) has been studied in [53, 54]. In contrast to previous work, the aggregators considered herein wish to maximize their profits from energy trading [66]. Such PEV aggregators will purchase the electric energy at wholesale by participating in the day-ahead markets, and then resell it to PEV owners at a predetermined fixed rate. The contracts will stipulate that PEVs are restricted to be charged only during off-peak hours, e.g., from 10 p.m. to 7 a.m. (This is reasonable because most of the vehicles are not in use and the wholesale electricity is inexpensive during this period.) Also,

aggregators are required to maximize the state of charge of the batteries within the specified charging period. As a reward for being restricted to a certain charging period and releasing the control of charging, PEV owners will receive a fixed retail rate which should be lower than the normal retail rate, and even lower than off-peak (time-of-use) rate for traditional non-PEV load. Therefore, the aggregator's profit will be maximized when the purchased energy cost will be minimum.

To achieve this, it is assumed that the aggregator utilizes advanced forecasting techniques for the day-ahead electricity locational marginal prices (LMPs), such as the ones presented in [57–60]. It is important to note that the LMP forecast's absolute value is not critical. Rather, for cost minimization, it is the ranking of the hourly LMPs that is critical, and should be predicted as accurately as possible [66].

In addition, the aggregator needs the statistics of electric energy consumption, charging duration, and arrival and departure time of the PEV fleet under control. Such data can be obtained by monitoring the actual composition, travel pattern, and energy consumption of the fleet as the penetration of PEVs increases in the future. For this analysis, synthetic data are generated by using the 2009 National Household Travel Survey (NHTS) database [34] in conjunction with certain assumptions about PEV drivetrain configuration and charger sizes [48]. It should be noted that this study only considers light-duty vehicles[1], which account for ca. 96% of household vehicles. Other vehicles, such as motorcycles, or other types of trucks are neglected.

The electric distribution system is modeled using one of the prototypical feeders provided by the Pacific Northwest National Laboratory (PNNL), which has developed a taxonomy of 24 prototypical feeder models that contain the fundamental characteristics of radial distribution feeders found in the U.S., based on 575 distribution feeders from 151 separate substations from different utilities across the nation [67, 68]. GridLAB-D [69] is used as a simulation platform. The PNNL feeder named R1-12.47-4 (feeder No. 4 with 12.47 kV primary distribution voltage in climate region 1) is selected for evaluation. This feeder serves 793 end-user loads, which

---

[1]The U.S. fleet of light-duty vehicles consists of cars and light trucks, including minivans, sport utility vehicles (SUVs), and trucks with gross vehicle weight less than 8,500 pounds [29].

include 652 residential and 141 commercial loads. The feeder is modeled with high fidelity from the substation down to the individual customer meters, including detailed end-use load representations (heating, ventilation, and air conditioning, and various other constant power, current, and impedance loads). It should be noted that some of the provided distribution transformers by PNNL were found to be improperly rated considering the load they serve, and had to be changed (their ratings had to be increased). The determination of appropriate distribution transformer size can be formulated as an optimization problem [70, 71]. In this study, the distribution transformers are reselected from the standard ratings [72] so that the insulation life (estimated based on IEEE Standard C57.91 [73]) is roughly no less than the normal insulation life without any PEV load.

6.3   Evaluation Method

The potential distribution system impacts from aggregator-controlled PEVs are studied for three PEV penetration levels: 10%, 25%, and 50%. Due to the uncertainty in the network location and individual PEV daily power consumption, the PEV load will exhibit a large degree of spatial and temporal diversity. Hence, a stochastic analysis is performed using 100 Monte Carlo simulations for each penetration level. In an uncontrolled charging scenario, the evaluation of PEV impacts during summer peak-hour days would be critical, because PEV load is superimposed on the traditional load peaks. However, for aggregator-controlled PEVs, where charging occurs during off-peak hours, it is not necessary to focus on summer peak-hour days. So, 100 randomly selected days selected from 2009 are used in the Monte Carlo simulations.

6.3.1   Spatial Diversity

To take into account the uncertainty of a PEV's connecting location, the probability mass function (PMF) of number of vehicles for a random household in the U.S. is obtained from [34]. In each simulation, the number of vehicles per residence is randomly generated based on the PMF in Table 6.1. The probability for a random vehicle to be a PEV is (by definition) the PEV penetration level.

Table 6.1   Vehicles per Household

Veh/HH	0	1	2	3	4	5	≥ 6
Prob.	0.087	0.323	0.363	0.144	0.053	0.019	0.01

6.3.2   Temporal Diversity

PEV aggregators who desire to maximize their profits from energy trading will schedule and dispatch the PEV load so that their energy cost is reduced (ideally minimized), using forecast information about the wholesale electricity price and the charging demand for the coming day. A PEV load repository is developed using the algorithms proposed in [66] with the travel pattern obtained from the 2009 NHTS, and certain assumed drivetrain parameters and charging circuits. This repository includes 141011 daily PEV load curves (including PEVs that do not travel on that specific day). The daily power consumption of individual PEVs in the distribution feeder is randomly selected from the repository.
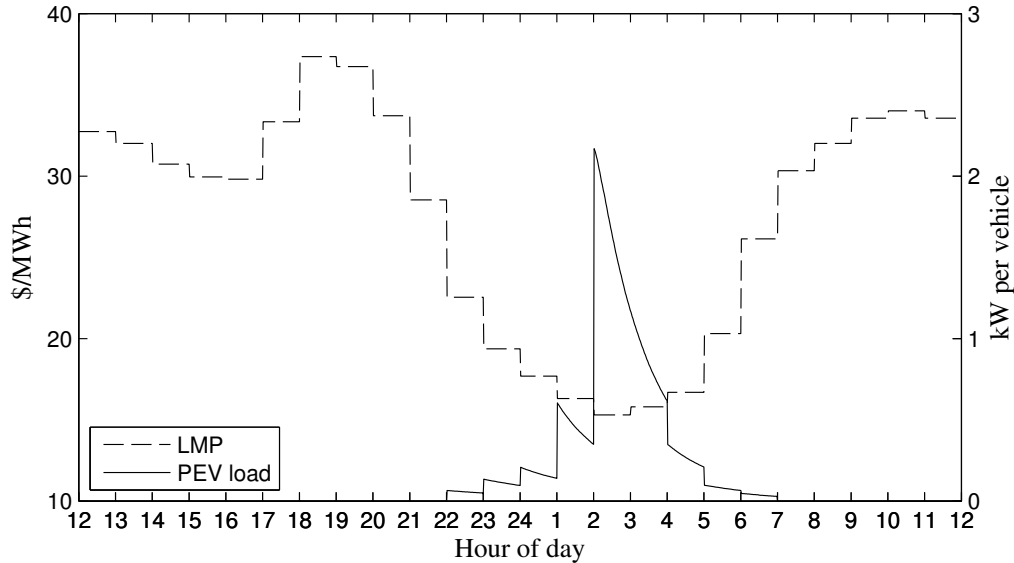

Figure 6.1   LMP and average PEV load.

Figure 6.1 depicts the average load per PEV within the repository that would be obtained under the energy cost minimization control strategy with a hypothetical day-ahead LMP variation. In the day-ahead market, the electricity price changes on an hourly basis. However, the

aggregator runs its scheduling and dispatch algorithms at a finer time resolution, say, using one minute-long time slots. So, all time slots of each hour have equal LMP. Nevertheless, the earlier time slots are favored because the sooner the vehicle starts charging, the more likely it can be fully charged by its departure time. Moreover, most PEVs' charging time is not an integer number of hours so, at the beginning of each hour, the PEV load has a relatively large spike that decreases with time due to those PEVs that finish charging before the hour is over.

6.4 Results and Discussion

This section discusses the simulation results regarding to asset loading, customer voltage, unbalanced phase loading, and system losses.

6.4.1 Loading

The daily peak of the power consumption of this feeder is below 60% of its rating (5334 kVA) except a small number of days in a year. It is not uncommon to design a feeder in such a way to ensure the ability to transfer load from adjacent feeders under emergency conditions. Due to the large amount of remaining capacity, adding PEV load during off-peak hours will not overload either substation transformer or primary trunks that are far away from the customer end. For example, the average apparent power consumption (in percentage of the feeder rating) at the substation under various penetration levels is shown in Figure 6.2.

However, the assets closest to customers are sensitive to overloading because i) no redundant capacity is reserved for reliability purposes; ii) they do not benefit much from spatial and temporal diversity [49]. For example, the average apparent power consumption (in percentage of the rating) for transformer 14—a center-tapped (3-wire single-phase) transformer that steps voltage from 7.2 kV down to 120 V and 240 V for 30 residential houses—under various penetration levels is shown in Figure 6.3. While exceeding normal ratings will not necessarily result in an immediate device failure, it does effectively reduce the insulation lifespan of the transformer [73]. In [25], it was shown that a distribution transformer's yearly failure rate could increase from 10% to 17%, which would increase utilities' expenses.
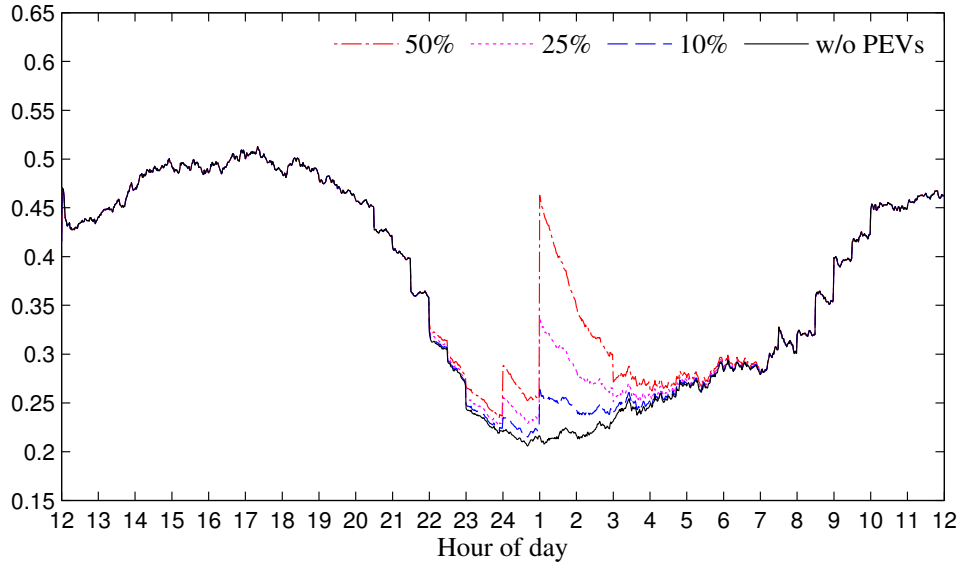
Figure 6.2   Average apparent power consumption at substation.
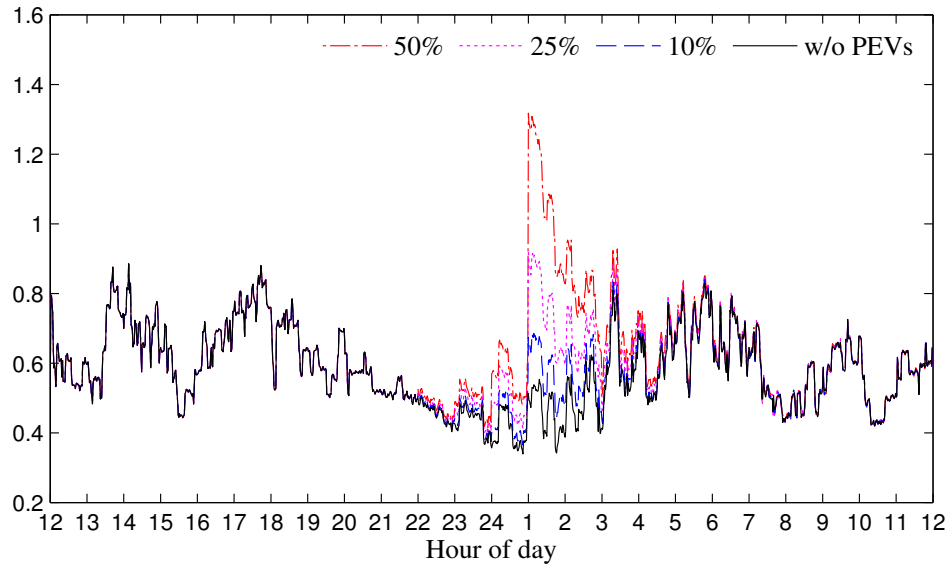
Figure 6.3   Average apparent power consumption for transformer 14.

6.4.2   Voltage Levels

The ANSI standard C84.1 [74] requires that the service voltage[2] remains within five percent from the nominal value (114∼126 V) at the customer level. Without PEVs and under mild

---

[2]Service voltage is the voltage at the point where the electrical system of the supplier and the electrical system of the user are connected.

penetration levels, such a requirement is satisfied for all the residential customers within the distribution system in all the simulations. However, low-voltage violations are detected for 50% penetration level. Figure 6.4 shows the minimum voltage of the distribution system in one simulation. As can be seen, the voltage is lower than 114 V for some residential customers for approximately 25 minutes, and occurs in 9 out of 100 simulations. This indicates that aggregator-controlled PEVs could create voltage problems.
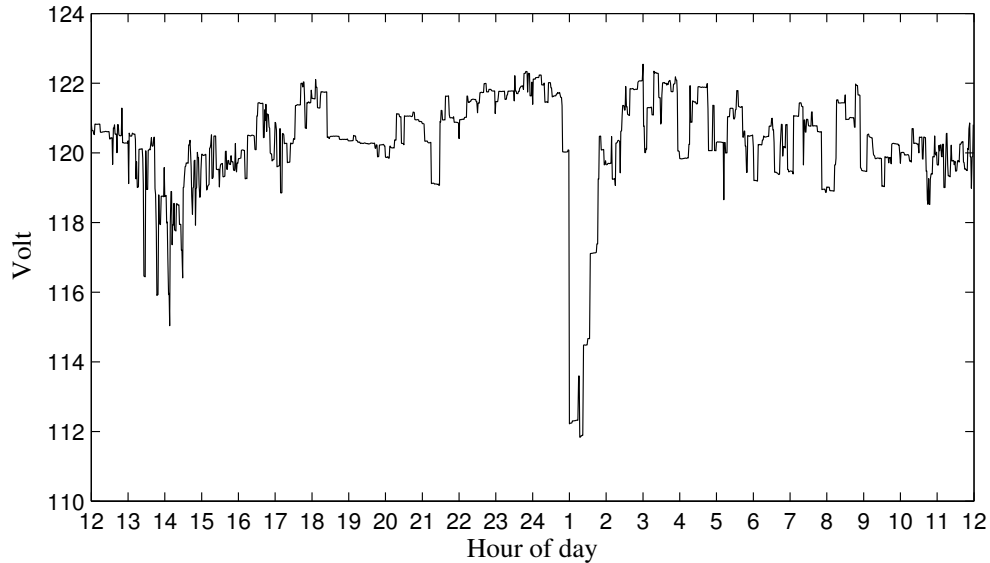
Figure 6.4   Minimum voltage within the distribution system.

6.4.3   Phase Unbalance

Although the actual distribution feeders are typically unbalanced in nature, aggregator-controlled PEVs could exacerbate this issue during the charging period. As an example, apparent power consumption in each phase at the substation from one simulation is shown in Figure 6.5. The load unbalance deteriorates the performance of the distribution system. Unbalanced loads cause voltage asymmetry which is harmful for customers' three-phase load, excessive losses and heating in three-phase electric machines and transformers, and inefficient utilization of feeder capacity [75]. Zero-sequence currents resulting from the unbalanced loads can cause not only extra power losses in neutral lines but also protection and interference problems [76]. In addition, zero-sequence currents may interfere with neighboring communication

circuits and induce voltages in gas pipelines through inductive coupling [77]. Possible measures to mitigate the above negative impacts include reactive power compensation [78] and feeder reconfiguration [79].
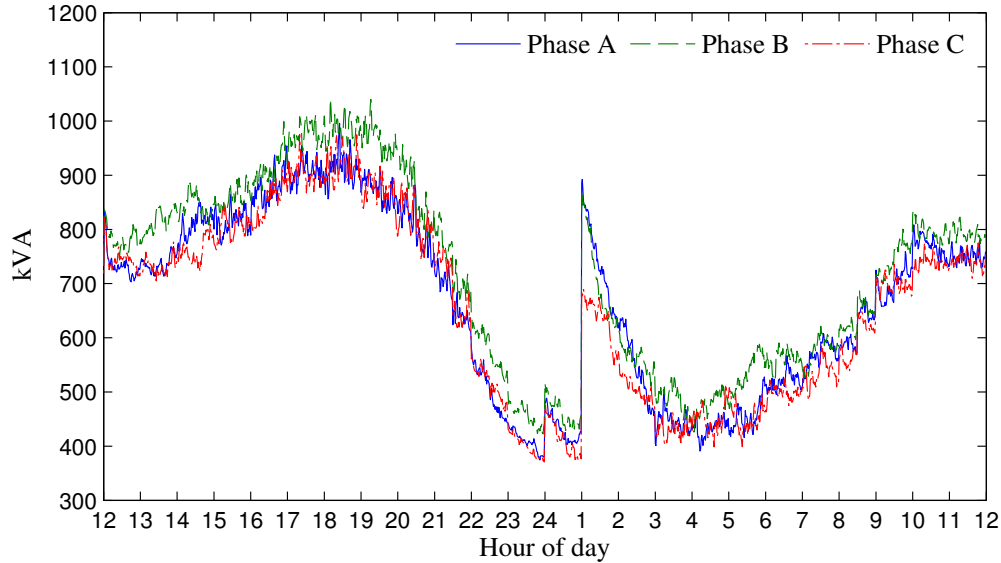
Figure 6.5   Average apparent power consumption in each phase.

6.4.4   Losses

The added PEV load will increase the system's ohmic losses. However, for the feeder under study, it is found that the distribution losses are less than one percent of the overall power consumption. (This low percentage is consistent with what is reported in [61].) The additional losses from charging PEVs are negligible. It should be noted that the losses could be higher for other distribution systems.

6.4.5   Recommendations

These negative impacts could be mitigated by modifying the control strategy. The performance metric of interest (such as asset loading, customer voltage, or system losses) could be perhaps incorporated into the optimization constraints or the objective function. The desired power consumption of each individual PEV from the optimization results can be realized by modulating the charging power magnitude (for chargers with such capability) or adjusting the

charging duration (turning the chargers on and off) [54]. However, this can reduce the aggregators' profits from energy trading. Without suitable incentives (or regulations), aggregators (especially those who do not have an interest in maintaining the distribution system's reliability) will have no motivation to modify their control strategy. Finally, the associated impact in battery lifespan from frequent charging cycles is another concern.

6.5   Conclusion

This paper proposes a stochastic simulation method to evaluate the potential distribution system impacts from aggregator-controlled PEVs. The simulation results indicate that appropriate optimization and control algorithms might be beneficial in order to avoid the negative impacts caused by the PEV load.

7. MODELING LIGHT-DUTY PLUG-IN ELECTRIC VEHICLES FOR NATIONAL ENERGY AND TRANSPORTATION PLANNING

A paper to be submitted

Di Wu and Dionysios C. Aliprantis

Abstract

This paper presents models of light-duty plug-in electric vehicles, appropriate for conducting long-term national-level planning studies of the energy and transportation sectors. Four models of varying degree of complexity are set forth. Parameters for the models are obtained from a variety of sources, including the U.S. National Household Travel Survey. Three case studies of integrated energy and transportation planning are performed to illustrate portfolios of optimum investments in the two sectors over a 40-year horizon, with and without the introduction of plug-in electric vehicles in the fleet.

Index Terms

Energy planning, infrastructure, plug-in electric vehicles.

Nomenclature

a_v	Equivalent all-electric range of a plug-in electric vehicle (PEV) of technology type v.
$costVehInv_v(\mathbf{t})$	Investment cost (in today's U.S. dollars) per light-duty vehicle (LDV) of technology type v at time $\mathbf{t} \in \mathcal{T}_{\mathrm{LDV}}$.

$d_i^{E\text{-}LDV}(\mathbf{t})$	Demand for energy from LDVs at node i ($i \in \mathcal{N}_{\text{elec}}$ or $i \in \mathcal{N}_{\text{gas}}$) at time $\mathbf{t}$ ($\mathbf{t} \in \mathcal{T}_{\text{elec}}$ or $\mathbf{t} \in \mathcal{T}_{\text{gas}}$).
$d_j^{LDV}(\mathbf{t})$	Demand for LDVs (cumulative number) at node $j \in \mathcal{N}_{\text{LDV}}$ at time $\mathbf{t} \in \mathcal{T}_{\text{LDV}}$.
d_v	Charge-depleting range (CDR) of a PEV of technology type v.
$e_{\text{elec}}(d_v, \xi_v)$	Average daily electric energy demand (from the high-voltage transmission system) per PEV of CDR d_v and fuel displacement factor (FDF) ξ_v.
$e_{\text{gas}}(d_v, \xi_v)$	Average daily gasoline demand (gallons) per LDV of CDR d_v and FDF ξ_v; could represent gasoline demand of conventional and hybrid LDVs, which have $d_v = 0$.
$e_{j,v}(\mathbf{t})$	Average energy demand per LDV of technology type v at node $j \in \mathcal{N}_{\text{LDV}}$ at time $\mathbf{t}$ ($\mathbf{t} \in \mathcal{T}_{\text{elec}}$ or $\mathbf{t} \in \mathcal{T}_{\text{gas}}$).
f_x	Probability density function (PDF) of continuous random variable x, or probability mass function (PMF) of discrete random variable x.
$f_{x\|y}$	Conditional PDF (or PMF) of random variable x given y.
G	Vehicle group, according to annual miles traveled.
$h_{\text{tr},v}$	Tractive energy per mile at the wheels for a vehicle of technology type v.
$\text{I}[\cdot]$	Indicator function that equals to 1, if the condition in the bracket holds, or 0, otherwise.
m	A vehicle's miles traveled on a given day.
$m_{\text{cd}}(m, d_v)$	Miles traveled in charge-depleting mode for a PEV of CDR d_v that traveled m miles on a given day.
$m_{\text{cd}}^{\text{avg}}(d_v)$	Average (per PEV of CDR d_v) daily miles traveled in charge-depleting mode.
$m_{\text{cs}}(m, d_v)$	Miles traveled in charge-sustaining mode for a PEV of CDR d_v that traveled m miles on a given day.
$m_{\text{cs}}^{\text{avg}}(d_v)$	Average (per PEV of CDR d_v) daily miles traveled in charge-sustaining mode.
M	A vehicle's annual miles traveled.
MPG_v	Fuel economy (miles per gallon) for vehicle of technology type v. For hybrid electric vehicles, this represents the fuel economy in charge-sustaining mode.
$\mathcal{N}_{\text{elec}}$	Set of electricity network nodes.

$\mathcal{N}_{\text{gas}}$	Set of gasoline network nodes.
$\mathcal{N}_{\text{LDV}}$	Set of LDV network nodes.
$\mathcal{N}^i_{\text{LDV}}$	Subset of $\mathcal{N}_{\text{LDV}}$ containing nodes that create an energy demand at node i ($i \in \mathcal{N}_{\text{elec}}$ or $i \in \mathcal{N}_{\text{gas}}$).
r	Real discount rate.
$\mathbf{t}$	Vector that defines time for subsystem s, $\mathbf{t} = [t_1, t_2, \ldots, t_{z_s}] \in \mathcal{T}_s$. The dimension of the vector (z_s) varies among subsystems.
$\mathcal{T}_{\text{elec}}$	Domain of time for the electricity subsystem.
$\mathcal{T}_{\text{gas}}$	Domain of time for the gasoline subsystem.
$\mathcal{T}_{\text{LDV}}$	Domain of time for the LDV subsystem.
$\mathcal{T}_s$	Domain of time for subsystem s. The domain is divided into z_s levels of time scales, i.e., $\mathcal{T}_s = [1, \ldots, T_1] \times [1, \ldots, T_2] \times [1, \ldots, T_{z_s}]$, where z_s can vary among subsystems. For example, in this study, for the natural gas subsystem, time is divided into "years" and "months"; for the electricity subsystem, simulation time is divided into "years", "months", and three subdivisions of a month (see Section 7.2).
v	Vehicle technology type, $v \in \mathcal{V}$.
$vehCum_{j,v}(\mathbf{t})$	Cumulative number of LDVs of technology type v at node $j \in \mathcal{N}_{\text{LDV}}$ at time $\mathbf{t} \in \mathcal{T}_{\text{LDV}}$.
$vehInit_{j,v}(\mathbf{t})$	Number of remaining LDVs of technology type v at node $j \in \mathcal{N}_{\text{LDV}}$ at time $\mathbf{t} \in \mathcal{T}_{\text{LDV}}$ from the initially existing ones, decreasing monotonically over time.
$vehInv_{j,v}(\mathbf{t})$	Investment (number) in new LDVs (i.e., new LDVs produced) of technology type v at node $j \in \mathcal{N}_{\text{LDV}}$ at time $\mathbf{t} \in \mathcal{T}_{\text{LDV}}$.
$vehLife_v(\mathbf{t})$	Lifetime (years) of an LDV of technology type v produced at time $\mathbf{t} \in \mathcal{T}_{\text{LDV}}$.
$\mathcal{V}$	Set of LDV technologies, including conventional gasoline vehicles, hybrid electric vehicles, plug-in hybrid electric vehicles, and pure electric vehicles.
η_v	Energy conversion efficiency for PEVs of technology type v, from high-voltage electricity to kinetic energy at the wheels.
ξ_v	Fuel displacement factor (FDF) in charge-depleting mode for PEVs of tech-

nology type v, which represents the fraction of tractive energy obtained from the battery pack in charge-depleting mode.

7.1 Introduction

In the United States, the two largest consumers of energy are the electricity and transportation sectors. To power the electric grid, approximately 40 Quads of energy are absorbed annually, obtained from a mix of primary energy sources such as coal, natural gas, and uranium, whereas transportation uses approximately 27 Quads, mostly extracted from petroleum [80]. Notably, as of today there is very little interdependence between the two sectors, since petroleum provides but a fraction of the overall electricity in the U.S., and the power grid provides very little energy for transportation purposes. However, this is bound to change in the U.S. and other nations with the electrification of the transportation sector, which will involve the introduction of potentially millions of plug-in electric vehicles (PEVs) in the fleet of light-duty vehicles (LDVs). A PEV can be either a plug-in hybrid electric vehicle (PHEV) or a pure battery electric vehicle (EV). LDVs are defined as cars and light trucks, including minivans, sport utility vehicles, and trucks with gross vehicle weight less than 8,500 pounds [29]. They account for the majority of highway vehicle miles traveled, energy consumed by highway travel modes, and carbon dioxide emissions from on-road sources.

A major consequence of such a technological shift will be the reduction of our dependence on petroleum, which is an insecure and generally unsustainable energy source, and a corresponding increase of our dependence on the electric grid and its primary energy sources, including renewable resources such as hydro, wind, and solar energy. Hence, further investments will be necessary in the electric grid to support this additional load, and the operational costs of the electricity sector will change according to the mix of generation technologies adopted. On the other hand, the investment costs in the transportation sector will be different than the ones that would be incurred by conventional vehicles. Moreover, emissions from vehicle tailpipes will shift to power plants, thus affecting the net emissions of the integrated system.

This work sets forth four PEV models appropriate for studying the national energy and transportation infrastructures for long-term planning purposes in an integrated manner. The

models are implemented within an advanced planning tool called NETPLAN that has been recently developed at Iowa State University [81–83]. NETPLAN utilizes models of an array of power generation technologies, and numerous details about the existing energy transport and storage networks as well as the transportation system in the U.S. The proposed PEV models could be adapted for other planning software, such as the MARKAL/TIMES suite [84], the National Energy Modeling System (NEMS) [85], and the Regional Energy Deployment System (ReEDS) [86], which currently do not have this kind of modeling capability.

Previous related system-level work on the integration of PEVs with the power system can be classified according to the problem that has been addressed as follows: (i) charging control strategies and algorithms with various objectives [53, 54, 61, 66, 87–89]; (ii) load estimation at the distribution level [90–93]; and (iii) load estimation at the transmission level [21–23, 48, 51, 94–96]. The methods and results in the first two categories are not appropriate for studying the long-term national-scale planning problem at hand. The studies in the third category are more suitable, even though the level of modeling therein usually corresponds to the simplest of the four models that are proposed in this paper (Model 0.0). Furthermore, PEV models have not been expressly developed for studying the energy and transportation sectors in an integrated manner. For instance, the LDV submodule of the transportation module of NEMS [97] estimates the gasoline consumption of PEVs, without explicitly accounting for their electricity consumption.

The paper is organized as follows: Section 7.2 briefly describes the modeling approach of the integrated energy and transportation systems of NETPLAN. In Section 7.3, four LDV models for national energy and transportation planning are presented. Section 7.4 illustrates the implementation of the most advanced model. In Section 7.5, three case studies are discussed. Section 7.6 concludes the paper.

7.2 Modeling approach background

The modeling framework of NETPLAN permits long-term planning analyses at the national scale of the energy and transportation systems in an integrated fashion. This is depicted within the dashed frame in Figure 7.1, wherein the energy system includes coal, natural gas,
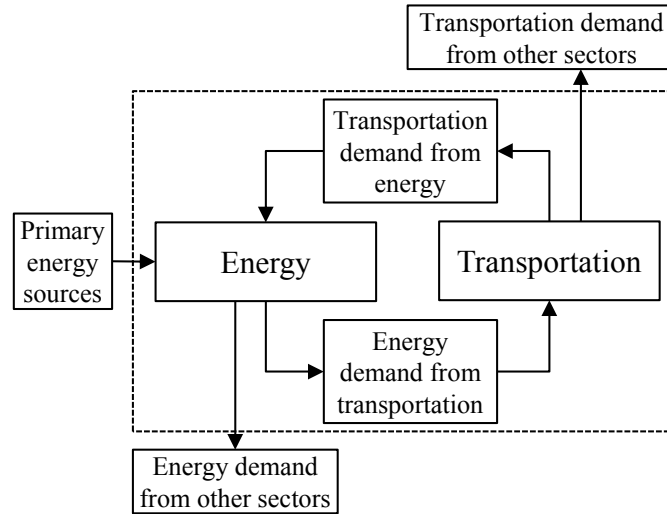
Figure 7.1   Interdependent energy and transportation systems.

electricity, and petroleum subsystems, the transportation system includes freight and passenger transportation, and "other sectors" refers to the residential, commercial, and industrial sectors. Details about NETPLAN can be found in [82, 83, 98, 99], so only a brief description is provided here.

The integrated system is modeled using networks defined by nodes and arcs. Within the energy system, nodes are used to represent points where the law of conservation of energy is enforced; they correspond to geographical region and type of energy. For example, natural gas and electricity demand at the same location is modeled using two separate nodes. Arcs connect nodes, and represent energy conversion paths (e.g., power plants) or geographical flows (e.g., natural gas pipelines). Arc flows are limited by their designated capacity, which can be increased by investment. The freight transport system is modeled as a multicommodity flow network, where flows are measured in tons. Energy conversion or transport is modeled to occur within infrastructures (e.g., power plants and natural gas pipelines). However, the modeling of commodity movements involves either infrastructures (e.g., rail and roads) or fleets (e.g., trains and heavy-duty trucks), resulting in two layers: multicommodity flows that are limited by fleet capacities, and fleet flows that are limited by infrastructure capacities. Although nodes and arcs could be formed at an arbitrary level of granularity, usually aggregations are used. The dimensions of the energy and transportation networks used in this study to model the U.S.

systems are provided in Table 7.8 on page 99.

This type of network modeling leads to the formulation of a linear program that minimizes the present value of the combined energy and transportation infrastructures' investment and operational costs over a specified period of time (on the order of years or decades), under constraints related to meeting demands on energy and transportation while satisfying the networks' capacity constraints:

$$\textbf{minimize} \quad \textit{present value of } \{investment + operational\} \textit{ costs}$$

$$\textbf{subject to}$$

$$\textit{Energy demand,}$$

$$\textit{Transportation demand,} \tag{7.1}$$

$$\textit{Capacity constraints of energy network,}$$

$$\textit{Capacity constraints of transportation network.}$$

The integrated system cost in the objective function accounts for: investments in the energy and transportation infrastructures; cost of primary energy extraction at the sources; operational costs of power plants including labor and maintenance (O&M costs); and operational costs of the transportation sector. In particular, fuel costs are accounted for at the sources and during the transportation of the primary energy carriers. Therefore, the retail cost of electricity or the fuel expenses at the pump of individual vehicle drivers are not calculated. The decision variables include capacity investments in energy infrastructure, transportation infrastructure, and transportation fleets (such as trains, heavy-duty trucks, and LDVs), and operational flows of energy and freight.

In NETPLAN, rather than selecting a single time step that is small enough to capture the dynamics of the smallest subsystem, time steps of different size are used for each subsystem in order to capture the essential dynamics and to eliminate the burden of redundant simulation details [83, 100]. The longest time scale is in terms of years (i.e., t_1 has units of years); this is common to all subsystems. A yearly time step is chosen for the coal subsystem due to its relatively slow dynamics. A monthly time step is chosen for the natural gas subsystem due to its faster dynamics. However, for the dynamics of the electric system, a time step

of one month is inappropriately large. For example, if such a time step were to be used, one could only use monthly average electric demands to represent load levels. The resulting model would be unable to represent periods of high demand when relatively more expensive peaking units (typically, natural gas plants) are committed. Therefore, the model will tend to overestimate the generation from coal-fired units and underestimate the generation from natural gas units. An hourly time step would be able to take most of the demand variability into account. Nevertheless, due to weak time coupling and redundant operating conditions [101], hours with a similar demand level can be aggregated to reduce the computational burden. This leads to the well known load duration curve (LDC), which is obtained by ordering the demand data in descending order of magnitude, rather than chronologically. Here, the LDC is discretized into three parts as described in Section 7.5, which represent the "time steps" of the electrical subsystem (strictly speaking these do not represent steps in time).

7.3 LDV modeling approach

The LDV technologies considered include conventional gasoline vehicles (CVs), hybrid electric vehicles (HEVs), plug-in hybrid electric vehicles (PHEVs), and pure electric vehicles (EVs). However, the proposed methods could be used for other vehicle technologies, such as natural gas, hydrogen fuel cell, and biodiesel vehicles, by estimating their energy demand and adding it to the appropriate network. A yearly time step is selected for the LDV subsystem, whose domain of simulation time is denoted by $\mathcal{T}_{\mathrm{LDV}}$.

The proposed LDV models are classified with respect to two aspects, namely:

1. whether the share of each vehicle technology type among new LDVs is exogenously provided, or in other words, whether the numbers of new LDVs of every technology type at each node over time ($vehInv_{j,v}(\mathbf{t})$) are external input parameters or decision variables;

2. whether LDV groups are formed to represent different travel patterns.

The four models proposed for LDVs are outlined in Table 7.1. The models are assigned a numerical designation as $x.y$, with x and $y \in \{0, 1\}$. The choice of model is left to the user, who might be willing to adopt a lower ranked model and thus sacrifice accuracy due to lack of

Table 7.1   Classification of proposed LDV models

	Is $vehInv_{j,v}(\mathbf{t})$ a decision variable?	Are LDV groups formed to represent different travel patterns?
Model 0.0	No	No
Model 0.1	No	Yes
Model 1.0	Yes	No
Model 1.1	Yes	Yes

data or for increased computational efficiency.

The total investment cost for LDVs can be expressed as

$$costLDVInv = \sum_{\mathbf{t}\in\mathcal{T}_{\text{LDV}}} \sum_{j\in\mathcal{N}_{\text{LDV}}} \sum_{v\in\mathcal{V}} (1+r)^{-t_1}\, costVehInv_v(\mathbf{t})\, vehInv_{j,v}(\mathbf{t}), \qquad (7.2)$$

which is added to the total cost of the integrated system. NETPLAN minimizes the present value of cost using a constant real discount rate r [102]. The parameters r and $costVehInv_v(\mathbf{t})$ are specified by the user. In Models 0.0 and 0.1, $vehInv_{j,v}(\mathbf{t})$ is an input parameter; in Models 1.0 and 1.1, it becomes a decision variable.

The cumulative number of vehicles for each technology type $v \in \mathcal{V}$ at node $j \in \mathcal{N}_{LDV}$ at time $\mathbf{t} \in \mathcal{T}_{\text{LDV}}$ can be expressed as

$$vehCum_{j,v}(\mathbf{t}) = vehInit_{j,v}(\mathbf{t}) + \sum_{\mathbf{t}'\in\mathcal{T}_{\text{LDV}}} vehInv_{j,v}(\mathbf{t}') \cdot \mathrm{I}\left[0 \leq t_1 - t_1' < vehLife_v(\mathbf{t}')\right], \qquad (7.3)$$

where $vehInit_{j,v}(\mathbf{t})$ and $vehLife_v(\mathbf{t})$ are user-specified. The LDVs create demand for electricity and gasoline, and thus affect the underlying infrastructure.

The demand for electric energy (or gasoline) at node $i \in \mathcal{N}_{\text{elec}}$ (or $i \in \mathcal{N}_{\text{gas}}$) during time $\boldsymbol{\tau} \in \mathcal{T}_{\text{elec}}$ (or $\boldsymbol{\tau} \in \mathcal{T}_{\text{gas}}$) from LDVs on the road during time $\mathbf{t} \in \mathcal{T}_{\text{LDV}}$ (obviously, t_1 must be equal to τ_1) can be expressed as

$$d_i^{E\_LDV}(\boldsymbol{\tau}) = \sum_{j\in\mathcal{N}_{\text{LDV}}^i} \sum_{v\in\mathcal{V}} e_{j,v}(\boldsymbol{\tau})\, vehCum_{j,v}(\mathbf{t}), \qquad (7.4)$$

where the per-vehicle energy demands $e_{j,v}(\mathbf{t})$ are used-defined. This is added to the energy demand from other consumers at the corresponding electricity (or gasoline) node.

In Models 0.0 and 0.1, since $vehInv_{j,v}(\mathbf{t})$ is exogenously provided, the calculations described by (7.2) through (7.4) can be performed prior to solving the optimization problem. The result-

ing *costLDVInv* enters the objective cost function as a constant term, and $d_i^{E\text{-}LDV}(\boldsymbol{\tau})$ is added to the energy demand at the corresponding network nodes.

In Models 1.0 and 1.1, the $vehInv_{j,v}(\mathbf{t})$ are decision variables, which affect the objective function via (7.2). The following constraints are added to ensure that the cumulative demand for LDVs at each node $j \in \mathcal{N}_{\text{LDV}}$ at time $\mathbf{t} \in \mathcal{T}_{\text{LDV}}$ can be met:

$$\sum_{v \in \mathcal{V}} vehCum_{j,v}(\mathbf{t}) = d_j^{LDV}(\mathbf{t}), \tag{7.5}$$

where $vehCum_{j,v}(\mathbf{t})$ is expressed in (7.3), and $d_j^{LDV}(\mathbf{t})$ is an input parameter.

It should be noted that the LDV nodes j in Models 0.0 and 1.0 correspond to distinct geographical regions. But in Models 0.1 and 1.1, where LDV groups are formed to represent different travel patterns, each node j corresponds to a particular vehicle group within a geographical region.

7.3.1 Model 0.0

Model 0.0 represents the simplest formulation, where $vehInv_{j,v}(\mathbf{t})$ is exogenously specified. Forecasts of $vehInv_{j,v}(\mathbf{t})$ can be found in [103, 104]. Alternatively, one can use the forecasted total LDV sales in conjunction with the projected CV, HEV, and PEV market penetration (such as the ones in [105] and [22]) to obtain CV, HEV, and PEV annual sales first. The expected PEV composition from an array of PEV technology types (e.g., PHEV20, PHEV40, PHEV60, EV100) is then used to estimate $vehInv_{j,v}(\mathbf{t})$. The designation 'PHEVa_v' implies that the vehicle's equivalent all-electric range is a_v miles [27, 28, 106].

The operation of PEVs can be divided into the charge-depleting (CD) and charge-sustaining (CS) mode [28, 63]. In CD mode, the vehicle is gradually depleting the electric energy of its battery pack. The total distance a PHEV can travel in CD mode with a battery initially fully charged is defined as its charge-depleting range (CDR). This is determined with standardized testing procedures that are based on predetermined driving cycles [107]. Here, to simplify the analysis, the "average" vehicle is considered, so that all parameters (except the miles driven) correspond to their average values over the fleet. For the purposes of long-term national-scale planning, this approximation should be sufficient. When the minimum state of charge

is reached, a switch to the CS mode occurs, where the vehicle is operated similarly as an HEV. The CD mode can be further classified as pure EV or blended mode, according to the drivetrain design. In EV mode, all tractive energy is derived from electricity; in blended mode, the internal combustion engine occasionally assists the electric motor in supplying the tractive energy. The fuel displacement factor ξ_v represents the fraction of tractive energy obtained from electricity in CD mode for technology type v. Therefore, a vehicle's CDR is related to its equivalent all-electric range by [28]

$$d_v = \frac{a_v}{\xi_v} \,. \tag{7.6}$$

Here, $e_{j,v}(\mathbf{t})$ is estimated using the analytical method proposed in [48], where the average electric energy demands of different technology types are estimated using the travel pattern obtained from the 2009 U.S. National Household Travel Survey (NHTS) [34]. Assuming that the charging frequency is once per day (overnight) and that batteries are fully charged in the morning, the miles traveled in CD mode can be expressed as a function of miles traveled (m) and CDR (d_v) by

$$m_{\mathrm{cd}}(m, d_v) = \begin{cases} m & \text{for } m \le d_v \,, \\[2mm] d_v & \text{for } m > d_v \,. \end{cases} \tag{7.7}$$

The miles traveled in CS mode are

$$m_{\mathrm{cs}}(m, d_v) = \begin{cases} 0 & \text{for } m \le d_v \,, \\[2mm] m - d_v & \text{for } m > d_v \,. \end{cases} \tag{7.8}$$

Hence, the average (per vehicle) daily miles traveled in CD mode are

$$m_{\mathrm{cd}}^{\mathrm{avg}}(d_v) = \int_0^{d_v} x f_m(x) \, dx + d_v \int_{d_v}^{\infty} f_m(x) \, dx \,, \tag{7.9}$$

and the average daily miles traveled in CS mode are

$$m_{\mathrm{cs}}^{\mathrm{avg}}(d_v) = \int_{d_v}^{\infty} (x - d_v) f_m(x) \, dx \,. \tag{7.10}$$

In Model 0.0, vehicle groups of different travel patterns are not formed, and each technology type is assumed to be evenly distributed among LDVs irrespective of travel patterns. Therefore, the function f_m used in (7.9) and (7.10) is the PDF of daily miles traveled by all vehicles in the NHTS.

The average daily electric energy demand from the high-voltage transmission grid per vehicle of technology type v is

$$e_{\text{elec}}(d_v, \xi_v) = \frac{\xi_v h_{\text{tr},v} m_{\text{cd}}^{\text{avg}}(d_v)}{\eta_v}, \tag{7.11}$$

where $h_{\text{tr},v}$ is the average tractive energy per mile at the wheels, and η_v is the grid-to-wheels efficiency. The average daily gasoline demand per vehicle of technology type v is

$$e_{\text{gas}}(d_v, \xi_v) = \frac{(1 - \xi_v) m_{\text{cd}}^{\text{avg}}(d_v) + m_{\text{cs}}^{\text{avg}}(d_v)}{\text{MPG}_v}. \tag{7.12}$$

The average daily gasoline demand of conventional gasoline and hybrid electric vehicles is obtained by dividing the average daily miles traveled by their fuel economy.

Once $e_{\text{gas}}(d_v, \xi_v)$ is known for each technology type v, the annual gasoline demand per LDV for each node $j \in \mathcal{N}_{\text{gas}}$ ($e_{j,v}(\mathbf{t})$) can be readily obtained by multiplication. Similarly, the electric energy demand over a subdivision of a month per PEV at each node $j \in \mathcal{N}_{\text{elec}}$ (also denoted by $e_{j,v}(\mathbf{t})$) is found using the average daily electric energy consumption per vehicle ($e_{\text{elec}}(d_v, \xi_v)$) and an assumed distribution of charging energy among the subdivisions of the month (charging is not uniform, but mostly occurs overnight).

7.3.2   Model 0.1

In Model 0.0, LDVs are not grouped according to their travel pattern, and it is assumed that all technology types are evenly distributed among new LDVs irrespective of travel patterns. In reality, however, different PEV technology types will not penetrate evenly among LDVs with different travel patterns. It is reasonable to expect that LDV buyers will determine their preferred vehicle type based on their travel needs, and other factors such as income, vehicle price, fuel cost, environmental awareness, acceleration or other vehicle performance parameters, vehicle design, comfortableness, safety considerations, brand preference, etc. Therefore, it is expected that the penetration level of each technology type will vary among vehicle groups with distinct travel patterns. Nevertheless, the problem of understanding LDV buyers' choices [108–110] is very complicated and beyond the scope of the present study. Here, a simple model is used to capture the relation of a vehicle's technology type to its travel demand.

The determination of travel demand is complicated because vehicles do not travel the same on a daily basis. For instance, some vehicles may travel 40 miles on weekdays but less than 5 miles during the weekend, or vice versa. However, the NHTS records vehicle trips for only one designated sample day for each vehicle, which does not suffice to represent the travel pattern of each individual vehicle in its entirety. To deal with this difficulty, the best estimate of annual mileage provided in the 2009 NHTS Version 2.1 [111] is used to group vehicles with distinct travel patterns. In order to capture the interdependency between vehicle type and travel pattern, vehicles with similar annual miles traveled (M) are grouped together. As a result, now LDV network nodes j correspond to combinations of groups and geographical regions.

In order to obtain $vehInv_{j,v}(\mathbf{t})$, a conditional probability mass function (PMF) of group given the vehicle technology type, denoted by $f_{G|v}$, can be assigned. Then, new LDVs of each technology type are distributed among vehicle groups based on $f_{G|v}$, resulting in $vehInv_{j,v}(\mathbf{t})$ (recall that the index j in this model corresponds to a particular vehicle group in a region). Alternatively, a conditional PMF of vehicle type given the group, denoted by $f_{v|G}$, can be assigned. For a given grouping, f_G can be readily obtained from the NHTS. In this case, the total LDV sales for each group and region every year ($\sum_v vehInv_{j,v}(\mathbf{t})$) can be obtained using a forecast of LDV sales in conjunction with f_G, and $vehInv_{j,v}(\mathbf{t})$ is found using the assumed $f_{v|G}$. (For simplicity, it is assumed that all PMFs are the same among all geographical regions.)

It should be noted that vehicle grouping is based on the *annual* miles traveled M. Since vehicle charging is performed on a daily basis, and vehicles travel differently every day, annual data is not particularly useful when one needs to determine the daily consumption of electricity and gasoline. In other words, the division of daily miles traveled m into m_{cd} and m_{cs} is not readily found using M. Replacing m by $M/365$ will misrepresent the variance of daily miles traveled, and will lead to an overestimation of electric energy demand and an underestimation of gasoline demand from PHEVs. An illustrative example is provided in Table 7.2. As can be seen, m_{cd} and m_{cs} need to be determined on a daily basis, and cannot be estimated using the total miles traveled over a week (154 miles), since using the average miles traveled (22 miles) would yield the wrong answer (the split would be 20 miles in CD mode vs. 2 miles in CS mode instead of 15 miles and 7 miles, respectively).

Table 7.2   Miles traveled in CD and CS modes for a PHEV with CDR of 20 miles

Day	m	m_{cd}	m_{cs}
Mon	15	15	0
Tue	15	15	0
Wed	23	20	3
Thu	15	15	0
Fri	26	20	6
Sat	60	20	40
Sun	0	0	0
Total	154	105	49
Average	22	15	7

In order to estimate $e_{j,v}(\mathbf{t})$, the travel pattern of each vehicle group ($f_{m|G}$) is extracted first using NHTS data. The formulas of (7.9) through (7.12) are still valid, but $f_{m|G}$ rather than f_m should be used. Model 0.1 considers the correlation between the technology type of new LDVs and travel pattern more carefully. The conditional PMF $f_{G|v}$ or $f_{v|G}$ is proposed to capture this interdependency, which in turn enters into the estimation of $vehInv_{j,v}(\mathbf{t})$ and $e_{j,v}(\mathbf{t})$. Presently, however, only a hypothetical "best guess" function $f_{v|G}$ or $f_{G|v}$ can be used.

7.3.3   Model 1.0

In Model 1.0, the composition of new LDVs added to the fleet is not exogenously predefined, and so $vehInv_{j,v}(\mathbf{t})$ is added to the set of decision variables. Since LDV groups are not formed to represent different travel patters, each LDV network node corresponds to geographical location only. The demand for LDVs at node j during time $\mathbf{t}$ is modeled as an input parameter, denoted by $d_j^{LDV}(\mathbf{t})$, which can be estimated based on historical and projected LDV sales. The method for estimating $e_{j,v}(\mathbf{t})$ is the same as in Model 0.0.

7.3.4   Model 1.1

Model 1.1 is an improvement over Model 1.0, because LDVs are grouped according to annual miles traveled. Each LDV network node j represents a geographical region and vehicle group combination. This allows vehicle technologies to penetrate in different percentages among LDV groups, and therefore enables NETPLAN to identify the optimal composition of LDVs in a less

Table 7.3   Vehicles grouped by annual mileage

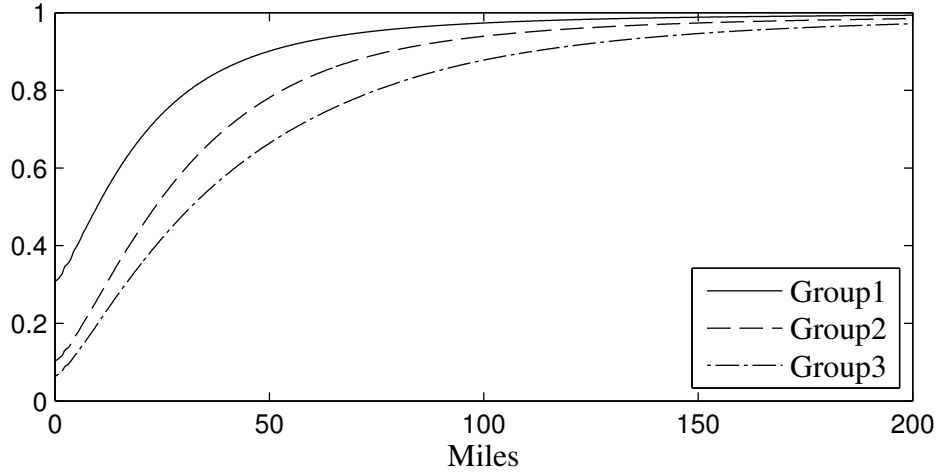|	Annual mileage	Percentage of total LDVs
Group 1	less than 10,000 miles	54%
Group 2	between 10,000 and 20,000 miles	34%
Group 3	20,000 miles and above	12%

Figure 7.2   CDF of daily miles traveled for different vehicle groups.

constrained manner than Model 1.0. The estimation of $d_j^{LDV}(\mathbf{t})$ is based on f_G and total demand for LDVs in each geographical region. The estimation of $e_{j,v}(\mathbf{t})$ proceeds in the same manner as in Model 0.1.

7.4   Model implementation

In this section, Model 1.1 is used as an example. LDVs are divided into three groups based on their annual miles traveled, namely, less than 10,000 miles, between 10,000 and 20,000 miles, and more than 20,000 miles, representing vehicles with low, medium, and high travel demand. The PMF f_G can be obtained from NHTS data, as in Table 7.3. This is later (in step 3 of subsection 7.4.1) used to calculate $d_j^{LDV}(\mathbf{t})$ based on the total LDV demand. Next, the travel pattern is extracted for each group. For example, the cumulative distribution function (CDF) of daily miles traveled for each vehicle group is shown in Figure 7.2. These travel patterns are later used (in subsection 7.4.3) to estimate $e_{j,v}(\mathbf{t})$.

7.4.1 Estimation of LDV demand

Depending on the modeling granularity of the electric and petroleum subsystems, demand for LDVs can be modeled either at the state level or at a regional level, such as the supply regions used in NEMS, which are based on the regions defined by the North American Electric Reliability Corporation [85]. Here, the latter approach is used, using the energy system developed in [83], where the electricity subsystem is based on NEMS regions.

The estimation of $vehInit_{j,v}(\mathbf{t})$ and $d_j^{LDV}(\mathbf{t})$ proceeds in three steps:

1. First, data are obtained for the entire U.S., i.e., estimates of $\sum_j \sum_v vehInit_{j,v}(\mathbf{t})$ and $\sum_j d_j^{LDV}(\mathbf{t})$.

   The historical and projected LDV sales can be found in [112] and [103], respectively. The expected vehicle lifespan is ca. 14 years for conventional gasoline vehicles, derived from data in [112]. The estimates thus obtained of the existing conventional gasoline vehicles and the cumulative demand for LDVs in the U.S. over the planning horizon are shown in Figure 7.3.
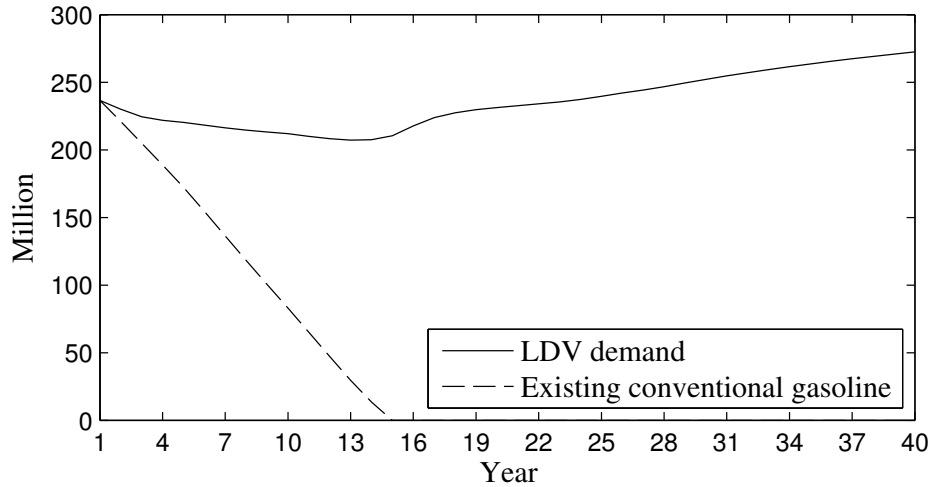
Figure 7.3   Existing conventional gasoline vehicles and LDV demand in U.S.

2. Second, the distribution of LDVs among regions is found.

   The present distribution of LDVs among different States can be found in [113], and can be used to obtain the LDV distribution among the NEMS regions, as shown in Table 7.4. Here, it is assumed that the ratio of LDV demand among regions will remain the same over the planning horizon. Hence, the existing CVs and total LDV demand over the planning

horizon are found for each region.

Table 7.4   LDV distribution among NEMS regions

Region	Percentage
East Central Area Reliability Coordination Agreement (ECAR)	12.2%
Electric Reliability Council of Texas (ERCOT)	7.6%
Mid-Atlantic Area Council (MAAC)	9%
Mid-America Interconnected Network (MAIN)	6%
Mid-Continent Area Power Pool (MAPP)	5.8%
New York Power Pool (NY)	4.4%
New England Power Pool (NE)	4.9%
Florida Subregion of SERC (FL)	6.7%
Southeastern Electric Reliability Council Excluding Florida (STV)	14.7%
Southwest Power Pool (SPP)	5.7%
Northwest Pool (NWP)	6.2%
Rocky Mountain and Arizona-New Mexico Power Areas (RA)	3.1%
California-Southern Nevada Power Area (CNV)	13.7%

3. Third, the number of LDVs in each group of each region is determined.

   The number of initial CVs and the demand of LDVs for each group in each region in each year are obtained using the percentages listed in Table 7.3. Alternatively, one can use the travel pattern of LDVs within each region rather than the average national travel pattern to group vehicles, which could lead to more accurate results. The number of vehicle groups could also vary, but the method remains essentially the same.

7.4.2   Alternative LDV technologies

The LDV technologies considered here are listed in Table 7.5. LDV cost is estimated using information found in [114–116] and the prices of PEVs commercially available today. It is assumed that the cost of vehicle technologies—except CVs—will linearly decrease with time during the first 20 years due to advances in technology, and will remain the same for the remaining years of the study. The lifespan is assumed to be $vehLife_v(\mathbf{t}) = 14$ years for all $v \in \mathcal{V}$. Battery replacement costs for PEVs over their lifespan can be included in the original investment cost.

Table 7.5   Vehicle technology parameters

Technology	ξ_v	d_v	Cost (thousand \$)	
			Year 1	Year 20
Conventional	N/A	N/A	24	24
HEV	N/A	N/A	28	26
PHEV20	0.8	25	35	31
PHEV40	0.85	44	41	34
PHEV60	0.9	60	50	36
EV100	1	100	45	35

Table 7.6   Daily electricity (kWh) and gasoline (gallon) demand per LDV

Technology	Group 1		Group 2		Group 3	
	Elec.	Gas.	Elec.	Gas.	Elec.	Gas.
CV	N/A	0.94	N/A	1.65	N/A	2.27
HEV	N/A	0.64	N/A	1.14	N/A	1.56
PHEV20	4.10	0.29	6.14	0.60	6.79	0.97
PHEV40	5.80	0.17	9.41	0.36	11.06	0.65
PHEV60	6.79	0.12	11.39	0.25	14.03	0.47
EV100	9.20	N/A	N/A	N/A	N/A	N/A

7.4.3   Estimation of gasoline and electricity demand

The fuel economy and the tractive energy per mile are estimated on a fleet-wise basis, i.e., by averaging the parameters of different kinds of vehicles (cars, SUVs, minivans, pick-up trucks) according to the fleet composition. The average fuel economy for CVs is 22 miles per gallon, based on information found in [29]. The average LDV tractive energy for PEVs is $h_{\mathrm{tr},v} = 0.31$ kWh/mile, based on information found in [25, 35, 36]. Since the energy content per gallon of gasoline is ca. 33.7 kWh [117] and the tank-to-wheels efficiency is ca. 0.25–0.3 [118], the fuel economy of HEVs and PEVs in charge-sustaining mode is $\mathrm{MPG}_v = 32$ miles per gallon. This is consistent with data about available HEV models found in [119]. Furthermore, it is assumed that the efficiencies of charger, battery (roundtrip), on-board power electronics, traction motor, and mechanical transmission plus accessory loads (e.g., air-conditioning, on-board electronics) are: 95% [25], 92% [37], 95% [25, 38], 92% [38], and 88% [39], respectively; losses within distribution systems are assumed to be 3%; this results in an overall grid-to-wheels efficiency for PEVs of $\eta_v = 65.2\%$. The estimated daily energy demands $e_{j,v}(\mathbf{t})$ are shown in

Table 7.6. Here, it has been assumed that EV100 technology will only penetrate vehicles in Group 1, whose drivers would not need to modify their driving behavior substantially to accommodate their limited electric range (see Figure 7.2).

7.5   Case studies

In this section, Model 1.1 is used in a 40-year planning study of the U.S. energy and transportation infrastructures. Three interesting case studies are presented:

Case 1: All LDVs are conventional gasoline vehicles over the planning horizon.

Case 2: The vehicle technologies listed in Table 7.6 are considered using Model 1.1.

Case 3: Same as Case 2 with an additional constraint imposed on net greenhouse gas (GHG) emissions from electricity generation and LDVs.

The data of Section 7.4 are used. The modeling assumptions and data reported in [83] are adapted for the other components of the U.S. energy and transportation systems. For the electricity subsystem, the existing capacity, capacity factors, and economic parameters (shown in Table 7.7) for various generation technologies are updated to reflect the current state using statistics from [120]. The other subsystems are used without any modification whatsoever. In particular, no investments or improvements are considered for the coal and natural gas subsystems, nor for electricity transmission lines; the existing petroleum network is simplified assuming a single node connected to an unlimited supply due to the lack of publicly available data. A summary of the system network model is shown in Table 7.8.

Here, the LDC in each region is divided into three blocks (the first block has the highest load level), as in Table 7.9. The magnitude of each block is the average load during the corresponding time period, varying among nodes in the electricity subsystem. The LDCs among regions have been obtained based on data customized for Iowa State University from the Ventyx Velocity Suite [121]. PEV charging is assumed to take place mostly during off-peak hours, which leads to the distribution shown in Table 7.9. The real discount rate is 5% and the annual non-PEV load growth rate is 1%.

Table 7.7   Electricity generation technologies and parameters

Technology	Overnight capital (million \$/GW)	Fixed O&M per year (million \$/GW)	Variable O&M (\$/MWh)
PC	2,844	29.67	4.25
IGCC	3,221	48.90	6.87
NGCC	1,003	14.62	3.11
CT	665	6.70	9.87
Nuclear	5,335	88.78	2.04
Hydro	3,076	13.44	0
Inland wind	2,000	28.07	0
Offshore wind	5,975	53.33	0
Oil	1,270	15.67	3.21
Solar PV	3,000	16.70	0
Solar Thermal	4,692	64.00	0
Geothermal	4,141	84.27	9.64

PC = Pulverized coal

IGCC = Integrated gasification combined cycle

NGCC = Natural gas combined cycle

CT = Combustion turbine

PV = Photovoltaic

All studies are solved using NETPLAN [122], which utilizes IBM ILOG CPLEX Concert Technology [123] to perform the linear optimization. The cost minimization problem is a linear program with ca. 1.47 million decision variables and 745 thousand inequality constraints (the exact number depends on the case study). The problem is solved by an Iowa State University server with 24 2.67-GHz CPUs and 47 GB of RAM. The solution time varies between 40 minutes and 1.5 hour for Case 1, between 50 minutes and 2 hours for Case 2, and between 1.5 and 2.5 hours for Case 3.

The model is validated by comparing the simulation results in year 1 (the same initial point for all three cases) with the actual data from 2009. Table 7.10 lists the initial generation capacity from different primary energy sources in the simulation, which is the sum of the capacity in each region (input parameters). Table 7.10 also juxtaposes simulation results in year 1 with the actual data in 2009 regarding electricity generation and GHG emissions from different primary energy sources. In particular, data for the capacity and electricity generation in 2009 were obtained from [120], while the corresponding CO_2 emissions were obtained from [124]. Non-

Table 7.8   Nodes and arcs by subsystem

Subsystem	Type	Size
Coal	Production	24 nodes
	Demand	46 nodes
Natural gas	Production	25 nodes
	Demand	50 nodes
	Pipelines	108 arcs
	Import pipelines	9 arcs
	Storage	30 nodes
Electricity	Generation	168 arcs
	Demand	13 nodes
	Transmission lines	19 arcs
	Import transmission	8 arcs
Petroleum	Gasoline	13 nodes
	Diesel	13 nodes
Freight	Transportation	95 arcs
LDV	Demand	13 (region) nodes

Table 7.9   Load duration curves blocks and PEV load distribution

	1st	2nd	3rd
Duration	10%	40%	50%
PEV load distribution	0	20%	80%

CO_2 GHG emissions from electricity generation are not considered here since they account for less than 1% of total GHG emissions in the electricity sector.

As can be seen in Table 7.10, in year 1, generation and emissions from coal are overestimated, whereas they are underestimated for natural gas and other energy sources. This is mainly because only three blocks are used to represent the LDCs. In consequence, this reduces the time period of high load level and shifts some generation from natural gas and other primary energy sources to coal. With increased granularity in the LDC representation, the simulation results are expected to become closer to the actual data at the expense of computational burden. For example, representing the LDC by four blocks will increase by ca. 359 thousand the number of decision variables and by ca. 140 thousand the number of constraints. According to [125], the total GHG emissions from LDVs are 1.11 billion metric tons carbon dioxide equivalent (BMTCO$_2$e). In the simulation, the GHG emissions from LDVs in year 1 are 1.07 BMTCO$_2$e,

Table 7.10   Capacity, generation, and CO_2 emissions in year 1 vs. 2009 data

Description	Capacity (GW)		Generation (TWh)		Emissions (MMT)	
	Year 1	2009	Year 1	2009	Year 1	2009
Coal	319	314	2,086	1,756	1,911	1,742
Natural gas	408	401	548	921	210	373
Nuclear	103	101	805	799	N/A	N/A
Hydro	78	79	275	273	N/A	N/A
Others	102	130	124	201	9	45
Total	1,010	1,025	3,838	3,950	2,130	2,160

only 3% less than the actual data for 2009.

7.5.1   Case 1

Case 1 represents a business-as-usual scenario wherein all LDVs are assumed to be CVs over the next 40 years, without introducing HEVs or PEVs. Consequently, all the energy for LDVs is uniquely derived from petroleum. The annual gasoline consumption is shown in Figure 7.4, and is proportional to the LDV demand (cf. Figure 7.3).
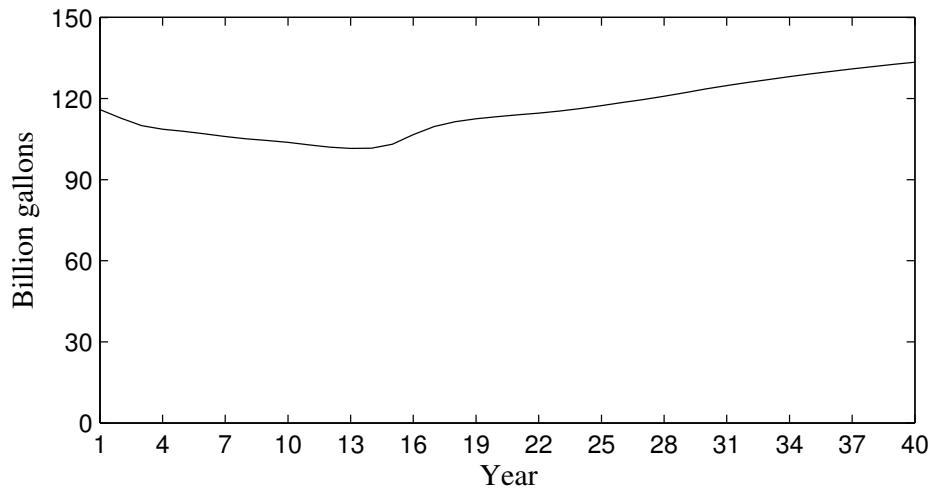

Figure 7.4   Annual gasoline demand from LDVs in Case 1.

In this case, the minimum total cost of the integrated system is 18.33 trillion in today's U.S. dollars. The total GHG emissions from electricity generation and LDV tailpipes over the next 40 years are 128.7 BMTCO$_2$e. Here, time value of GHG emissions [126] is not considered, and the above number is the sum of annual GHG emissions over the planning horizon.

Figure 7.5 displays generation capacity mix over the planning horizon. Extra capacity (15% of the peak load) is reserved for each region. The cumulative hydro generation capacity is capped due to limited suitable sites, but new hydro generation plants are allowed to be built when old ones retire. The maximum cumulative capacity of nuclear generation in each region is assumed to be twice as high as today's capacity. Generally, delaying the investment in new generation helps to reduce the present value of total cost. Therefore, an investment will not be made unless the existing capacity cannot meet the demand. At the beginning of the planning period, as existing generation units retire, investments in nuclear, coal, and natural gas units are made in order to meet the load. Under strict cost minimization, no investments in wind are made for the first 24 years. Investment in wind is observed after year 24, due to a further increase in load and since expansion of the coal subsystem is not allowed. Natural gas units contribute increasingly to the required generation capacity, but at low capacity factor since natural gas is more expensive (in terms of dollars per MMBTU) than other energy sources. (It should be noted that natural gas prices in the U.S. have decreased considerably over the last couple of years, and are now almost comparable to coal prices. These results were generated using slightly older data, when natural gas was still twice as expensive as coal.)
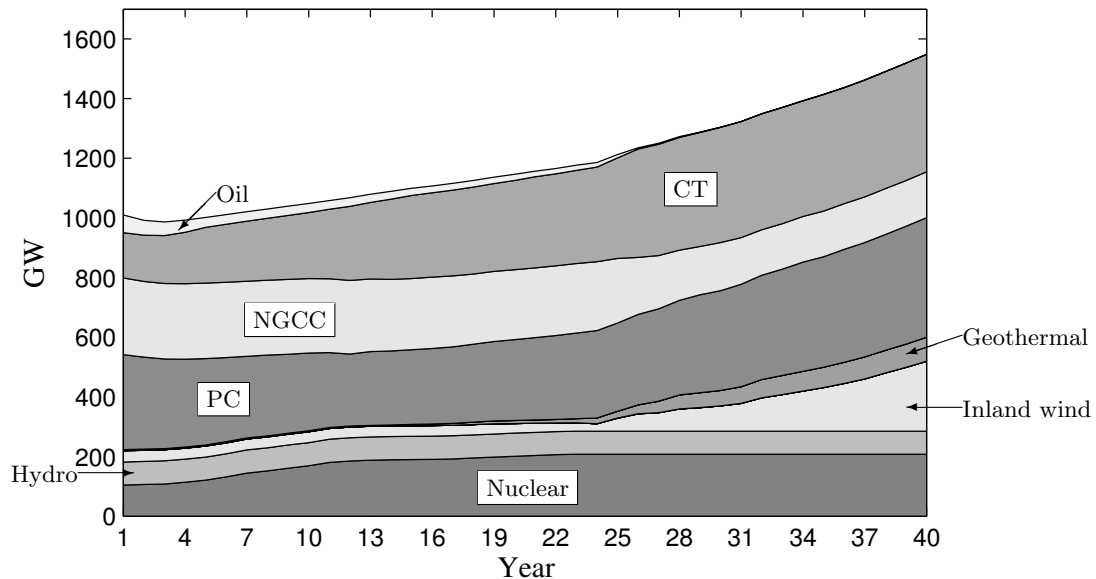

Figure 7.5 Generation capacity mix over time in Case 1.

Figure 7.6 displays the annual GHG emissions from electricity generation and LDV tailpipes.

As can be seen, without HEVs and PEVs, GHG emissions from LDVs increase slightly over the planning horizon, proportionally to the LDV demand (cf. Figure 7.3). GHG emissions from electricity generation decrease at the beginning of the planning horizon due to the investment in nuclear plants that replace coal and natural gas units.
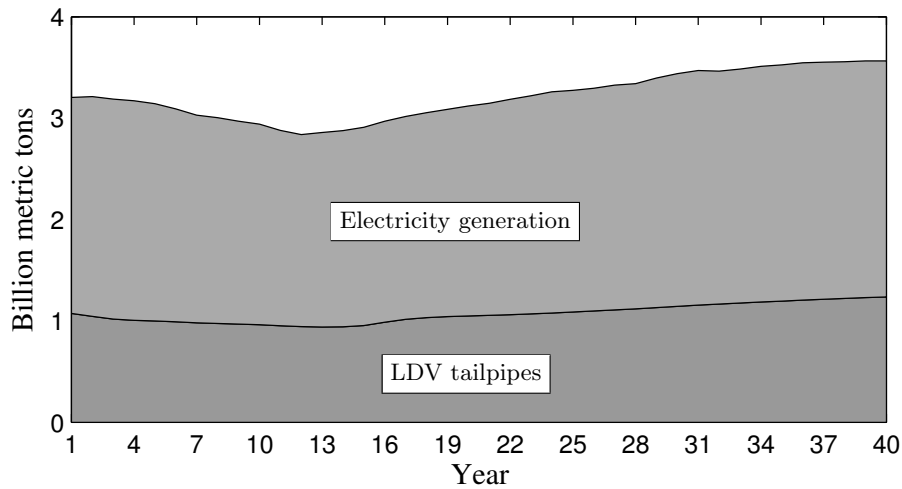

Figure 7.6   Annual GHG emissions (CO_2 equivalent) in Case 1.

7.5.2   Case 2

In Case 2, all the vehicle technologies listed in Table 7.6 are considered using Model 1.1. The resulting minimum cost is \$17.32 trillion, 5.5% less than Case 1. The total GHG emissions are 116.5 $BMTCO_2e$, 9.6% less than Case 1. These results demonstrate that HEV and PEV technology can help to reduce both system cost and GHG emissions substantially.

The national LDV fleet composition over time is shown in Figure 7.7, which indicates that HEV technology is the most economical in the near future, with PEVs penetrating the market in later years. The optimal LDV fleet composition per vehicle group is shown in Figure 7.8. As CVs are gradually retired, investment in new LDVs must be made in order to satisfy the demand. New LDVs can be selected among CVs, HEVs, and PEVs. If CVs are selected, then capital cost is minimum but fuel cost is maximum. Switching from CVs to HEVs and then to PEVs increases the capital cost but reduces the fuel cost. Because the reduction in fuel

cost depends on the travel pattern, it can be observed that the optimal composition of LDVs varies among groups. The additional electricity consumption due to PEV charging increases not only capital and O&M costs in the electricity sector, but also the cost of extracting and transporting primary energy sources (e.g., coal and natural gas). It should be noted that the optimal composition of LDVs also varies slightly across regions (not shown here due to space limitations) even among vehicles of the same travel pattern; this is because electric energy costs vary among regions. The annual gasoline demand in Figure 7.9 drops as the penetration of HEVs and PEVs rises, whereas electricity demand is increased significantly. At the end of the planning horizon, electricity consumption from PEV charging accounts for 12% of the total electricity consumption.
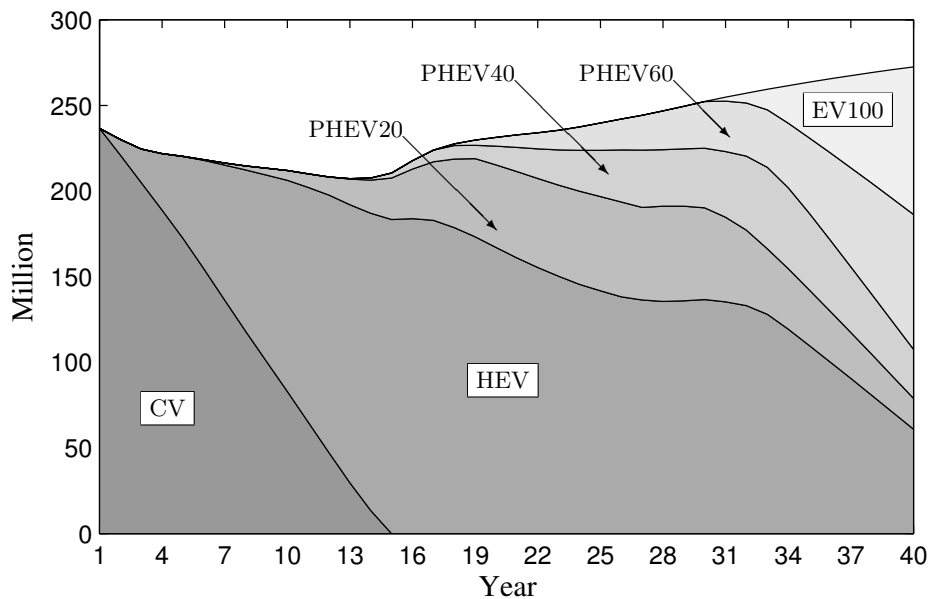

Figure 7.7   LDV fleet composition over time in Case 2.

Figure 7.10 displays the generation capacity mix over the planning horizon. PEVs increase the electricity load, especially during off-peak hours. Compared with Case 1 (cf. Figure 7.5), the capacity of geothermal and wind energy increases, and NGCC generation capacity decreases slightly.
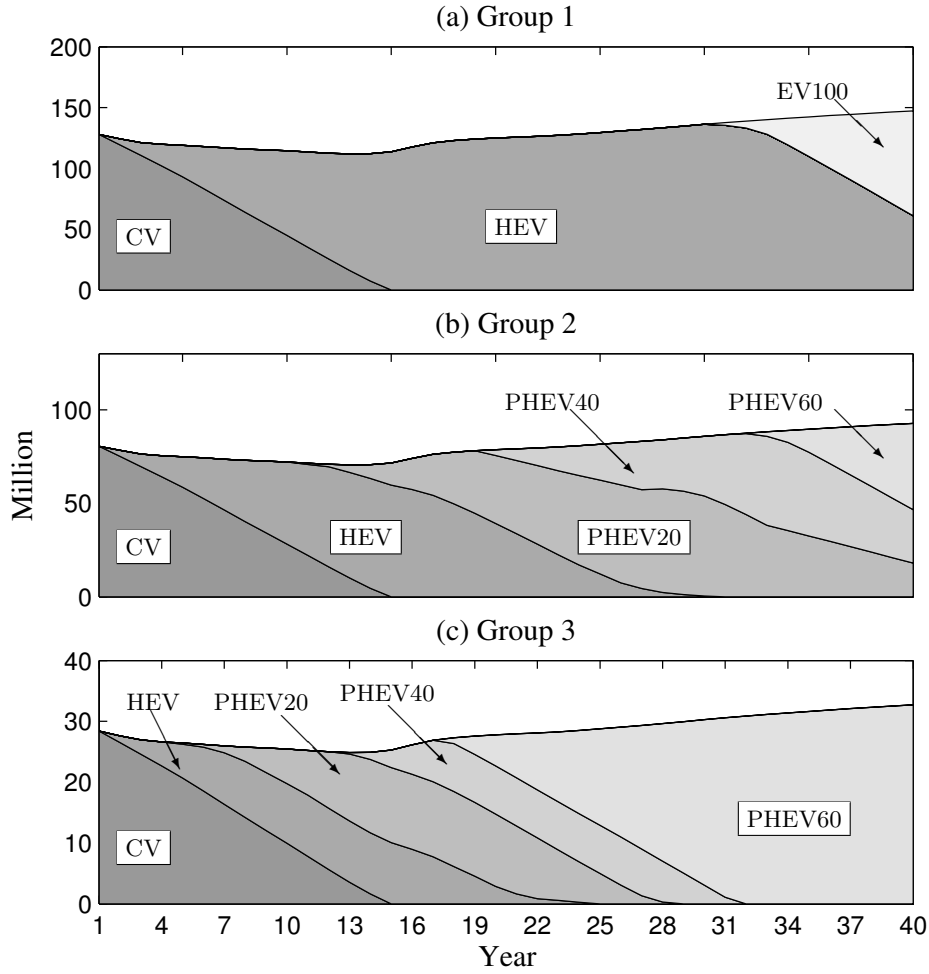
Figure 7.8   LDV fleet composition in each group over time in Case 2.
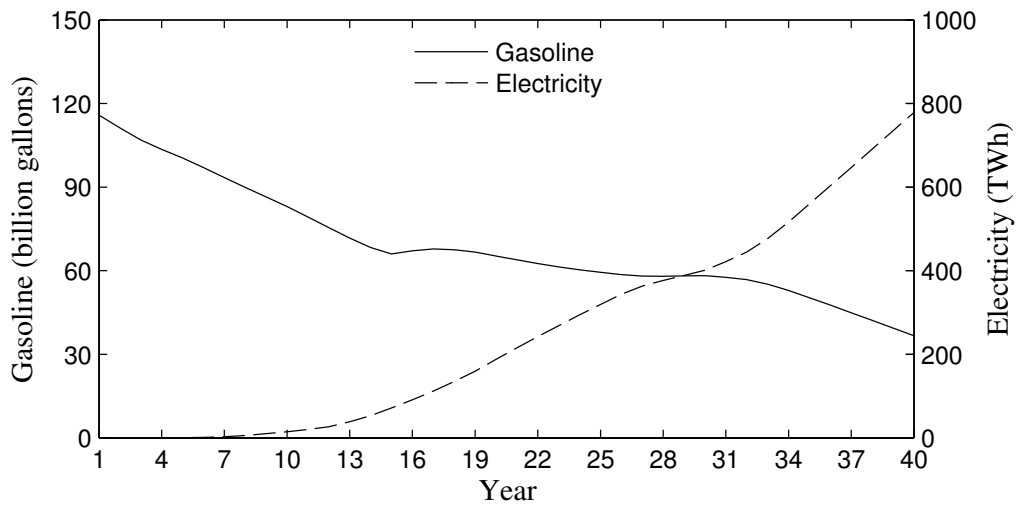

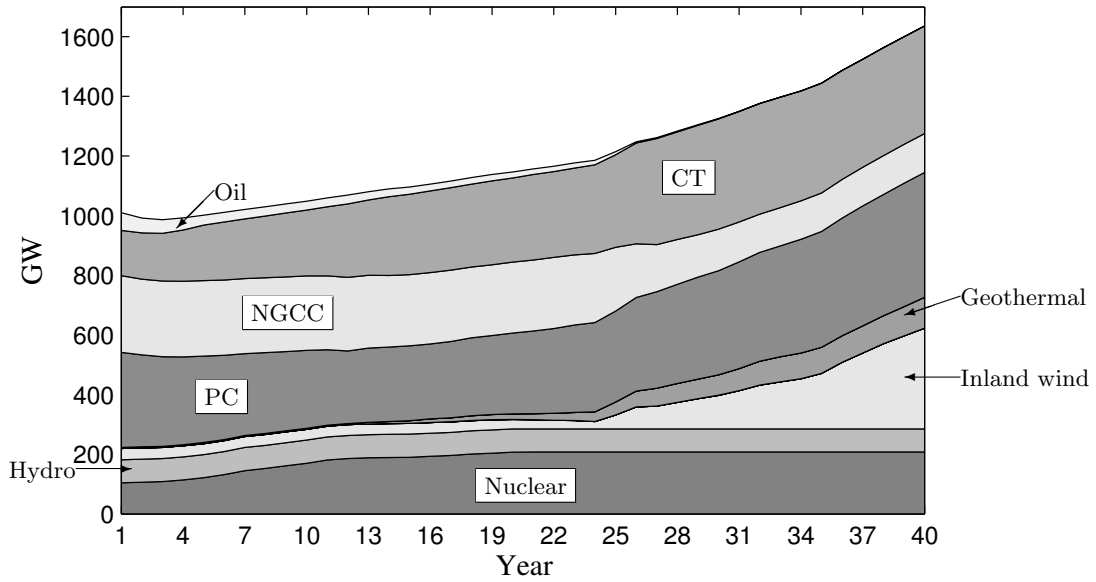Figure 7.9   Annual gasoline and electricity demand from LDVs in Case 2.

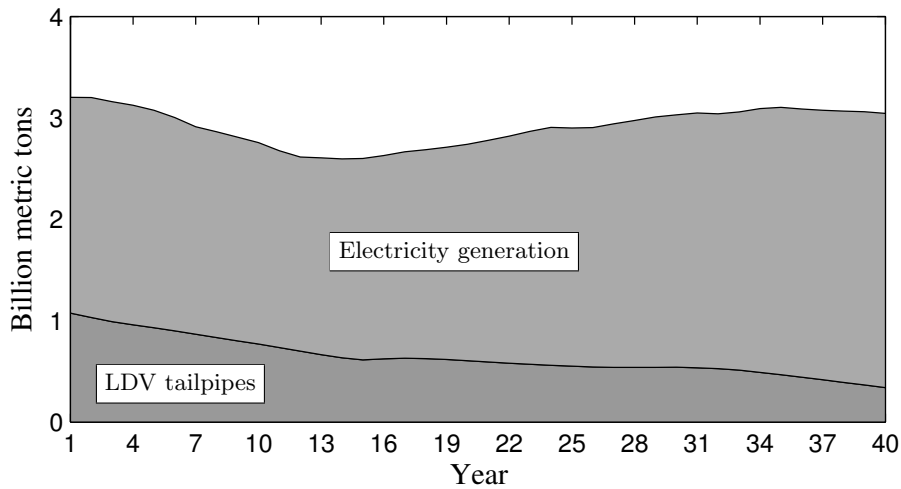Figure 7.10   Generation capacity mix over time in Case 2.

Figure 7.11   Annual GHG emissions (CO$_2$ equivalent) in Case 2.

Figure 7.11 displays annual GHG emissions from electricity generation and LDV tailpipes. As the degree of electrification in LDVs increases, GHG emissions from LDV tailpipes drop significantly over the years. Although the additional electricity consumption due to PEV charging leads to increased CO$_2$ emissions from the electricity sector, the total GHG emissions still decrease compared with Case 1.

7.5.3 Case 3

In Case 3, an additional constraint related to total annual GHG emissions is added. This is based on the emissions reduction target proposed in the U.S. Congress, as derived by [99], which corresponds to a linear decrease to ca. 26% of year-1 emissions in year 40. This is imposed as an upper bound on total GHG emissions from electricity generation and LDVs.

In this case, the minimum cost of the integrated system is \$17.47 trillion, only 0.9% more than Case 2. The total GHG emissions are 81.8 BMTCO$_2$e, 29.7% less than Case 2. Compared with Case 2 (cf. Figure 7.7), the degree of electrification of LDVs in this case increases slightly due to the additional constraint imposed on GHG emissions, as can be seen in Figure 7.12. Compared with Case 2 (cf. Figure 7.9), the annual gasoline (electricity) demand is further decreased (increased) over the time horizon, as shown in Figure 7.13. For comparison purposes, Figure 7.14 illustrates the variation of system cost vs. GHG emissions from power plants and LDV tailpipes for the three cases.
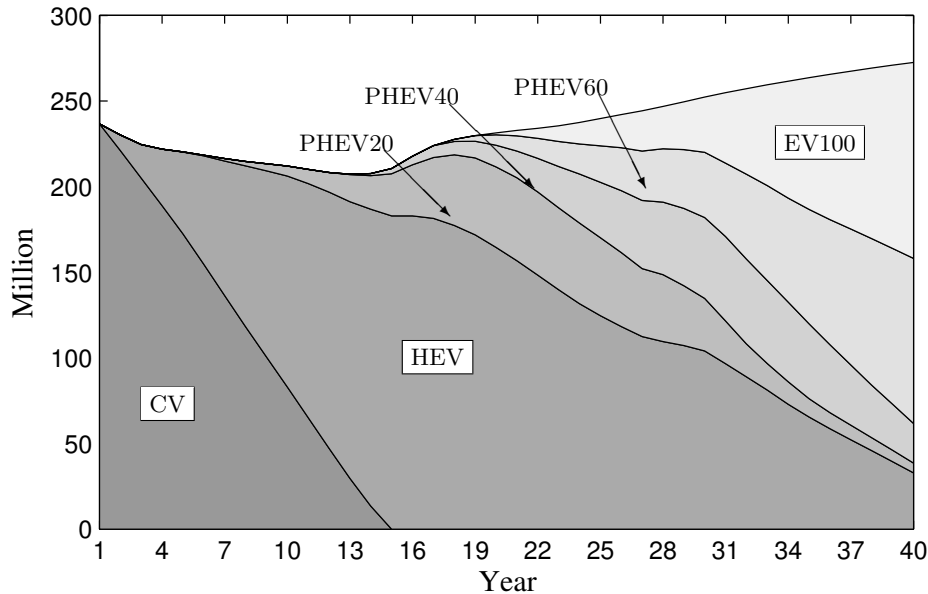

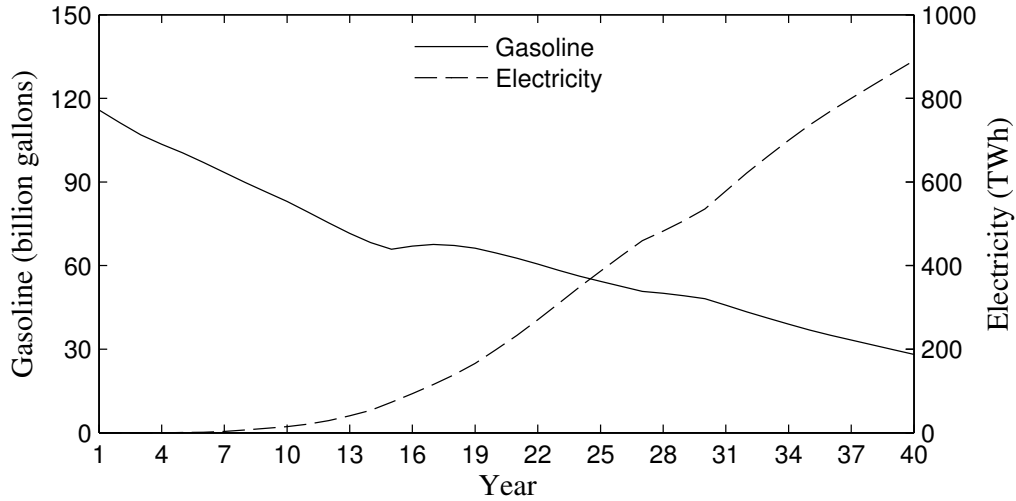Figure 7.12   LDV composition over time in Case 3.

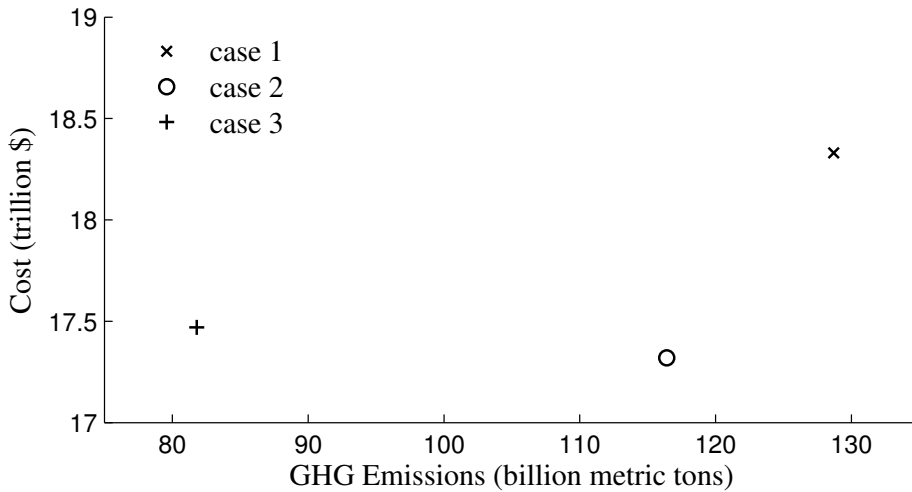Figure 7.13   Annual gasoline and electricity demand from LDVs in Case 3.

Figure 7.14   System cost and GHG emissions from power plants and LDV tailpipes.

Figure 7.15 displays the generation capacity mix over the planning horizon. Due to additional constraints on GHG emissions, compared with Case 2 (cf. Figure 7.10), a significant amount of generation capacity is shifted from coal to wind (mostly) as well as CT and NGCC (to a lesser extent). Figure 7.16 shows the annual GHG emissions from electricity generation and LDV tailpipes. As can be seen, GHG emissions from LDV tailpipes further decrease compared with Case 2. However, the majority of GHG emissions reduction comes from the shifting of electricity generation from coal to renewable sources (wind and solar).
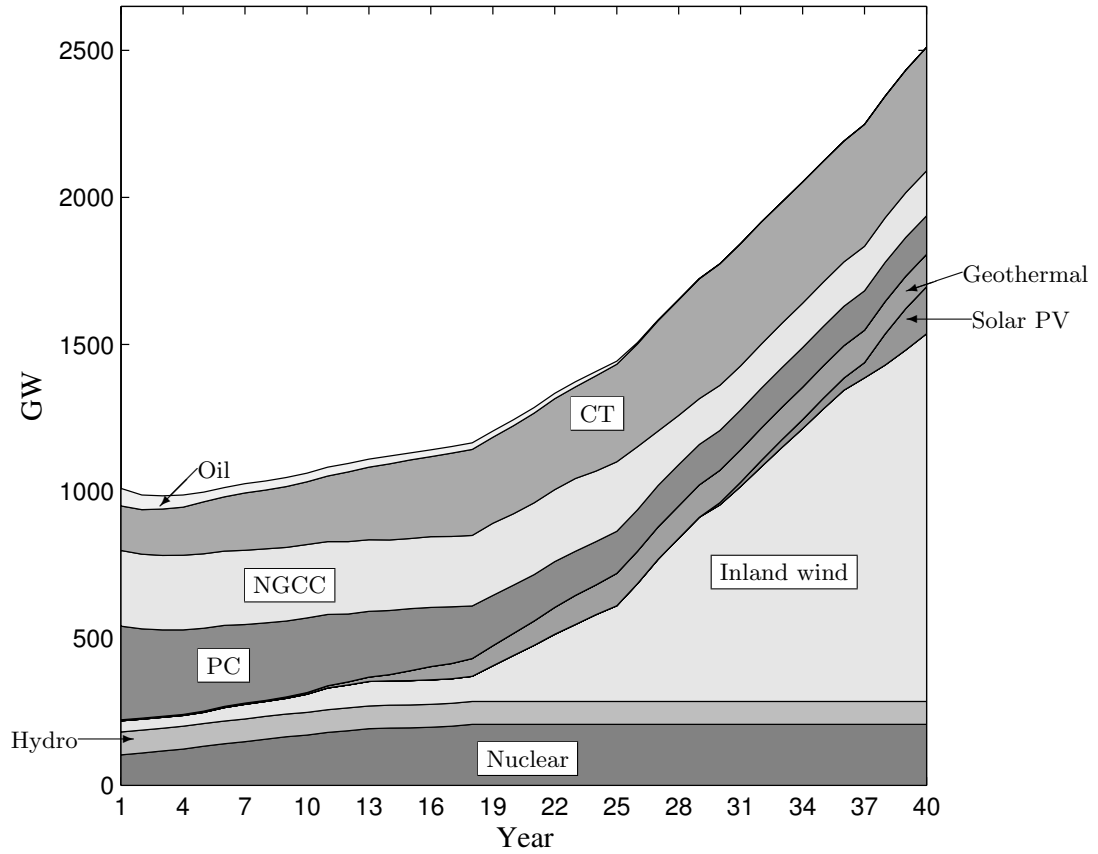
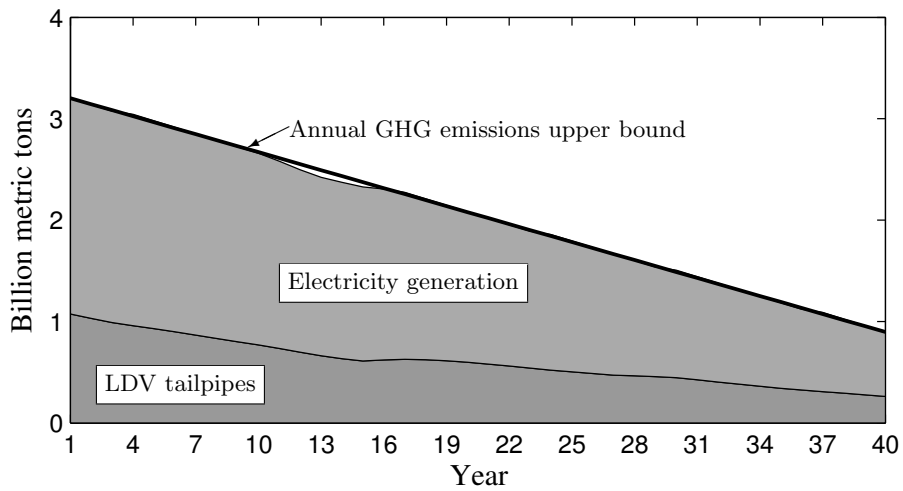Figure 7.15   Generation capacity mix over time in Case 3.

Figure 7.16   Annual GHG emissions (CO_2 equivalent) in Case 3.

7.5.4   Discussion

The case studies demonstrate the degree of interdependence between the energy and transportation systems, especially after the introduction of PEVs, and the importance of performing joint analyses. However, it is rather unrealistic to expect that an optimization by a single central entity of the LDV fleet composition in terms of cost and sustainability can be performed in a country like the U.S. The same argument can be made for the other decision variables, e.g., investments in different types of generation plants, or the fleet of highway trucks. Such decisions are made by individual market participants, and will be different from the optimal solutions obtained from NETPLAN. Nevertheless, these solutions should be interpreted as *targets* that could be achieved with the right planning and appropriate policy decisions [82]. Policies that can help approach the desired optimal solution (such as production tax credits for wind generation, carbon taxes, or tax credits for PEV buyers) have been discussed in [127–130].

Certainly, modeling the national energy and transportation systems over such a long-term planning period is an ambitious goal. The case study results should not be construed as definitive but as indicative. Our main objective is to provide the mathematical framework and basic modeling approach for incorporating PEVs in such studies. There are several aspects of NETPLAN that could be further expanded or improved, as discussed in [83]. For example, distribution-level investments have not been accounted for (e.g., for serving traditional non-PEV or PEV load) when calculating the total system investment cost. Neither have we accounted for transmission expansion investments, or environmental externalities.

7.6   Conclusion

This paper set forth LDV models for national energy and transportation planning studies. The models were parameterized using an array of publicly available data, and three case studies were presented. The results indicate that HEVs and PEVs can help to reduce the cost of the integrated system, and can play a significant role in an effort to realize an aggressive reduction target for GHG emissions. In future work, the proposed LDV models could be used to identify optimal energy and transportation infrastructure designs under multiple objectives, including

more detailed metrics of sustainability and resiliency.

Acknowledgment

8.   CONCLUSIONS AND FUTURE WORK

8.1   Conclusions

First, a novel power electronics topology was proposed for grid-to-vehicle or vehicle-to-grid power flow. This could be an enabling technology for active participation of PEVs in the "smart grid," allowing for instance PEVs to participate in ancillary service markets or to act as distributed energy resources in micro-grids.

However, the main contributions of this dissertation are related to system-level analysis. To this end, we used the most authoritative source of national travel patterns (i.e., the NHTS database) as a means to assess the impacts of fleets of PEVs on the electric power system. Our results were markedly different from previous work, because of the more careful consideration of the vehicles' travel patterns. Furthermore, we found that uncontrolled PEV charging will almost certainly increase the power system's peak load in the U.S.

In addition, algorithms were set forth for the scheduling and dispatch of electric power by aggregators of PEV fleets, under the premise that their main objective would be the maximization of energy trading profits. A major implication of our findings is that aggregator-controlled PEVs could cause problems with system frequency regulation under current market regulations and policies, due to a possible synchronization of the charging start times of massive numbers of PEVs. We also discovered certain interesting facts about the pricing of electricity by PEV aggregators, most notably that off-peak charging rates must be set substantially lower than normal rates in order to attract owners.

Another important contribution is the development of PEV models for use in national energy and transportation planning studies. Our findings indicate that PEVs can help reduce the cost of the integrated system, and can play a significant role in efforts to achieve aggressive

reduction targets for carbon dioxide emissions.

Finally, at the distribution level, we proposed a simple stochastic simulation method for simulating feeders with PEVs.

8.2   Directions of Future Research

This dissertation is not without limitations. For future research, we propose the following directions:

- Cost comparison between vehicle-to-grid (V2G) and dedicated energy storage systems.

  PEVs can participate in the market for various ancillary services to the power system, as reported in [4]. Most of these can be realized to some extent through controlling vehicle charging, without requiring V2G capability. Nevertheless, V2G would further increase the capacity of the ancillary service that a PEV fleet could provide (e.g., for frequency regulation and non-spinning reserve). Moveover, with V2G technology, the battery energy storage of PEVs can be controlled to shift load from peak to off-peak hours. However, vehicle batteries are not designed for power system support, since their main function is to assist in propelling the vehicle. V2G-based ancillary services would reduce the lifespan of PEV batteries further than their normal wear-and-tear, so the associated cost should be carefully evaluated. Alternatively, these ancillary services could be provided using dedicated energy storage systems. It would be of interest to perform a comprehensive comparison of cost-effectiveness between the two schemes.

- Operating framework and strategies for PEV aggregators who participate in both energy and ancillary markets.

  PEV aggregators could provide various ancillary services to the power system. Revenue maximization from frequency regulation through controlling PEVs with or without V2G capability is discussed in [53] and [54], respectively. On the other hand, this dissertation examined the actions of an aggregator who strives to maximize his energy trading-related profits only. It is reasonable to expect that PEV aggregators would prefer to maximize the combined revenue from both energy trading and ancillary services. This would require the

formulation of an integrated optimization problem with constraints accounting for realistic travel patterns, charging circuit rates, and even from local distribution feeders. The aggregators could also engage in arbitrage through charging PEVs during off-peak hours and discharging them during peak hours. Appropriate financial contracts should be designed so that costs associated with battery lifespan reduction due to V2G services is recovered.

- Modeling PEVs in unit commitment.

  In the U.S., ca. 50% of generating capacity participates in wholesale power markets [131]. Nevertheless, a significant portion of electricity is still managed by vertically integrated utilities (in the U.S. and worldwide), which control the entire process of power generation, transmission and distribution. In an electricity market, the PEV load would be represented by PEV aggregators who would be bidding in the day-ahead market in a similar fashion as other load serving entities. Therefore, as far as a market operator or balancing authority is concerned, the unit commitment problem would be formulated and solved in the same manner as previously. However, a vertically integrated utility could obtain the right to control the PEV load through special financial contracts with PEV owners. An interesting problem is how to reformulate the unit commitment problem so that flexible PEV load is appropriately modeled and utilized.

- Coordinating PEVs with other distribution energy resources to improve the performance of distribution systems.

  The efficiency and reliability of distribution systems can be improved by coordinating PEVs with other distributed energy resources (DERs), such as distributed generation, demand response, and energy storage systems. For example, PEV charging could be controlled to follow the power generation from intermittent distributed wind and solar generation. The design of such systems would require investments in communication infrastructure, and devising appropriate centralized or distributed control strategies.

BIBLIOGRAPHY

[1] N. Tanaka *et al.*, "Technology roadmap: Electric and plug-in hybrid electric vehicles," International Energy Agency, Tech. Rep., Jun. 2011.

[2] D. Sutanto, "Alternative energy resource from electric transportation," in *Proc. IEEE Int. Conf. Power Electron. Syst. Appl.*, Nov. 2004, pp. 149–154.

[3] W. Kempton and J. Tomić, "Vehicle-to-grid power fundamentals: Calculating capacity and net revenue," *J. Power Sources*, vol. 144, no. 1, pp. 268–279, Jun. 2005.

[4] K. Fell *et al.* (2010, Mar.) Assessment of plug-in electric vehicle integration with ISO/RTO systems. KEMA, Inc. and ISO/RTO Council. [Online]. Available: http://www.isorto.org/

[5] C. C. Chan, "The state of the art of electric and hybrid vehicles," *Proc. IEEE*, vol. 90, no. 2, pp. 247–275, Feb. 2002.

[6] A. Emadi, K. Rajashekara, S. S. Williamson, and S. M. Lukic, "Topological overview of hybrid electric and fuel cell vehicular power system architectures and configurations," *IEEE Trans. Veh. Technol.*, vol. 54, no. 3, pp. 763–770, May 2005.

[7] G. Zorpette, "The smart hybrid," *IEEE Spectr.*, vol. 41, no. 1, pp. 44–47, Jan. 2004.

[8] C. C. Chan and K. T. Chau, *Modern Electric Vehicle Technology*.   Oxford New York: Oxford University Press, 2001.

[9] A. Emadi, M. Ehsani, and J. M. Miller, *Vehicular electric power systems land, sea, air, and space vehicles*.   Marcel Dekker, 2004.

[10] H. Oyobe, M. Nakamura, T. Ishikawa, S. Sasaki, Y. Minezawa, Y. Watanabe, and K. Asano, "Development of ultra low-cost, high-capacity power generation system using drive motor and inverter for hybrid vehicle," in *Proc. IAS Ann. Meet. IEEE Ind. Appl. Conf.*, Oct. 2005, pp. 2029–2034.

[11] J. M. Miller, *Propulsion Systems for Hybrid Vehicles*. Institution of Electrical Engineers, 2004.

[12] W. Kramer, S. Chakraborty, B. Kroposki, and H. Thomas, "Advanced power electronic interfaces for distributed energy systems," National Renewable Energy Laboratory (NREL), Tech. Rep. NREL/TP-581-42672, Mar. 2008.

[13] J. Vithayathil, *Power Electronics: Principles and Applications*. New York, NY: McGraw-Hill, 1995.

[14] P. C. Krause, O. Wasynczuk, and S. D. Sudhoff, *Analysis of Electric Machinery and Drive Systems*, 2nd ed. New York, NY: Wiley-IEEE Press, 2002.

[15] C.-M. Ong, *Dynamic Simulation of Electric Machinery Using Matlab/Simulink*. New Jersey: Prentice Hall, 1998.

[16] D. C. Aliprantis, N. Wu, C. E. Lucas, and M. A. Masrur, "Automated evolutionary design of a hybrid-electric vehicle power system using distributed heterogeneous optimization," in *Proc. SAE Power Syst. Conf.*, New Orleans, Louisiana, Nov. 7–9 2006.

[17] S. Morimoto, M. Sanada, and Y. Takeda, "Wide-speed operation of interior permanent magnet synchronous motors with high-performance current regulator," *IEEE Trans. Ind. Appl.*, vol. 30, no. 4, pp. 920–926, Nov./Dec. 1994.

[18] C. C. Chan, "The state of the art of electric, hybrid, and fuel cell vehicles," *Proc. IEEE*, vol. 95, no. 4, pp. 704–718, Apr. 2007.

[19] P. Denholm and W. Short, "An evaluation of utility system impacts and benefits of optimally dispatched plug-in hybrid electric vehicles," National Renewable Energy Laboratory, Golden, CO, Tech. Rep. NREL/TP-620-40293, Oct. 2006.

[20] K. Parks, P. Denholm, and T. Markel, "Costs and emissions associated with plug-in hybrid electric vehicle charging in the Xcel Energy Colorado service territory," National Renewable Energy Laboratory, Golden, CO, Tech. Rep. NREL/TP-640-41410, May 2007.

[21] M. Kintner-Meyer, K. Schneider, and R. Pratt, "Impacts assessment of plug-in hybrid vehicles on electric utilities and regional U.S. power grids. Part 1: Technical analysis," *J. EUEC*, vol. 1, no. 4, 2007.

[22] S. W. Hadley and A. Tsvetkova, "Potential impacts of plug-in hybrid electric vehicles on regional power generation," Oak Ridge National Laboratory (ORNL), Oak Ridge, TN, Tech. Rep. ORNL/TM-2007/150, Jan. 2008.

[23] S. Letendre and R. A. Watts, "Effects of plug-in hybrid electric vehicles on the Vermont electric transmission system," in *Transport. Res. Board 88th Annu. Meet.*, Washington DC, Jan. 2009.

[24] "Alternate route: Electrifying the transportation sector. Potential impacts of plug-in hybrid electric vehicles on New York state's electricity system," New York Independent System Operator, Tech. Rep., Jun. 2009.

[25] S. Meliopoulos, J. Meisel, G. Cokkinides, and T. Overbye, "Power system level impacts of plug-in hybrid vechiles," Power Systems Engineering Research Center (PSERC), Tech. Rep., Oct. 2009.

[26] A. Hajimiragha, C. A. Cañizares, M. W. Fowler, and A. Elkamel, "Optimal transition to plug-in hybrid electric vehicles in Ontario, Canada, considering the electricity-grid limitations," *IEEE Trans. Ind. Electron.*, vol. 57, no. 2, pp. 690–701, Feb. 2010.

[27] M. Duoba, R. Carlson, and J. Wu, "Test procedures and benchmarking blended-type and EV-capable plug-in hybrid electric vehicles," in *EVS 23: sustainability - The future of transportation*, Anaheim, CA, Dec. 2007.

[28] M. Duoba, R. Carlson, and D. Bocci, "Calculating results and performance parameters for PHEVs," presented at the SAE World Congr. Exhibit., Detroit, MI, Apr. 2009.

[29] U.S. Energy Information Administration. Fuel economy of the light-duty vehicle fleet. [Online]. Available: http://www.eia.doe.gov/oiaf/aeo/otheranalysis/aeo_2005analysispapers/feldvf.html

[30] U.S. Dept. of Transportation, Federal Highway Administration. Highway statistics 2006. Table VM-1. [Online]. Available: http://www.fhwa.dot.gov/policy/ohim/hs06/htm/vm1.htm

[31] U.S. Dept. of Transportation, Bureau of Transportation Statistics. National transportation statistics. Table 4-6. [Online]. Available: http://www.bts.gov/publications/national_transportation_statistics/html/table_04_06.html

[32] ——. Transportation statistics annual report 2008. Table 1-1-1. [Online]. Available: http://www.bts.gov/publications/transportation_statistics_annual_report/2008/html/chapter_01/table_01_01_01.html

[33] L. Turcksin, S. Van Moll, C. Macharis, N. Sergeant, and J. Van Mierlo, "How green is the car purchase decision? A review," in *10th Int. Conf. Applic. Adv. Techn. Transportation*, Athens, Greece, 27–31 May 2008.

[34] U.S. Dept. of Transportation, Federal Highway Administration. National household travel survey (NHTS). [Online]. Available: http://nhts.ornl.gov/download.shtml

[35] "Comparing the benefits and impacts of hybrid electric vehicle options," Electric Power Research Institute (EPRI), Palo Alto, CA, Tech. Rep. 1000349, Jul. 2001.

[36] "Comparing the benefits and impacts of hybrid electric vehicle options for compact sedan and sport utility vehicles," Electric Power Research Institute (EPRI), Palo Alto, CA, Tech. Rep. 1006892, Jul. 2002.

[37] N. Shidore, T. Bohn, M. Duoba, H. Lohse-Busch, and P. Sharer, "PHEV 'All electric range' and fuel economy in charge sustaining mode for low SOC operation of the JCS VL41M Li-ion battery using battery HIL," in *Proc. 23rd Int. Electr. Veh. Symp. (EVS23)*, Anaheim, CA, Dec. 2007.

[38] T. A. Burress, C. L. Coomer, S. L. Campbell, A. A. Wereszczak, J. P. Cunningham, L. D. Marlino, L. E. Seiber, and H. T. Lin, "Evaluation of the 2008 LEXUS LS 600h hybrid synergy drive system," Oak Ridge National Laboratory (ORNL), Oak Ridge, TN, Tech. Rep. ORNL/TM-2008/185, Jan. 2009.

[39] U.S. Dept. of Energy, Office of Energy Efficiency and Renewable Energy, and U.S. Environmental Protection Agency. Advanced technologies & energy efficiency. [Online]. Available: http://www.fueleconomy.gov/feg/atv.shtml

[40] *Utility Factor Definitions for Plug-In Hybrid Electric Vehicles Using 2001 U.S. DOT National Household Travel Survey Data*, Society of Automotive Engineers (SAE) Std. J2841, Mar. 2009.

[41] A. Moawad, G. Singh, S. Hagspiel, M. Fellah, and A. Rousseau, "Impact of real world drive cycles on PHEV fuel efficiency and cost for different powertrain and battery characteristics," in *24th Int. Electr. Veh. Symp. (EVS24)*, Stavanger, Norway, May 2009.

[42] *SAE Electric Vehicle and Plug in Hybrid Electric Vehicle Conductive Charge Coupler*, Society of Automotive Engineers (SAE) Std. J1772, Jan. 2010.

[43] D. Danilov and P. H. L. Notten, "Adaptive battery management systems for the new generation of electrical vehicles," in *IEEE Veh. Power Prop. Conf. (VPPC)*, Dearborn, MI, Sep. 2009, pp. 317–320.

[44] Midwest ISO. Market information. [Online]. Available: https://www.midwestiso.org/

[45] U.S. Dept. of Transportation, Bureau of Transportation Statistics. State transportation statistics. [Online]. Available: http://www.bts.gov/publications/state_transportation_statistics/

[46] "Annual energy review," Energy Information Administration, U.S. Dept. of Energy, Washington, DC, Tech. Rep. DOE/EIA-0384(2009), 2010.

[47] J. T. Chambers *et al.*, "Fleet electrification roadmap. Revolutionizing transportation and achieving energy security," Electrification Coalition, Tech. Rep., Nov. 2010.

[48] D. Wu, D. C. Aliprantis, and K. Gkritza, "Electric energy and power consumption by light-duty plug-in electric vehicles," *IEEE Trans. Power Syst.*, vol. 26, no. 2, pp. 738–746, May 2011.

[49] J. Taylor, A. Maitra, M. Alexander, D. Brooks, and M. Duvall, "Evaluations of plug-in electric vehicle distribution system impacts," in *Proc. IEEE Power Energy Soc. Gen. Meet.*, Minneapolis, MN, Jul. 2010.

[50] M. Mahalik, L. Poch, A. Botterud, and A. Vyas, "Impacts of plug-in hybrid electric vehicles on the electric power system in Illinois," in *Proc. IEEE Innovative Technologies for an Efficient and Reliable Electricity Supply (CITRES)*, Waltham, MA, Sep. 2010, pp. 341–348.

[51] R. Sioshansi, R. Fagiani, and V. Marano, "Cost and emissions impacts of plug-in hybrid vehicles on the Ohio power system," *Energy Policy*, vol. 38, no. 11, pp. 6703–6712, Nov. 2010.

[52] C. Guille and G. Gross, "A conceptual framework for the vehicle-to-grid (V2G) implementation," *Energy Policy*, vol. 37, no. 11, pp. 4379–4390, Nov. 2009.

[53] S. Han, S. Han, and K. Sezaki, "Development of an optimal vehicle-to-grid aggregator for frequency regulation," *IEEE Trans. Smart Grid*, vol. 1, no. 1, pp. 65–72, Jun. 2010.

[54] A. Brooks, E. Lu, D. Reicher, C. Spirakis, and B. Weihl, "Demand dispatch," *IEEE Power Energy Mag.*, vol. 8, no. 3, pp. 20–29, May/Jun. 2010.

[55] "Characterizing consumers' interest in and infrastructure expectations for electric vehicles: Research design and survey results," Electric Power Research Institute, Tech. Rep. 1021285, May 2010.

[56] P. Fairley. Nissan gets into the electric vehicle charging business. [Online]. Available: http://staging.spectrum.ieee.org/energywise/energy/the-smarter-grid/nissan-gets-into-the-electric-vehicle-charging-business

[57] T. Niimura, "Forecasting techniques for deregulated electricity market prices," in *Proc. IEEE Power Syst. Conf. Expos.*, Atlanta, GA, Oct. 2006.

[58] G. Li, C.-C. Liu, C. Mattson, and J. Lawarree, "Day-ahead electricity price forecasting in a grid environment," *IEEE Trans. Power Syst.*, vol. 22, no. 1, pp. 266–274, Feb. 2007.

[59] N. Amjady and F. Keynia, "Day-ahead price forecasting of electricity markets by mutual information technique and cascaded neuro-evolutionary algorithm," *IEEE Trans. Power Syst.*, vol. 24, no. 1, pp. 306–318, Feb. 2009.

[60] L. Wu and M. Shahidehpour, "A hybrid model for day-ahead price forecasting," *IEEE Trans. Power Syst.*, vol. 25, no. 3, pp. 1519–1530, Aug. 2010.

[61] E. Sortomme, M. M. Hindi, S. D. J. MacPherson, and S. S. Venkata, "Coordinated charging of plug-in hybrid electric vehicles to minimize distribution system losses," *IEEE Trans. Smart Grid*, vol. 2, no. 1, pp. 198–205, Mar. 2011.

[62] Z. Ma, D. Callaway, and I. Hiskens, "Decentralized charging control for large populations of plug-in electric vehicles: Application of the Nash certainty equivalence principle," in *Proc. IEEE Int. Conf. Control Appl. (CCA)*, Yokohama, Sep. 2010, pp. 191–195.

[63] J. Gonder and T. Market, "Energy management strategies for plug-in hybrid electric vehicles," presented at the SAE World Congr. Exhibit., Detroit, MI, Apr. 2007.

[64] U.S. Energy Information Administration. Annual Energy Outlook 2011. Main Reference Case, Electricity Supply, Disposition, Prices, and Emissions. [Online]. Available: http://www.eia.doe.gov/oiaf/aeo/excel/aeotab_8.xls

[65] ——. Annual Energy Outlook 2011. Main Reference Case, Petroleum Product Prices. [Online]. Available: http://www.eia.doe.gov/forecasts/aeo/excel/aeotab_12.xls

[66] D. Wu, D. C. Aliprantis, and L. Ying, "Load scheduling and dispatch for aggregators of plug-in electric vehicles," *IEEE Trans. Smart Grid (Special Issue on Transportation Electrification and Vehicle-to-Grid Applications)*, vol. 3, pp. 368–376, 2012.

[67] K. P. Schneider, Y. Chen, D. P. Chassin, R. Pratt, D. Engel, and S. Thompson, "Modern grid initiative distribution taxonomy final report," Pacific Northwest National Laboratory, Tech. Rep., Nov. 2008.

[68] K. P. Schneider, Y. Chen, D. Engle, and D. Chassin, "A taxonomy of North American radial distribution feeders," in *Proc. IEEE Power Energy Soc. Gen. Meet.*, Calgary, AB, Jul. 2009.

[69] GridLAB-D. [Online]. Available: http://www.gridlabd.org/

[70] K. C. Schneider and R. F. Hoad, "Initial transformer sizing for single-phase residential load," *IEEE Trans. Power Del.*, vol. 7, no. 4, pp. 2074–2081, Oct. 1992.

[71] J. D. Luze, "Distribution transformer size optimization by forecasting customer electricity load," in *IEEE Rural Elec. Power Conf. (REPC)*, Apr. 2009.

[72] T. Shoemaker, J. Mack, and E. Kurtz, *The lineman's and cableman's handbook*, 10th ed. McGraw-Hill, 2002, ch. 15.

[73] *IEEE Guide for Loading Mineral-Oil-Immersed Transformers*, The Institute of Electrical and Electronics Engineers (IEEE) Std. C57.91-1995, 1996.

[74] *American National Standard for Electric Power Systems and Equipment–Voltage Ratings (60 Hz)*, American National Standards Institute (ANSI) Std. C84.1-2006.

[75] T. Short, *Electric power distribution handbook*, L. L. Grigsby, Ed. Boca Raton, FL: CRC Press, 2004.

[76] P. Anderson, *Analysis of faulted power systems.* New York, NY: IEEE Press, 1995.

[77] S. T. Sobral, J. Castinheiras, W. G., M. M. Nielsen, V. S. Costa, and D. Mukhedkar, "Interferences between faulted power circuits and communication circuits or pipelines-simplification using the decoupled method," *IEEE Trans. Power Del.*, vol. 6, no. 4, pp. 1599–1606, Oct. 1991.

[78] S.-Y. Lee and C.-J. Wu, "On-line reactive power compensation schemes for unbalanced three phase four wire distribution feeders," *IEEE Trans. Power Del.*, vol. 8, no. 4, pp. 1958–1965, Oct. 1993.

[79] V. Borozan, D. Rajicic, and R. Ackovski, "Minimum loss reconfiguration of unbalanced distribution networks," *IEEE Trans. Power Del.*, vol. 12, no. 1, pp. 435–442, Jan. 1997.

[80] Lawrence Livermore National Laboratory (LLNL). Energy flow. [Online]. Available: https://flowcharts.llnl.gov/energy.html

[81] NETSCORE-21 Web page. [Online]. Available: http://www.ece.iastate.edu/research/research-projects/netscore-21.html

[82] J. McCalley, E. Ibáñez, Y. Gu, K. Gkritza, D. Aliprantis, L. Wang, A. Somani, and R. Brown, "National long-term investment planning for energy and transportation systems," in *Proc. IEEE Power Energy Soc. Gen. Meet.*, Minneapolis, MN, Jul. 2010.

[83] E. Ibanez, "A multiobjective optimization approach to the operation and investment of the national energy and transportation systems," Ph.D. dissertation, Iowa State University, 2011.

[84] Energy Technology Systems Analysis Program. MARKAL and TIMES model documentation. [Online]. Available: http://www.iea-etsap.org/web/Documentation.asp

[85] U.S. Energy Information Administration. The national energy modeling system: An overview. [Online]. Available: http://www.eia.gov/oiaf/aeo/overview/electricity.html

[86] National Renewable Energy Laboratory. Regional Energy Deployment System (ReEDS). [Online]. Available: http://www.nrel.gov/analysis/reeds

[87] S. Acha, T. C. Green, and N. Shah, "Effects of optimised plug-in hybrid vehicle charging strategies on electric distribution network losses," in *Proc. IEEE Power Energy Soc. Transm. Distrib. Conf. Expos.*, New Orleans, LA, Apr. 2010.

[88] M. A. A. Pedrasa, T. D. Spooner, and I. F. MacGill, "Coordinated scheduling of residential distributed energy resources to optimize smart home energy services," *IEEE Trans. Smart Grid*, vol. 1, no. 2, pp. 134–143, Sep. 2010.

[89] N. Rotering and M. Ilic, "Optimal charge control of plug-in hybrid electric vehicles in deregulated electricity markets," *IEEE Trans. Power Syst.*, vol. 26, no. 3, pp. 1021–1029, Aug. 2011.

[90] A. Maitra, J. Taylor, D. Brooks, M. Alexander, and M. Duvall, "Integrating plug-in-electric vehicles with the distribution system," in *Proc. IEEE Electr. Distrib. - Part 1, CIRED 2009. 20th Int. Conf. Exhib.*, Prague, Czech Republic, Jun. 2009.

[91] C. Farmer, P. Hines, J. Dowds, and S. Blumsack, "Modeling the impact of increasing PHEV loads on the distribution infrastructure," in *Proc. HICSS 43rd Hawaii Int. Conf. Sys. Sci.*, Jan. 2010.

[92] L. Pieltain Fernández, T. Gómez San Román, R. Cossent, C. M. Domingo, and P. Frías, "Assessment of the impact of plug-in electric vehicles on distribution networks," *IEEE Trans. Power Syst.*, vol. 26, no. 1, pp. 206 –213, Feb. 2011.

[93] D. Wu, C. Cai, and D. C. Aliprantis, "Potential impacts of aggregator-controlled plug-in electric vehicles on distribution systems," in *Proc. IEEE workshop 4th Comput. Adv. Multi-Sensor Adap. Process.*, San Juan, Puerto Rico, Dec. 13–16, 2011, pp. 105–108.

[94] L. Wang, A. Lin, and Y. Chen, "Potential impact of recharging plug-in hybrid electric vehicles on locational marginal prices," *Nav. Res. Log.*, vol. 57, no. 8, pp. 686–700, 2010.

[95] J. Wang, C. Liu, D. Ton, Y. Zhou, J. Kim, and A. Vyas, "Impact of plug-in hybrid electric vehicles on power systems with demand response and wind power," *Energy Policy*, vol. 39, no. 7, pp. 4016–4021, Jul. 2011.

[96] C. Weiller, "Plug-in hybrid electric vehicle impacts on hourly electricity demand in the United States," *Energy Policy*, vol. 39, no. 6, pp. 3766–3778, Jun. 2011.

[97] U.S. Energy Information Administration, "Transportation sector module of the national energy modeling system: Model documentation 2010," Tech. Rep., 2010, available online at ¡http://www.eia.gov/analysis/model-documentation.cfm¿.

[98] E. Ibáñez, J. McCalley, D. Aliprantis, R. Brown, K. Gkritza, A. Somani, and L. Wang, "National energy and transportation systems: Interdependencies within a long term planning model," in *Proc. IEEE Energy 2030*, Atlanta, GA, Nov. 2008.

[99] E. Ibanez and J. D. McCalley, "Multiobjective evolutionary algorithm for long-term planning of the national energy and transportation systems," *Energy Systems*, vol. 2, no. 2, pp. 151–169, 2011.

[100] A. Quelhas, E. Gil, J. D. McCalley, and S. M. Ryan, "A multiperiod generalized network flow model of the U.S. integrated energy system: Part I—model description," *IEEE Trans. Power Syst.*, vol. 22, no. 2, pp. 829–836, May 2007.

[101] J. McCalley, "National planning tools," 2010, lecture notes. Iowa State University.

[102] W. Short, D. J. Packey, and T. Holt, "A manual for the economic evaluation of energy efficiency and renewable energy technologies," National Renewable Energy Laboratory (NREL), Golden, CO, Tech. Rep. NREL/TP-462-5173, Mar. 1995.

[103] U.S. Energy Information Administration. Annual Energy Outlook 2011. Main Reference Case, Light-Duty Vehicle Sales by Technology Type. [Online]. Available: http://www.eia.gov/forecasts/aeo/data.cfm

[104] VISION 2011 AEO Base Case Model. Argonne National Laboratory. [Online]. Available: http://www.transportation.anl.gov/modeling_simulation/VISION/

[105] M. Duvall, E. Knipping, M. Alexander, L. Tonachel, and C. Clark, "Environmental assessment of plug-in hybrid electric vehicles," Electric Power Research Institute (EPRI), Palo Alto, CA, Tech. Rep. 101532, Jul. 2007.

[106] *Hybrid Electric Vehicle (HEV) & Electric Vehicle (EV) Terminology*, Society of Automotive Engineers (SAE) Std. J1715, Feb. 2008.

[107] *Recommended Practice for Measuring the Exhaust Emissions and Fuel Economy of Hybrid-Electric Vehicles, Including Plug-in Hybrid Vehicles*, Society of Automotive Engineers (SAE) Std. J1711, Jun. 2010.

[108] Z. Lin and D. L. Greene, "A plug-in hybrid consumer choice model with detailed market segmentation," in *Transport. Res. Board 89th Annu. Meet.*, Washington DC, Jan. 2010.

[109] J. Axsen and K. S. Kurani, "Reflexive layers of influence (RLI): A model of interpersonal influence, vehicle purchase behavior, and pro-societal values," in *Transport. Res. Board 90th Annu. Meet.*, Washington DC, Jan. 2011.

[110] M. J. Eppstein, D. K. Grover, J. S. Marshall, and D. M. Rizzo, "An agent-based model to study market penetration of plug-in hybrid electric vehicles," *Energy Policy*, vol. 39, no. 6, pp. 3789–3802, Jun. 2011.

[111] "Developing a best estimate of annual vehicle mileage for 2009 NHTS vehicles," Oak Ridge National Laboratory (ORNL), Tech. Rep., Feb. 2011.

[112] S. C. Davis, S. W. Diegel, and R. G. Boundy, *Transportation Energy Data Book*, 30th ed., 2011.

[113] U.S. Bureau of Transportation Statistics. (2010) State transportation statistics. [Online]. Available: http://www.bts.gov/publications/state_transportation_statistics/state_transportation_statistics_2010/html/table_05_01.html

[114] A. Simpson, "Cost-benefit analysis of plug-in hybrid electric vehicle technology," National Renewable Energy Laboratory (NREL), Tech. Rep. NREL/CP-540-40485, Nov. 2006.

[115] U.S. Dept. of Energy, Office of Energy Efficiency and Renewable Energy. New car prices: The past 100 years. [Online]. Available: http://www1.eere.energy.gov/vehiclesandfuels/facts/2008_fotw541.html

[116] U.S. Energy Information Administration. Annual Energy Outlook 2011. Main Reference Case, New Light-Duty Vehicle Prices. [Online]. Available: http://www.eia.gov/forecasts/aeo/data.cfm

[117] "Electric and hybrid vehicle research, development, and demonstration program; petroleum-equivalent fuel economy calculation," Energy Efficiency and Renewable Energy Office, Tech. Rep. 00-14446, Jun. 2000. [Online]. Available: http://federalregister.gov/a/00-14446

[118] F. An and D. Santini, "Assessing tank-to-wheel efficiencies of advanced technology vehicles," presented at the SAE World Congr. Exhibit., Detroit, MI, Mar. 2003.

[119] U.S. Environmental Protection Agency – Fuel Economy. [Online]. Available: http://www.fueleconomy.gov/feg/findacar.htm

[120] U.S. Energy Information Administration. Electric power annual: Summary statistics for the united states. [Online]. Available: http://www.eia.gov/cneaf/electricity/epa/epates.html

[121] Ventyx. Velocity suite: Investment grade data and analysis. [Online]. Available: http://ventyx.com/en/resources/type/brochures

[122] NETPLAN software. [Online]. Available: https://github.com/eibanez/NETPLAN

[123] IBM ILOG CPLEX . Optimization Studio Interfaces. [Online]. Available: http://www-01.ibm.com/software/integration/optimization/cplex-optimizer/interfaces/

[124] U.S. Energy Information Administration, "Emissions of greenhouse gases in the United States 2009," Mar. 2011.

[125] U.S. Dept. of Transportation, Bureau of Transportation Statistics. (2009) Transportation statistics annual report 2010. Table 5-2. [Online]. Available: http://www.bts.gov/publications/transportation_statistics_annual_report/2010/html/chapter_02/table_05_02.html

[126] L. Marshall, "Biofuels and the time value of carbon: Recommendations for GHG accounting protocols," WRI working papers, 2009.

[127] J. M. Loiter and V. Norberg-Bohm, "Technology policy and renewable energy: public roles in the development of new energy technologies," *Energy Policy*, vol. 27, pp. 85–97, 1999.

[128] T. Berry and M. Jaccard, "The renewable portfolio standard: design considerations and an implementation survey," *Energy Policy*, vol. 29, pp. 263–277, 2001.

[129] K. Palmer and D. Burtraw, "Cost-effectiveness of renewable electricity policies," *Energy Economics*, vol. 27, pp. 873–894, 2005.

[130] Z. Duan and L. Wang, "Heuristic algorithms for the inverse mixed integer linear programming problem," *J. Global Opt.*, vol. 51, no. 3, pp. 463–471, 2011.

[131] D. Aliprantis, S. Penick, L. Tesfatsion, and H. Zhao, "Integrated retail and wholesale power system operation with smart-grid functionality," in *Proc. IEEE Power Energy Soc. Gen. Meet.*, Jul. 2010.